# Mapping and quantifying the rate of soil and gully erosion in the dry areas of Jordan

Albertus Jozef van Peperstraten

Universiteit Utrecht

ICARDA
Science for resilient livelihoods in dry areas

# Mapping and quantifying the rate of soil and gully erosion in the dry areas of Jordan

**MSc Thesis**

**08-2020**

Author: A.J. van Peperstraten

Student number: 4103424

E-mail: a.j.vanpeperstraten@students.uu.nl

First supervisor: Geert Sterk

Co-supervisors: Stefan Strohmeier and Rens van Beek

MSc Programme: Earth Surface and Water

Faculty of Geosciences

Department of Physical Geography

Utrecht University

## Abstract

The arid and semi-arid regions of Jordan, also known as "Badia", are said to be increasingly degraded and soil erosion creating large gullies has become a common phenomenon. There are concerns that the rate of gully erosion has increased during the last decades due to enhanced desertification. Bedouin people in the Jordan Badia depend on herding sheep, and enhanced desertification hinders grazing and reduces a key source of income. The Jordanian government deemed it a priority to develop the Badia and reduce the damage of existing gully erosion. The objective of this research is to determine how gullies are initiated and what their progression speed is in the Jordan Badia.

A gully growth time lapse of the Wadi al Wala region inside the Jordan Badia has been made in Google Earth Pro and Google Earth Engine to determine gully growth over a period of 15 years. Rangeland Hydrology and Erosion Model (RHEM) is an event-based prediction model for runoff and water erosion that was used for surface runoff quantification. Cipoletti weirs were in addition used to directly measure runoff after events. A finite element model (Hydrus 2D) was used to simulate two-dimensional water movement inside gully channel walls.

Initiation of gullies was connected to water velocity and volume, as these factors determined soil detachment and transport. The correlation between critical slope and drainage area determined gully head boundaries but were influenced by obstacles and phenomena on the hillslope.

The growth speed was different inside the Wadi al Wala catchment. The lower catchment had an average growth of 6.1%, the middle catchment 4.05% and the high catchment 1.1% in 15 years. The growth did not increase gradually, as the largest rainfall events consisted often for >54% of yearly rainfall, which resulted in enhanced gully growth.

Keywords: Gully erosion, gully initiation, gully growth, Jordan, Badia

# Table of contents

## List of figures

## List of tables

## List of appendices

# 1.Introduction

Drylands occupy approximately 41% of the worldwide land surface and support livelihoods of about 2 billion people (Middleton et al., 2011; Reed et al., 2015). The West Asia and North Africa (WANA) region consists of vast dry environments known as arid and semi-arid zones (Karrou et al., 2011). These zones are defined as areas where rainfall relative to the level of evapotranspiration is inadequate to sustain reliable crop production. A large part of these arid zones is considered degraded as well (Dregne, 2002; Reed et al., 2015).

The United Nations Conference on Desertification (UNCOD) stated that land degradation or "desertification" results from various factors including climatic variations and human activities (Dregne, 2002). It is defined as diminution or destruction of the biological productivity of the land. Examples of desertification processes are water and wind erosion, soil salinization, soil compaction and vegetation degradation. Vegetation degradation is defined as "the temporary or permanent reduction in the density, structure, species composition or productivity of vegetation cover" (Conacher and Sala, 1998; Dis4Me, 2004). Long periods of human activity have greatly converted areas of natural vegetation into agricultural land and rangeland. This conversion has enhanced the rate of soil erosion, mainly due to a more sparse vegetation cover, as vegetation and soil organic matter stabilizes the soil (Conacher and Sala, 1998; Reed et al., 2015; Valentin et al., 2005).

Soil erosion is recognized as the major cause of land degradation worldwide (Valentin et al., 2005). An increasing number of publications are available describing its importance since the beginning of the 20$^{th}$ century (Castillo and Gomes, 2016). For instance, the arid and semi-arid regions of Jordan, also known as "Badia", are said to be increasingly degraded and soil erosion creating large gullies has become a common phenomenon (Karou et al., 2011). Bedouin people in the Jordan Badia depend on herding sheep and limited seasonal crop growth (Hashemite fund, 2019). Infrequent but heavy rainstorms in combination with bare crusted soils may lead to flash floods that cause serious gully erosion and damage to fields (Valentin et al., 2005). The gully erosion limits the economic potential of the Jordan Badia. The Jordanian government deemed it a priority to develop the Badia and reduce the damage of existing gully erosion (Hashemite fund, 2019).

It is currently unknown how many gullies are present in the Badia and what the growth speed of gully erosion is. There are concerns that the rate of gully erosion has increased during the last decades due to enhanced desertification. The enhanced desertification hinders grazing by sheep and thus reduces a key source of income for Bedouin farmers. The Jordanian government has deemed it a priority to reverse desertification and develop the Jordan Badia (Hashemite fund, 2019).

Gully erosion is the last stage of water erosion (Mishra, 2013). The stages of erosion can be subdivided to sheet, rill and gully erosion. Sheet erosion is the erosion caused by thin layers of surface runoff. The precipitation exceeds the infiltration capacity and flows down the slope, removing thin layers of the topsoil (sheetwash) (Figure 1-a). When the sheet flow increases in depth, it starts incising and erodes soil while flowing downslope. Then the sheet erosion changes to rill erosion. Rill erosion concentrates the flow of water into small streamlets (Figure 1-b). Finally, the concentrated surface runoff enlarges the rill in width and depth to a channel or miniature valley, advancing rill erosion to gully erosion (Figure 1-c).

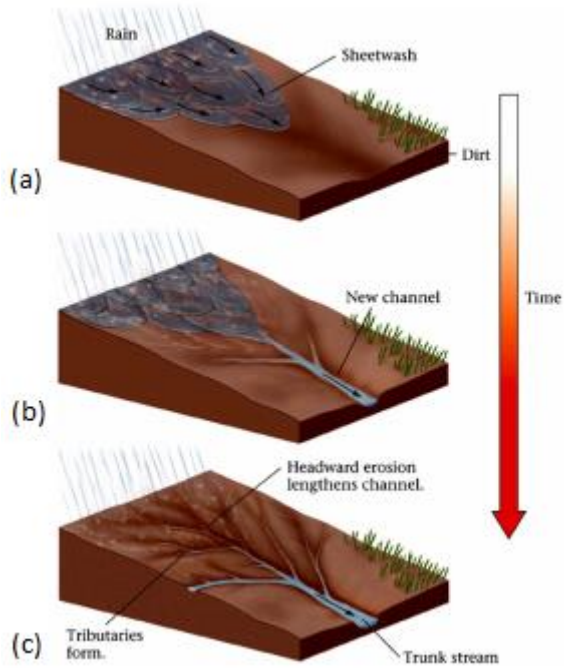


*Figure 1: Gully formation through time. a) Sheetwash erosion b) rill erosion at the top and start of a new channel or gully downslope. c) Gully erosion enlargement due to widening of rills and headward erosion. (Source: Pitt.edu).*

A given slope needs a critical drainage area to produce sufficient amounts of surface runoff to concentrate and initiate gullying (Morgan, 2005; Poesen et al., 2003; Valentin et al., 2005). If the velocity or tractive force of the runoff exceeds a critical or threshold value, gullying will occur. Under the same circumstances, steep slopes need smaller drainage areas to initiate gullying than more gentle slopes.

Steep slopes favor high runoff velocity and increase gully initiation. However, they produce lower runoff volumes than gentle slopes (Janeau et al., 2003; Poesen, 1986). Soil crusts mainly develop on gentle slopes due to the larger impact of the kinetic energy of raindrops. Janeau et al. (2003) found that the impact can decrease by 27% from the gentlest to steepest slopes. In addition, steep slopes are vulnerable to continuous erosion by shear stress. Consequently, soil crusts on the surface of steep slopes are less developed. The crusting of the soil on gentle slopes leads to excess rainwater being unable to infiltrate the surface. Surface runoff increases and concentrates on drainage lines, allowing gully erosion and sediment transport to take place in susceptible areas.

Shahrivar and Christopher (2012) conducted a study in Iran that connects gully volume and length with soil texture. They determined the relation between soil textures of loam, silt loam, silty clay loam and clay loam with gully activity. They found that gully volume was highest in silt loam soils, and gully length was highest for silty clay loam. Loam had in both cases the lowest gully erosion.

A secondary cause for the initiation of gullies could be subsurface- or interflow (Dunne, 1990). As precipitation infiltrates the surface, there is a chance it encounters soil with less vertical hydraulic conductivity. The moisture content becomes saturated and a perched zone develops. The perched zone starts to flow laterally, and a subsurface flow develops (figure 2). This subsurface flow can emerge and has a potential to initiate erosion. This could be due to entrainment of particles by water seeping out of the porous medium or by scouring the margins of macro pores. The macro pores may have originated independently of the water flow. For example, animal digging tunnels into the gully side banks. This could lead to pipe erosion and eventual collapse of the tunnel initiating a new gully channel.

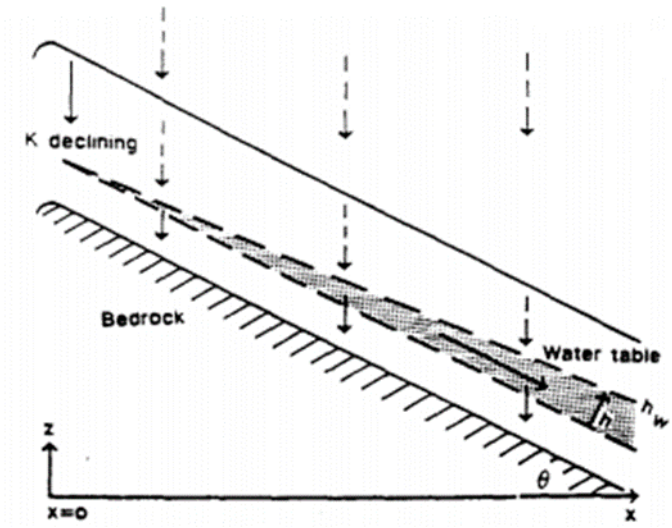

*Figure 2: Percolation of water to the water table on a slope. The water table increases downslope and starts to move as subsurface flow. (Source: Dunne, 1990).*

The main processes in the development of gullies are channel erosion, headward (waterfall) erosion and groundwater seepage (Kirkby and Bracken, 2009; Morgan, 2005; Mishra, 2013). Channel erosion is the scouring of the bottom and sides of the gully by water, which enlarges the depth and width of the gully. Severe scouring can result in the collapse of channel walls. Headward erosion takes place as surface water undercuts the topsoil and the soil falls under its own weight (plunge pool erosion and basal sapping). The soil particles are in turn detached and transported to the lower regions of the watershed. As a result, the gully advances towards the hill or mountain. When the drainage area and side steepness in the gully is high enough, depth and width of the existing gully can again grow by plunge pool erosion and basal sapping. Rapid soil collapse is often found at places where groundwater seepage is concentrated (Kirkby and Bracken, 2009). Seepage can also initiate gullies on fairly gentle slopes or leveled fields. Soil crusting can delay the initiation of gullies due to stronger shear strength, but headward erosion occurs often at points where cracks have developed in surface crusts (Prasad and Römkens, 2004).

Standing water can be found inside a gully after a rainstorm. Infiltration will not take place due to oversaturation. This water has the potential to infiltrate inside the gully side bank, increasing the soil moisture content. When soil moisture is high in these side banks, pore pressure increases and overpressure could initiate the growth of the gully's cross section (Gui and Wu, 2014). Oversaturation of the soil can cause the side banks to collapse.

The impacts of gully erosion can be significant. One of the main issues of soil erosion is the reduction of soil fertility (Dis4Me, 2004; Dregne, 2002; Valentin et al., 2005). The removal of a significant proportion of the topsoil increases the stress that vegetation experiences in the field. Gullies can in addition include loss of available land and an increase in labor costs. Another main issue of gully erosion is the enhanced drainage and accelerated aridification processes. The gullies prevent floodwater from irrigating the surrounding land by concentrating the runoff into narrow valleys. This reduces the soil moisture and reduces the growth of vegetation. A large part of sediment in catchments downstream has its origin by gully and channel erosion. Several studies discussed in Valentin et al. (2005) showed that identification by tracers, had identified gully walls as the main source of sediment. They contributed between 80-98% to the sediment in downstream pools.

Rainwater harvesting (RWH) is locally implemented in the arid and semi-arid regions of Jordan to counteract on water scarcity (Karrou et al., 2011). The structures in treated sites are placed to increase the soil moisture for water uptake by vegetation. One of the most promising RWH techniques is the Vallerani water harvesting structure (Vallerani, 2013). A special type of plow creates micro water harvesting catchments that are placed

perpendicular to the slope. When rainfall is captured by these structures, it is assumed that the total runoff becomes less as more rainfall infiltrates into the soil. In addition, the Vallerani structures slow down the velocity of runoff. This decreases the potential soil erosion in the field and thus rill and gully growth and initiation (Karrou et al., 2011; Kirkby and Bracken, 2009; Morgan, 2005; Valentin et al., 2005; Vallerani, 2013). The vegetation growth caused by the RWH systems increases the soil roughness and slows down runoff as well. Currently it is unknown what the impact of water harvesting structures is on gully formation and growth, and needs to be studied to relate water harvesting efficiency and locations to gully erosion.

The number of gullies and the speed of gully erosion in the Jordan Badia are not fully determined yet. Hence, there is a need to understand the existing processes for gully initiation and monitoring the speed of gully erosion. Understanding the initiation of gullies in the field, with and without RWH structures in place, could help to map susceptible areas for gully erosion. This knowledge could eventually help to prevent gully erosion. The objective of this thesis research was to determine how the gullies are initiated and what the speed of their progression is in the Jordan Badia. Sub questions to answer this objective are:

- Why do certain areas in the Jordan Badia have more active gullies?
- What is the speed of the growth of identified gullies?
- How does the Vallerani RWH technique influence gully growth?
- How is the hillslope hydrology connected to the initiation and growth of gullies?
- What is the impact of an extensive rainstorm on the gully erosion inside the Al-Majidyya watershed?

# 2 Site description

The research area is located in the Badia of Jordan, which covers 80% of the country (Figure 3). It extends from the east, across to where the western mountains border the Jordan valley. The whole Badia extends throughout the Middle East, and in Jordan the area has an extent of 73000 $km^2$ (Hashemite fund, 2019). The area is elevated between 700 and 1100 meters above sea level.

The highest population density in Jordan is concentrated in the west (Figure 3). The east is less inhabited due to the dry conditions and related water scarcity of the Badia (Hashemite fund, 2019; Karrou et al., 2011). Most of the people that live in the less dense populated area are Bedouins who depend on sheep herding. The vegetation cover is low and it is claimed that the desertification in the area is becoming an increasing problem (Dregne et al., 2002; Hashemite fund, 2019; Reed et al., 2015).

The major geological formation in Jordan is composed of finely dissected limestone, chert and marl (Karrou et al., 2011). The soil is highly calcareous and weakly saline, has high silt contents, hard crusts and weak aggregation of the surface layer. The most common soil texture classes are silty clay loam, silty clay and silty loam (Karrou et al., 2011). The water infiltration rate of the soil is low and ranges between 4-20 mm/h (Karrou et al., 2011). Soil crusts are common, leading to high quantities of runoff. Consequently, rill and gully erosion are a common sight in the area.

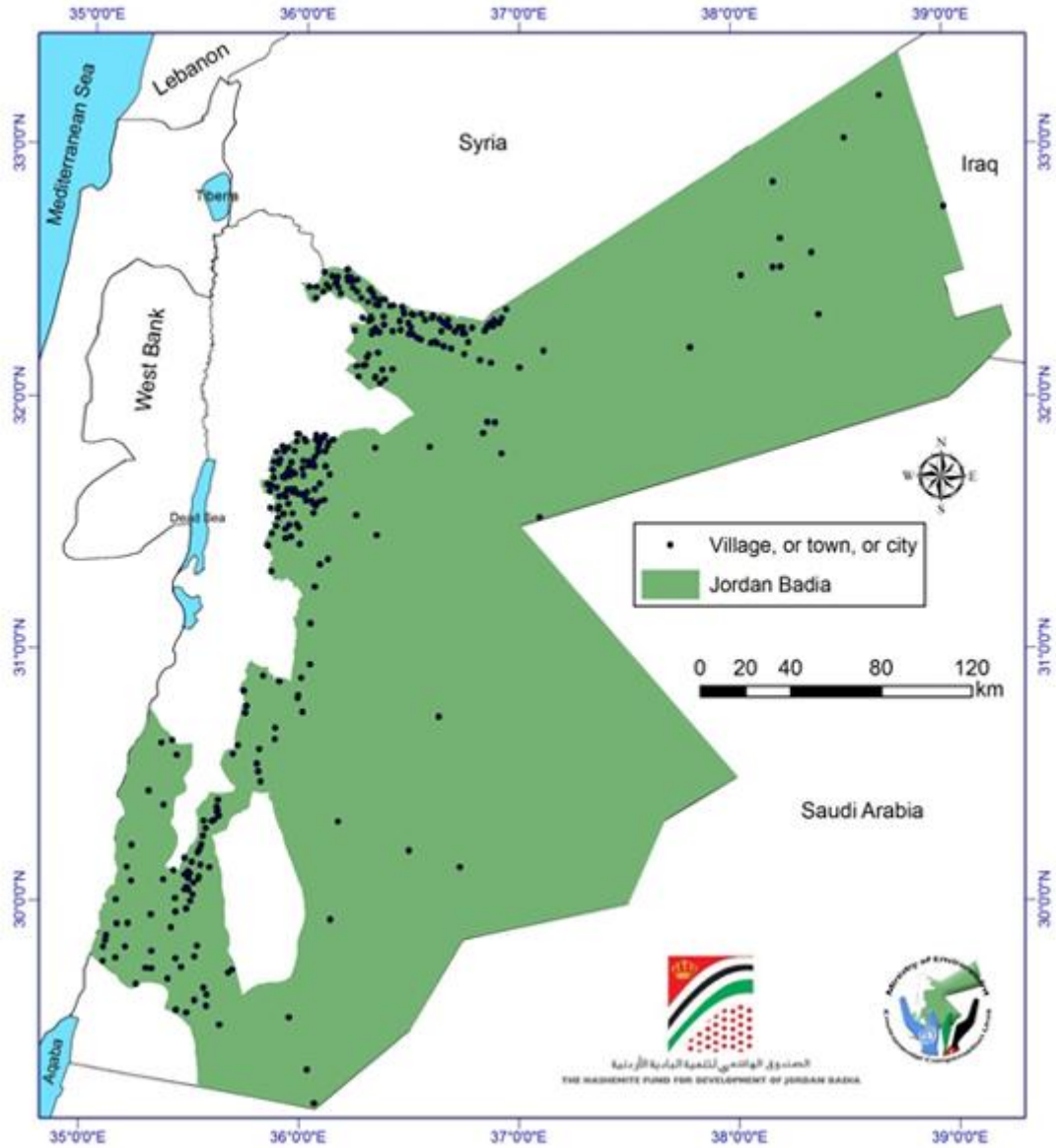


*Figure 3: Map of the Jordan Badia in green. The black dots show villages, cities and towns. (Source: Hashemite fund, 2019)*

The Badia region experiences high average daytime temperatures and low average nighttime temperatures. Average daily temperatures are 24.5°C in summer and 10.0°C in winter (Karrou et al., 2011). Precipitation is less than 200 mm of rain per year (Hashemite fund, 2019; Karrou et al., 2011). Although rainstorms are limited in the region, they have a high intensity. The precipitation amounts vary with and within each season (Figure 4). The rainy season starts in September and continues until May (Karrou et al., 2011).

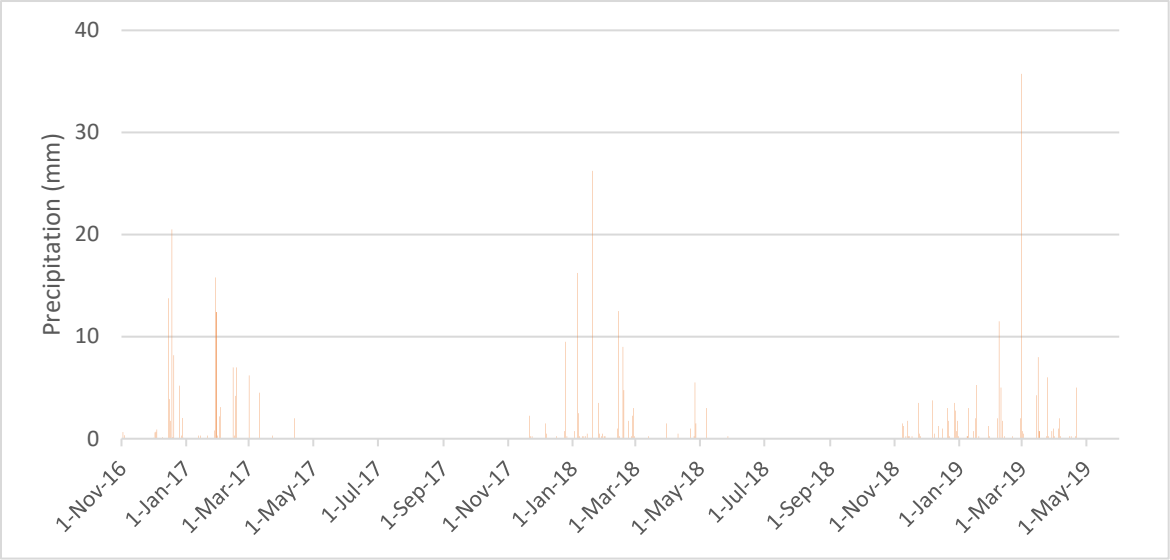


*Figure 4: Rainfall per day between the 1st of November 2016 and the 1st of June 2019. The rainy seasons start in September and ends in May. The rainfall data was gathered from Queen Alia airport Amman, located at 13 km from the Al-Maydiyya research site.*

The study area of the thesis research is located in the Wadi al Wala catchment inside the Jordan Badia. Its location is south of the capital Amman and east of the city of Madaba (figure 5). This catchment is one of the wadi catchments that start at the higher elevated Badia and flows into the Dead Sea (Karrou et al., 2011; WRMD, 2010). The term wadi is Arabic for valley or ephemeral river. These wadis are dry most of the year, but can become active during the rainy season. The gullies inside this wadi catchment were studied at three different scales.

The first scale is the largest scale and consisted of the whole Wadi al Wala catchment (figure 5). The large scale study provides general information on the spatial distribution and temporal changes of high-activity gullies. The aim was localization of gully systems, and monitoring gully growth rates in different areas and for different circumstances. The Wadi al Wala catchment was divided in three areas based on different overall precipitation, land use, vegetation cover, soil texture, elevation and slopes.

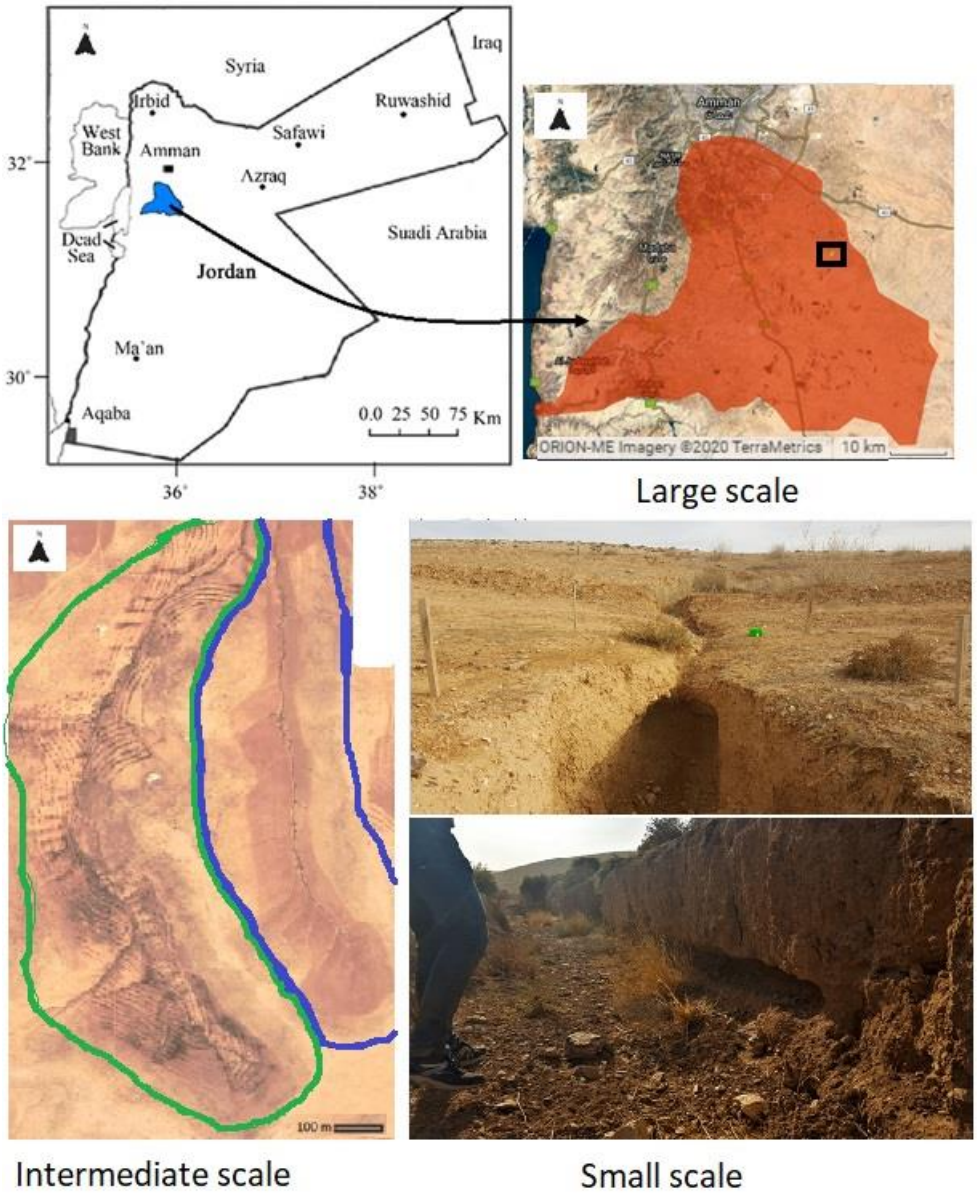


*Figure 5: The Wadi al Wala catchment (upper left and right), the treated (green) and untreated (blue) watersheds (down left) and the gully walls and head (down right).*

The second scale is the intermediate scale. This research was conducted at a site at the edge of the Wadi al Wala catchment (figure 5), close to the town of Al-Majidiyya where two small (30 ha and 14.5 ha) gully watersheds were accurately monitored. The elevation in this study area ranges from 780 to 940 meter. The slopes are on average 7% with a range from 2 to 30%. All soils in the watersheds show high carbonate concentrations. Two dominant soil texture types are common in the area (Karrou et al., 2011). These are silty loam and silty clay loam.

One of the watersheds is treated with RWH structures, which were installed at the site in 2017. This watershed has an area of 30 ha of which 12 ha has been used for Vallerani RWH structures. Vallerani structures have been placed throughout this area along the contour of the slope with a spacing of 6 to 9 meter (figure 6). These Vallerani structures support the growth of the shrub Atriplex Halimus which is used as fodder for the local livestock (Karrou et al., 2011). The surface runoff is directly captured by the Vallerani structures to decrease the erosion by water and sustain the shrub seedlings inside. The treated site has more vegetation than the surrounding area due to the increased soil

moisture generated by the RWH technique. The vegetation inside and outside the Vallerani structures is kept short by sheep grazing on the site. This is done to simulate the sustainable grazing processes before overgrazing took place in this location (Karrou et al., 2011).

The other watershed is located east of the treated watershed (figure 5). The size of this watershed is 14.5 ha, and was not treated by RWH structures. It had almost no vegetation cover during the period of field work. The two gullies come together in the lower area and are connected to a macro water harvesting system, the Marab. Marabs are natural formations that can be found in the Badia where water spreads naturally over relatively wide stream beds at a lower point of the watershed (Saba et al., 2017). The Marabs are often used for Barley cultivation.

*Figure 6: Vallerani structures as implemented in the treated watershed.*

The third scale focuses on detailed research sections of the treated and untreated gullies of the intermediate research scale (figure 5). The sections focus on the gully growth by describing, monitoring and measuring the cross sections and side walls of the gullies and gully heads.

# 3 Materials & methods

## 3.1 Large scale: Wadi al Wala catchment

The Wadi al Wala catchment does not have uniform landscape variables and gully growth was variable inside the whole area. Hence, the catchment was separated into three regions that had different landscape variables compared to each other but share similarities within their own region. Separation was achieved by comparing different landscape variable maps of the Wadi al Wala catchment which were collected on Google Earth Engine (GEE). The landscape variable data consisted of soil texture, land use, elevation, slope, vegetation and precipitation (table 1).

The speed of gully development and gully density in the Wadi al Wala catchment were monitored with Google Earth Pro (GEP) imagery. The gully development was studied for the three selected areas between 2008 and 2019. First, the main gullies were identified visually using the remotely sensed images of the studied areas. Subsequently, the density

and growth rates of the gullies were determined. GEP has a build-in time lapse, which showed the time and locations of when and where the erosion was more extensive during this period. The headward propagation of the gullies (m/timestep) was estimated using map measurements based on these timeseries of aerial imagery. These measurements were conducted manually by using the measurement tool in GEP.

*Table 1: Data sources of the landscape variable maps as found in Google Earth Engine. The slope was derived from the elevation.*

| Map | Soil texture | Land use | Elevation | Slope | EVI[a] | Precipitation |
|---|---|---|---|---|---|---|
| Provider | EnvirometriX Ltd | NASA | NASA/USGS / JPL-Caltech | (-) | NASA LP DAAC | UCSB/CHG |
| Image collection ID | OpenLandMap/SOL/SOL_TEXTURE-CLASS_USDA-TT_M/v02 | MODIS/006/MCD12Q1 | USGS/SRTMGL1_003 | (-) | NOAA/VIIRS/001/VNP13A1 | UCSB-CHG/CHIRPS/PENTAD |
| Resolution (m) | 250 | 500 | 30 | 30 | 500 | 5500 |

a: Enhanced Vegetation Index (optimized vegetation index which is responsive to canopy structural variations). The index ranges from -1 to 1 where -1 indicates no vegetation cover, 0 indicates low vegetation cover and 1 indicates complete vegetation cover.

## 3.2 Intermediate scale: Al-Majidiyya research site

At the intermediate scale, the hydrology of gully formation was studied using field data from the Al-Majidiyya research site and hydrological modeling. Two models were used that both require meteorological data as well as on-site measurements of drainage area and slope. The emphasis of this study was on the last 4 years of a 10-year period (2010-2020), as the Vallerani RWH structures were implemented in the treated watershed since 2017. This section will first elaborate on how the meteorological data was obtained. This is followed by an explanation of the on-site measurements for drainage area and slope. Then, the application of the collected data in the model for determining surface runoff is explained. This is followed by a section on the subsurface moisture content model.

### 3.2.1 Meteorology

The meteorological data was collected in the field as well as from the closest meteorology station at the Queen Alia international airport, which is located at 13 kilometers west of the Al-Majidyya research site. The meteorological data included daily precipitation and temperature over a period of 30 years. In addition, precipitation and temperature were measured using respectively rain gauges and thermometers in the fieldwork area. These measurements were carried out by the International Centre for Agricultural Research in the Dry Areas (ICARDA).

### 3.2.2 Slope and drainage area measurements

The critical slope threshold value was calculated for the initiation of gullies in the Al-Majidiyya area. Begin and Schumm (1979) and Moore et al. (1988) have established a function that determines the threshold for gully initiation which is as follows:

$$sA^b > t \qquad \text{(eq. 1)}$$

Where *s* is the slope (m/m), *A* is the size of the drainage area (ha), and *t* ($ha^b$) is the threshold value that indicates when slope stability is exceeded. The drainage area is the area upslope of the gully head and controls the discharge amount. The critical slope is the slope of this drainage area which controls the velocity of runoff. The variable *b* (-) is catchment dependent, determined by processes operating in the catchment. Values of *b* larger than 0.2 are associated with erosion by surface runoff and those below 0.2 are an indication of subsurface processes and mass movements. Figure 7 illustrates the relation between A and t for several regions in the world.

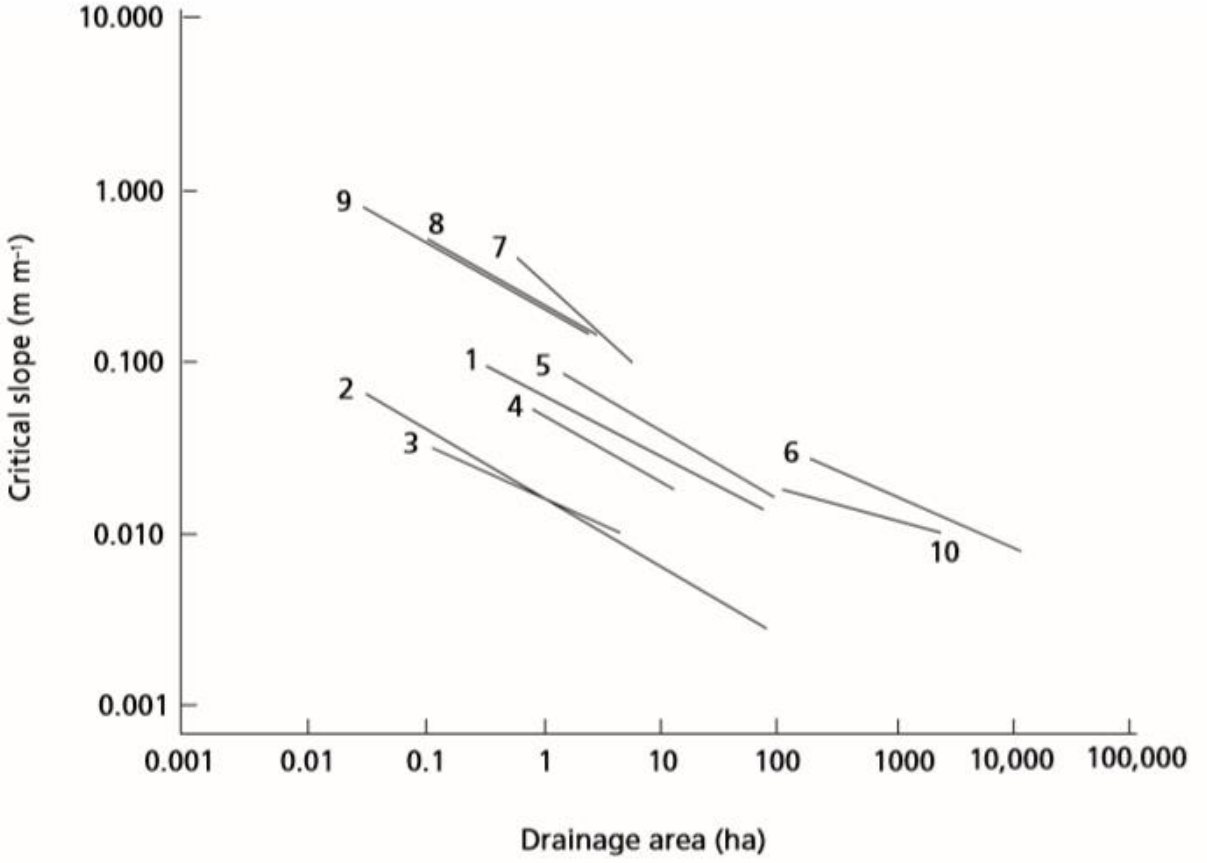


*Figure 7: Relationship between critical slope and drainage area for development of gullies. 1, Central Belgium; 2, Central Belgium; 3, Portugal; 4, France; 5, United Kingdom (South Downs); 6, Colorado, USA; 7, Sierra Nevada, USA; 8, California, USA; 9, Oregon, USA; 10, New South Wales, Australia (Source: Poesen et al, 2003).*

The drainage areas of gully heads in the fieldwork area of Al-Majidiyya were determined manually using elevation data in Google Earth Pro (figure 8). The gully head locations were determined in the field using a GPS device. The drainage areas were calculated from the manually determined polygons in GEP.

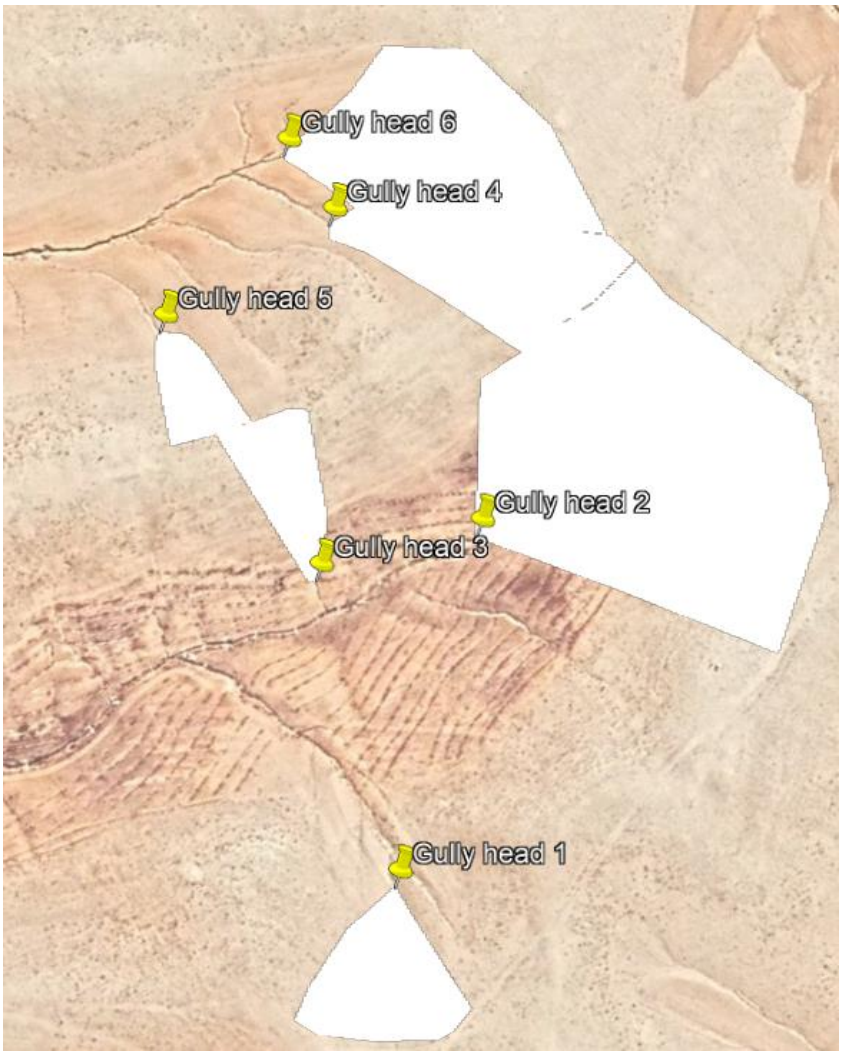

*Figure 8: Drainage area polygons and gully head locations of the Al-Majidiyya field site.*

The slope in the watershed was measured with a Leica Rugby 810 laser level altitude meter (figure 9). A tripod with the altitude meter was placed 15 meters upslope the gully head in the drainage area. The laser altitude meter measured the elevation inside every drainage catchment. It measured the elevation by capturing the light of the rotating laser with a receiver. The receiver was placed on top of a measurement bar and made a beeping noise when the laser was found. At this time, the height measurement was read on the bar.

*Figure 9: The measurement bar (left) and the Leica Rugby 810 laser level altitude meter and receiver (right).*

The drainage area slopes were measured using the elevation differences at nine- and thirteen-meter distances (figure 10). Local elevation differences (bumps, rocks etc.) were sufficiently diminished using these measurement distances. The first height measurement was taken at three meters downslope from the gully head. The next measurements were taken at six and ten meters upslope of the gully head. The elevation difference between the points downslope and upslope was divided by the distance between these points, resulting in a slope in m/m. Three different slopes in the RWH treated watershed and three different slopes in the untreated watershed were measured using this method.

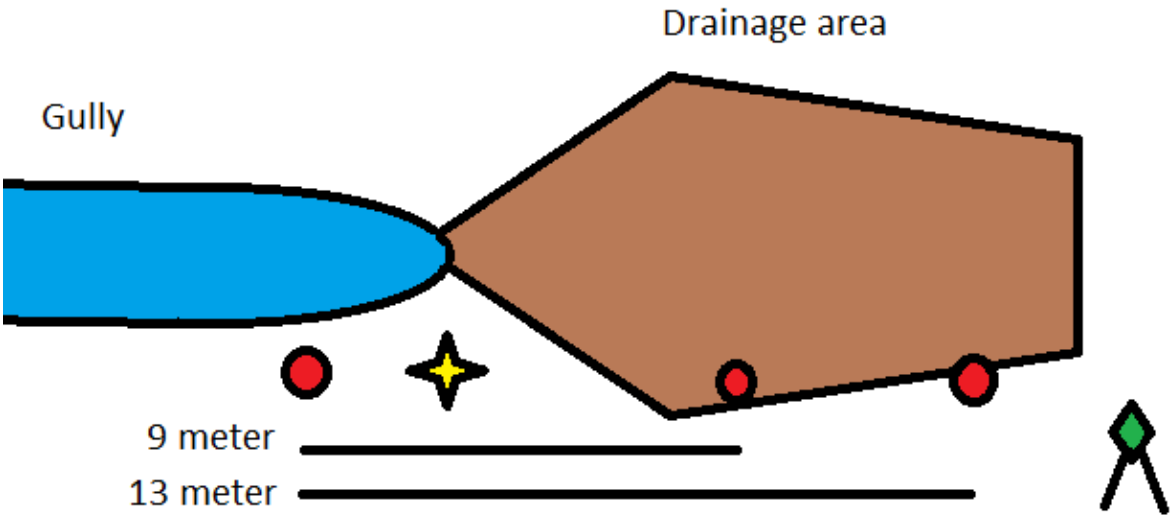


*Figure 10: The locations of the altitude meter and measurements. Red dots show the points where measurements were taken, the yellow star is the point between drainage area and gully. The green tripod represents the laser altitude meter.*

### 3.2.3 Surface runoff estimation

The progression of gully growth was determined in the large-scale catchment (see 3.1). The next step was to estimate the total surface runoff generated on the average hillslope inside the watershed of Al-Majidyya. This was determined by a hillslope model that calculates the amount of generated surface runoff after a rainfall event, which resulted in an estimation of the volume of surface runoff at the gully head.

The hillslope surface runoff was modeled using the Rangeland Hydrology and Erosion Model (RHEM). RHEM is an event-based prediction model for runoff and water erosion that is specifically used for rangeland conditions (Haddad, 2019). The model was developed by the Agricultural Research Service of the United States Department of Agriculture (USDA-ARS). RHEM simulates one-dimensional overland flow over a hillslope with uniform or curvilinear slope profiles as follows:

$$\frac{\partial h}{\partial t} + \frac{\partial q}{\partial x} = \sigma(x,t) \qquad \text{(eq. 2)}$$

Where $h$ is the flow depth at time $t$ and $x$ is the space coordinate along the direction of flow, $q$ is the volumetric water flux per unit plane width ($m^2s^{-1}$), and $\sigma(x,t)$ is the rainfall excess ($ms^{-1}$) calculated by rainfall minus infiltration (Hernandez et al., 2017). The effective saturated hydraulic conductivity (*Ke*) is an important factor in calculating generated surface runoff as it affects the infiltration. Saturated hydraulic conductivity (Ks) is needed to determine Ke. Rawls et al. (1982) developed a look-up table of Ks based on USDA soil texture classes, and Rawls et al. (1998) improved the look-up table by including two porosity classes and two bulk density classes within each textural class, the geometric means of the Ks along with the 25% and 75% percentile values. RHEM calculates *Ke* as follows:

$$Ke = Kb * e^{[p*(litter+basal)]} \qquad \text{(eq. 3)}$$

Where *Kb* is the 25% percentile saturated hydraulic conductivity for each soil texture class, *p* is defined as the natural log of the ratio between the 75% to the 25% percentile values of saturated hydraulic conductivity, *litter* is the litter cover (expressed as a fraction), and *basal* is the proportion of the plant that extends into the soil (expressed as a fraction) (Hernandez et al., 2017). Hence, slope profile, precipitation, soil texture and soil cover are the most important parameters needed to run the model.

The RHEM desktop model required as input a parameter file (.par), a storm/event file (.pre) and a connection file (kin.fil) (Haddad, 2019). The parameter file consisted of specific field parameters and was prepared using the online version of RHEM. The field parameters consisted of soil texture, slope and cover characteristics. Different parameter files were used for the calculation of the RWH treated and untreated watershed. The storm/event file covered rainfall events and amount of rainfall per 5 minutes. The connection file is a command option which connected all parameter and storm/event files.

The RHEM model calculated water volume of historical runoff events over the years 2016/2017 and 2017/2018. The runoff volume of each event was calculated for six different gullies, three in each watershed. The total surface runoff per gully head was determined for the complete season as well as for each individual rainfall event.

The total runoff at the gully head was calculated as the sum of all surface runoff that was generated on the slope of the gully head's drainage catchment. However, RHEM calculated the hillslope surface runoff on a straight slope of 50 $m^2$, which does not correspond to the whole gully head's drainage catchment as seen in figure 8. Therefore, the area of the RHEM slope needed to be converted to the area of the whole gully head's drainage catchment. This was done by dividing the volume of runoff from 50 $m^2$ slope area by 50, then multiplying this number by the drainage catchment corresponding to the gully head. The total runoff was calculated in both the treated and untreated watersheds to evaluate differences in water volume with and without field management.

The total surface runoff at the treated site was justified for runoff capture by the Vallerani RWH structures. First, the number of Vallerani's was counted inside the drainage area of every gully (figure 8). These structures have a volume of 223 liter each (Strohmeier, 2018). Second, the total storage volume of the Vallerani per drainage area was calculated. However, not all the surface runoff reaches the RWH structures as wide spacing and rills on the hillslope can bypass them. Structures can be broken down (by e.g. animals) and the total capture volume is never reached. The total capture volume or "efficiency" of the Vallerani RWH structure was estimated at 0.85 (Stefan Strohmeier, personal communication, May 18, 2020). The justified total Vallerani capture volume in each drainage area was subtracted from the runoff towards the gully head. This subtracted runoff gave the "true" runoff volume that would reach the gully head in the treated watershed.

### 3.2.4 Determining reoccurrence time of precipitation and peak discharge

The reoccurrence time of precipitation events and peak discharges were used to evaluate the magnitude of historic events. Return periods of 2, 5, 10, 25, 50 and 100 years were determined in this study to put recently monitored events into perspective. The return periods can only be calculated when enough rainfall data is available, which was not the case with only 30 years of Queen Alia airport data, as return periods of 50 and 100 years need a longer time frame. Therefore, the RHEM CLIGEN stochastic weather generator (USDA, 2016) was used to calculate a 300 year uniform distribution of events derived from 30 years of historic data. The generator produced daily estimates of precipitation, temperature, dewpoint temperature, wind speed and solar radiation, using daily parameters (means, standard deviation, skewness, etc.).

The peak discharges of the rainfall events over the last 10 years were not recorded in the watersheds of Al-Majidyya. But, the amount of rainfall was recorded at the Queen Alia airport station. Thus, the peak discharge could be estimated for the largest rainfall events over the last 10 years, as RHEM paired with CLIGEN calculated peak discharges for similar amounts of rainfall. This was done by comparing the historic rainfall data with similar generated rainfall, which was paired with generated peak discharge. This resulted in a peak discharge boxplot for the historic data.

### 3.2.5 Discharge measurements by Cipoletti weirs

Cipoletti weirs were installed at the end of both gully watersheds to determine the peak discharge directly in the season of 2019/2020. A Cipoletti weir is a trapezoidal weir, which is used to calculate discharge by the height of the water level (USBR, 1997). The front view of the Cipoletti weirs were monitored by a Bushnell 20 MP trophy camera with an interval of 5 minutes. The water level on the weir was used to calculate the discharge as follows:

$$Q = 1.026 * L * H^{1,5} \qquad \text{(eq. 4)}$$

Where $Q$ is the discharge ($m^3/s$), $L$ is the length of the weir (m) and $H$ is the head of the weir (m) (Dodge, 2001).

The Cipoletti weirs determined the peak discharge of the whole watershed, which includes the smaller sub-watersheds of the gully heads. Hence, the measured Cipoletti weir values needed to be converted to the peak discharge at the gully head only. This was calculated by first dividing the measured peak discharge at the weir by the whole watershed area, and then this number was multiplied by the gully head sub-watershed area.

### 3.2.6 Soil water content inside the gully

The behavior of soil moisture in the gully's cross-section was modeled in Hydrus 2D, which is a finite element model for simulating two-dimensional water, heat and solute movement in saturated and unsaturated soils (Šimůnek et al. 2018). The model numerically solves the Richards equation for uniform water flow in various degrees of saturated soil as follows:

$$\frac{\partial \theta(h)}{\partial t} = \frac{\partial}{\partial xi}\left[K(h)\left(K_{ij}^{A}\frac{\partial h}{\partial x_j} + K_{iz}^{A}\right)\right] \qquad \text{(eq. 5)}$$

Where θ is the volumetric water content ($L^3L^{-3}$), h is the pressure head (L), K is the unsaturated hydraulic conductivity ($LT^{-1}$), $K^A_{ij}$ and $K^A_{iz}$ are the dimensionless anisotropy tensor components for the unsaturated hydraulic conductivity, t is the time (T), and $x_i$ and $x_j$ are the spatial coordinates (L) (Šimůnek et al. 2018).

Hydrus 2D made it possible to see patterns of soil moisture inside a simulated 2D cross-section. Cross-sections of the gully system in the treated and untreated site were modeled. Silty clay loam texture was used in the model as this is the most common soil texture class in the field (Haddad, 2019; Karrou et al., 2011). A water input flux was implemented at the bottom of the gully to simulate the amount of standing water inside the gully after a rainstorm. The runoff photos made by the Bushnell 20 MP camera were used as the standing water height input.

The water content of the soil was simulated for one medium and two large rainfall events. The Hydrus 2D model started simulating 55 days prior to each rainfall event. This resulted in representative soil moisture content on the day of the event. The model simulated the changing patterns inside the cross-section for several days after the event.

Values of soil moisture in the side banks of the gully system were measured directly after a rainfall event to validate the Hydrus 2D model. The amount of soil moisture was measured using a handheld MP306 ICT Time Domain Reflectometer (TDR) (figure 11). A handheld TDR is a soil moisture meter that can directly measure the amount of water content in the soil using electric and dielectric properties of materials. This apparatus approximated water content once at 12 gully cross-sections in the RWH treated watershed and 6 cross-sections in the untreated watershed. The measurements were located at the bottom, in the middle and on top of the gully side banks.


*Figure 11: The handheld MP306 ICT TDR used to measure soil moisture content in the soil.*

## 3.3 Small scale: Gully erosion processes

A qualitative analysis of the erosional processes was made which were classified by the following types: scouring, plunge pools and headward erosion. These different types of erosion were marked on a map of both intermediate scale watersheds. Scouring is the erosion by water flow inside the channel to the side banks of the gully which can result in the collapse of the channel walls (Morgan, 2005). The first indication of collapse is spliced earth on top of the side walls. Preferential flow of water from the hillslope can result into funnel structures in the side banks due to irregularities like e.g. stones (Morgan, 2005). They can evolve into plunge pool erosion as overland flow scours a small basin or pool, which at first widens the gully but could evolve into tributaries. This develops when surface runoff falls into plunge pools, and plunge pools evolve into headward erosion by processes which undermine the head scarp. The locations of spliced earth and rill erosion were also marked on this map.

A detailed survey was performed to describe gully erosion processes by the external influences such as vegetation, animal perturbation and contour plowing. Observations and photographs were considered in explaining gully morphology, growth and initiation.

The growth of six gully heads were measured in three different locations at the RWH treated and untreated watersheds (Figure 2). The first measurement was located at the start of the primary gully (HE1), the second (HE2) and third (HE3) were located at tributaries of the treated watershed. The same was done for the untreated watershed. Profile measurements were plotted in a x-y coordinate system of the head of the gully (Figure 3-a). The origin of the x and y axis is the pole on the left seen in upstream direction. The first measurement point on the x-axis started at the location of the gully head. Each measurement was then taken at every 5 cm interval until the last point of the gully head. Profiles before and after rainstorms displayed the growth of headward erosion by these events.

The amount of gully erosion was determined through the changes in depth and width of the gullies before and after rainfall events. A total of eighteen cross sections of the two gullies were measured; at twelve different locations in the treated watershed, and at six different locations in the untreated watershed (Figure 2). The main gully and the tributaries were represented in the cross sections. The measurements were conducted by using two poles per cross section, which fixed the measurement locations of the cross section. The profile measurements were plotted in a x-y coordinate system with the origin starting at the pole on the left seen in upstream direction (Figure 3-b). The x-axis was represented by a rope with markings every 10 cm. Next, the depth of each 10 cm was measured with a measurement tape. The difference in erosion between both watersheds was compared.

The growth of cross sections and gully heads was plotted in Excel. The same cross sections and gully heads from before and after a rainfall event were plotted in the same graph. The difference indicates the gully growth. The growth between cross sections was compared and growth patterns within the watersheds were explained by their location.

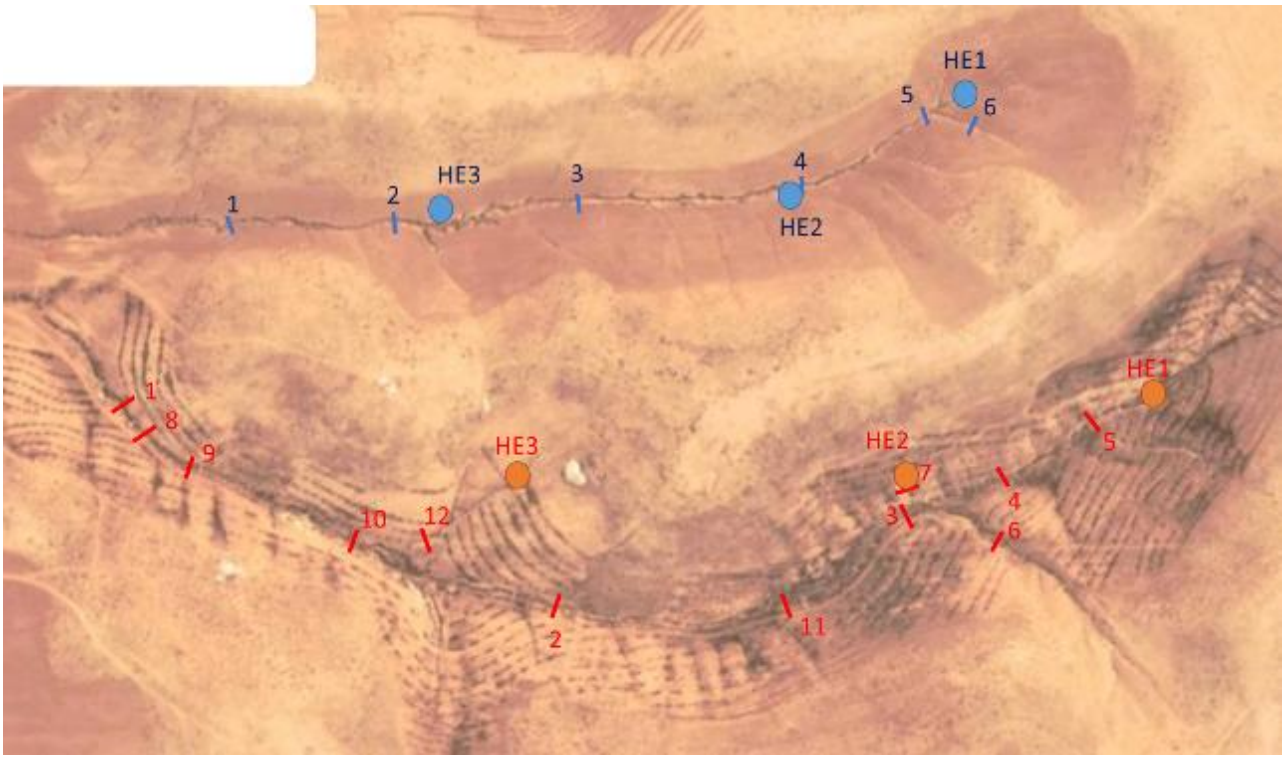


*Figure 12: The measurement locations of the untreated and treated gully systems. The untreated gully (blue) contains 6 cross sections and 3 gully heads. The treated gully (red) contains 12 cross sections and 3 gully heads.*

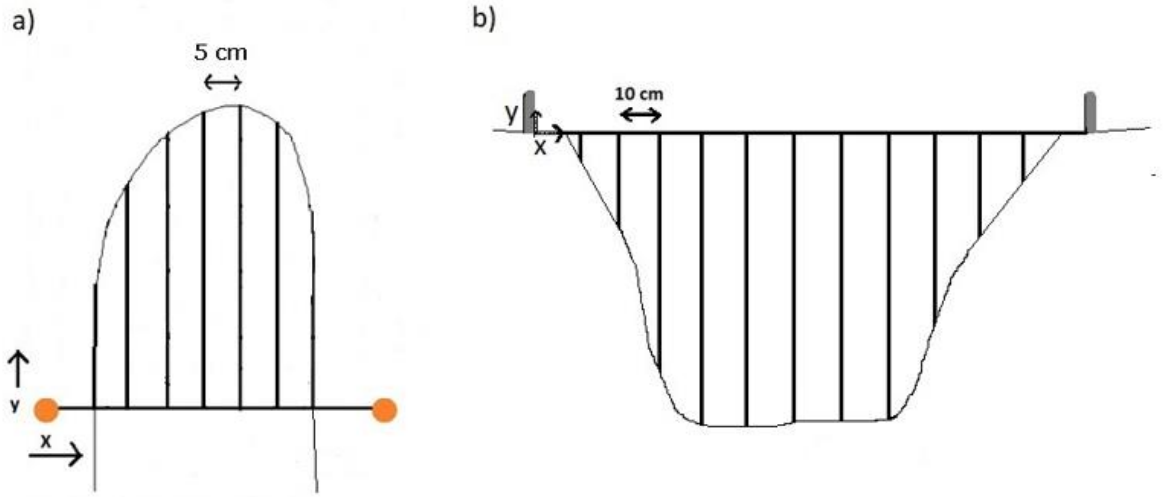


*Figure 13: a) Measurement setup of headward gully erosion (view from top). The orange dots are poles. The origin of the x-y coordinate system starts at the left seen in upstream direction. The contours were measured every 5 cm of the x-axis. b) Measurement setup of a cross section in the gully. The depth is measured each 10 cm on the x-axis. The x-y coordinate system starts at the left seen in upstream direction.*

# 4 Results

## 4.1 Gully development in the Wadi al Wala catchment

The Wadi al Wala catchment was subdivided into three more or less uniform regions for the gully growth assessment. This subdivision was based on the spatial distribution of six variables which were soil texture, land use, elevation, slope, Enhanced Vegetation Index (EVI) and annual precipitation (figure 14). This resulted in a lower, a middle and a higher region of the catchment (figure 15), which will be discussed in more detail in the following sections. The main characteristics of the three regions are shown in table 2.

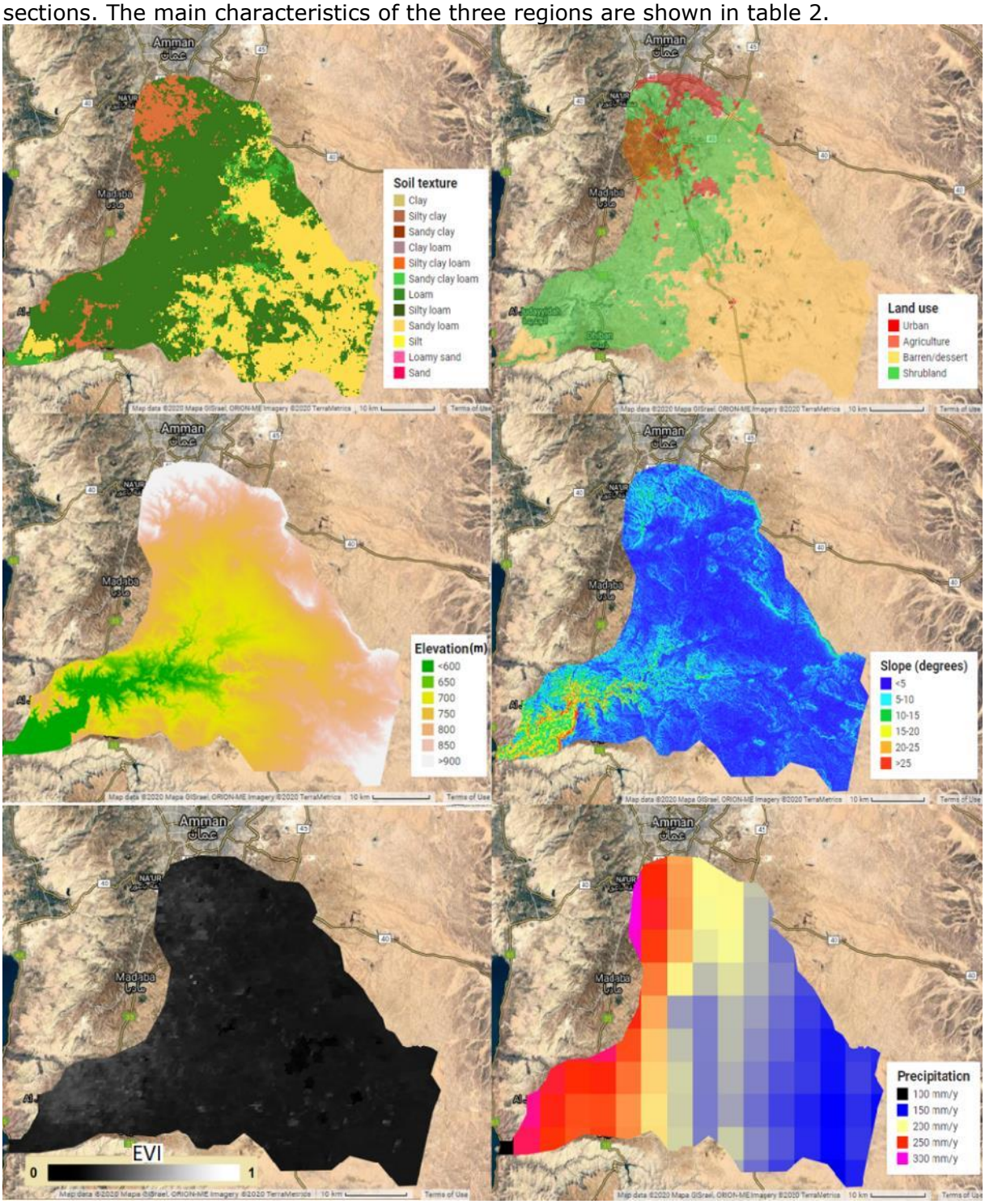


*Figure 14: The soil texture, land use, elevation, slope, Enhanced Vegetation Index (EVI) and annual precipitation of the Wadi al Wala catchment.*

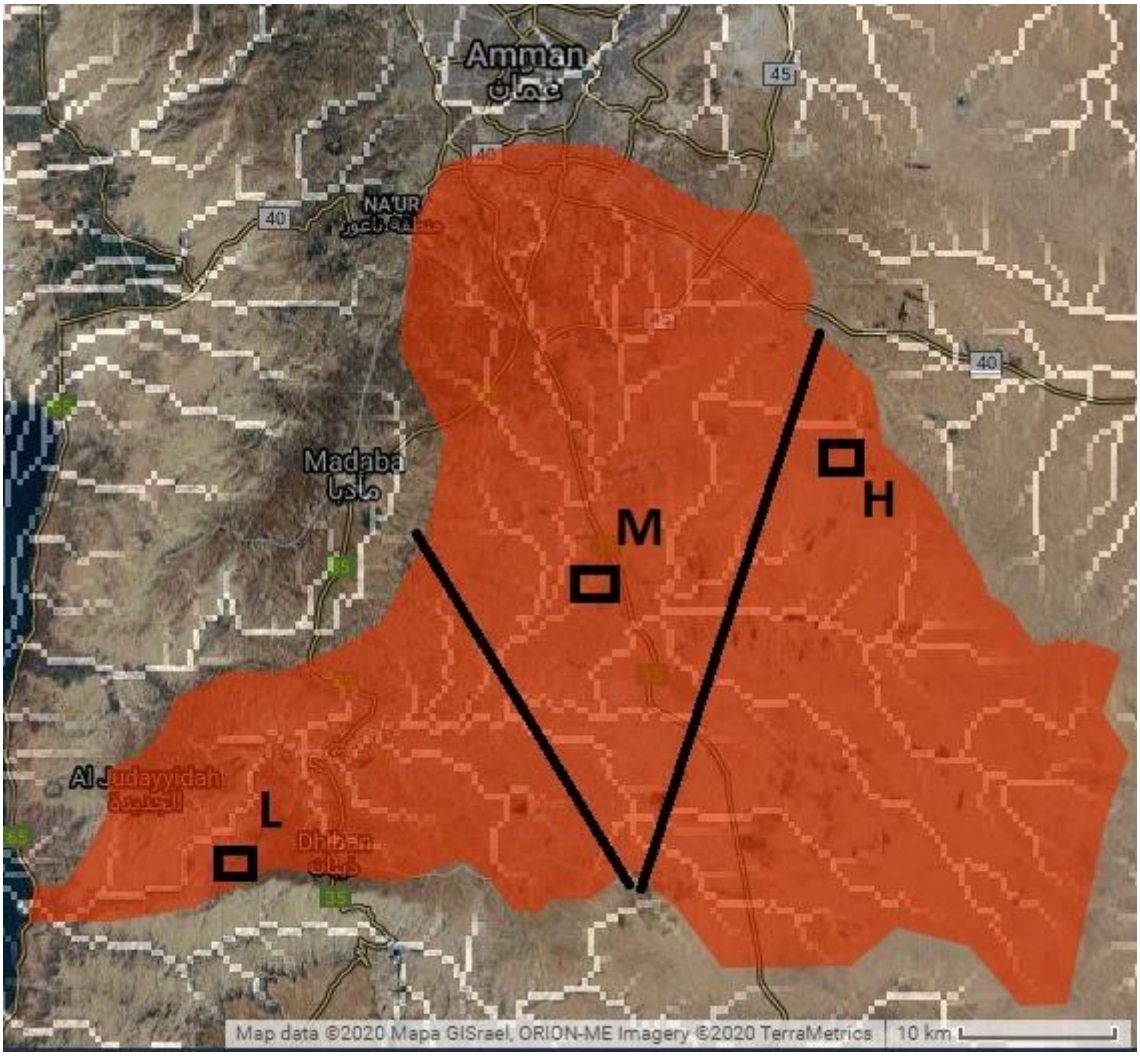


*Figure 15: The Wadi al Wala catchment and the three research sites. L identifies the location of the lower catchment research site, M identifies the middle catchment research site and H identifies the higher catchment research site.*

*Table 2: The landscape variables of the three research sites that identified active gullies and represent the separate regions of the Wadi al Wala catchment.*

| Wadi al Wala | Land use | Elevation (m) | Slope (°) | Soil texture | Veg (EVI) | Precip (mm) |
|---|---|---|---|---|---|---|
| Lower | Shrubland | -200 - 750 | >25 | SiCl/SiLo | 0.0947-0.0967 | >250 |
| Middle | Shrubland | 700 - 800 | 0-15 | SiCl/SiLo | 0.1048-0.1067 | >200 |
| High | Barren/dessert | 750 - 900 | 5-15 | SiLo/SaLo | 0.0562-0.1130 | <200 |

### 4.1.1 Gully growth in the lower catchment

In the lower catchment, which has a size of approximately 600 km$^2$, the gully density and growth rates were determined (table 3). The observed gully density is on average 4.19 km/km$^2$, and the gullies grew 6.1% in length during a time span of 15 years (from 2004 to 2019). The gully density did not change over these years, as no new gullies were observed inside the region. Older time series could not always recognize gullies well and in those cases newer time series were used to determine gully densities.

The high plateau and the hills inside the catchment had different characteristics. Two smaller areas of 10 km$^2$ inside these areas were monitored (table 3). The high plateau has

small elevation differences in which the gullies are located. The gullies are connected to cliffs surrounding the plateau, which transport the water towards the valleys. The hill areas have large elevation differences. The gullies are directly located on the slopes of these hills. The counted gullies and the gully densities were much larger in the hill area.

*Table 3: Gully density and growth in the lower part of the Wadi al Wala catchment of Jordan, over the period 2004-2020.*

| Selected area (10 km$^2$) | nr of gullies | gully density (km/km$^2$) | growth (%) |
|---|---|---|---|
| High plateau | 13 | 3.03 | 6.9 |
| Hills | 29 | 5.36 | 5.3 |
| Average | 21 | 4.19 | 6.1 |

As an example, the growth of a gully system in the lower catchment between 2004 and 2019 is shown in figure 16. Before 2010, growth was zero or could not be observed at this scale. However, fast growth in length (5 to 10 m) was observed inside the gully between the years 2010 and 2019. This growth was not uniform as other parts remained inactive. Hence, fast growth appeared locally, and the growth was different in every tributary.

One extreme case of growth was observed inside the gully in the agricultural field of figure 16, which grew substantially from 2015 onwards, with the largest increase of approximately 6 m between 2015 and 2017 and an increase of 4 m between 2017 and 2018 (figure 17). The peak rainfall was less than in previous years before 2015, while individual rainfall events became larger. However, the biggest precipitation event within these years was recorded in January 2018, when the erosion was at its peak.

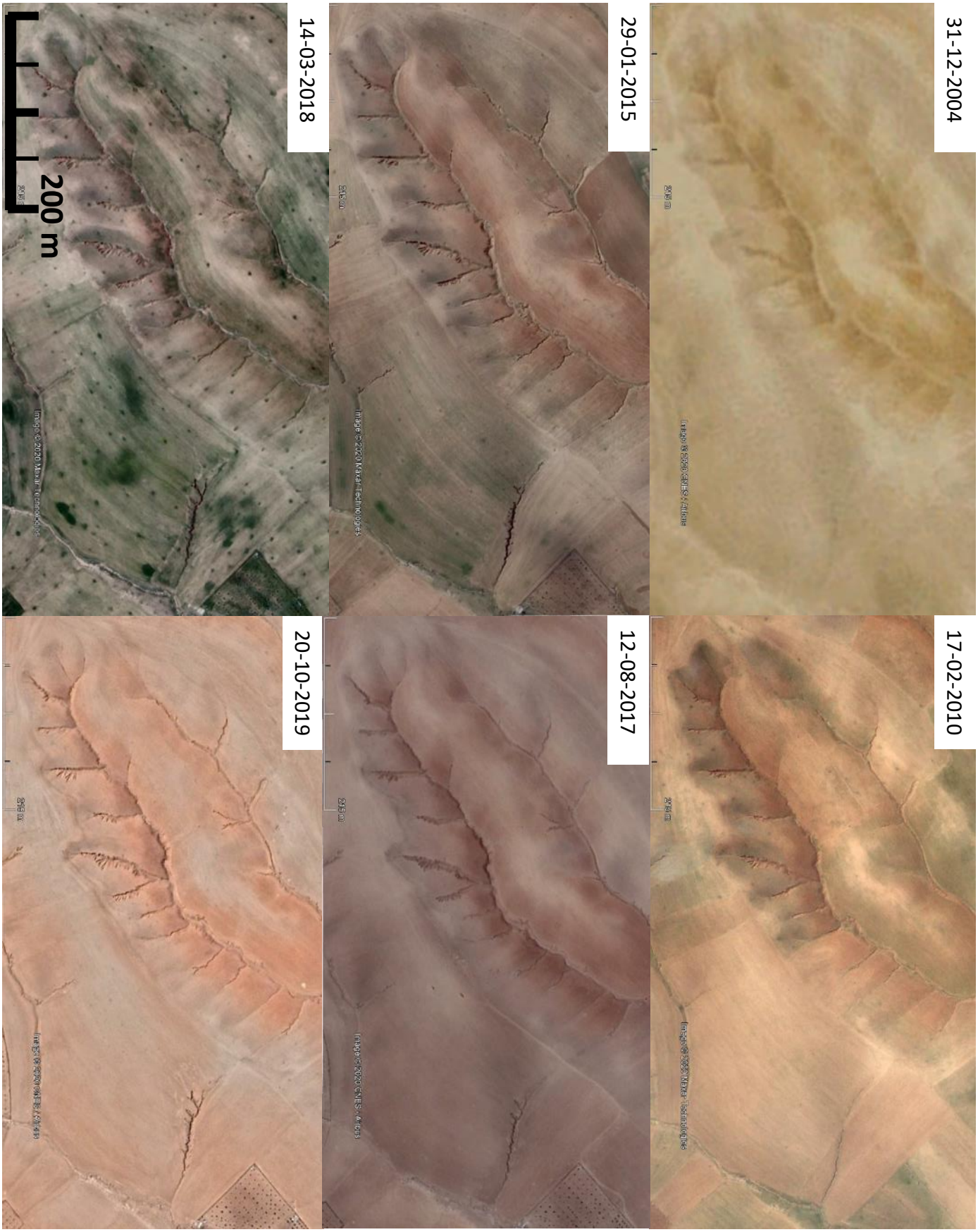


*Figure 16: Time lapse imagery of a watershed on the high plateau of the lower Wadi al Wala catchment in Jordan, over the period 2004-2019.*

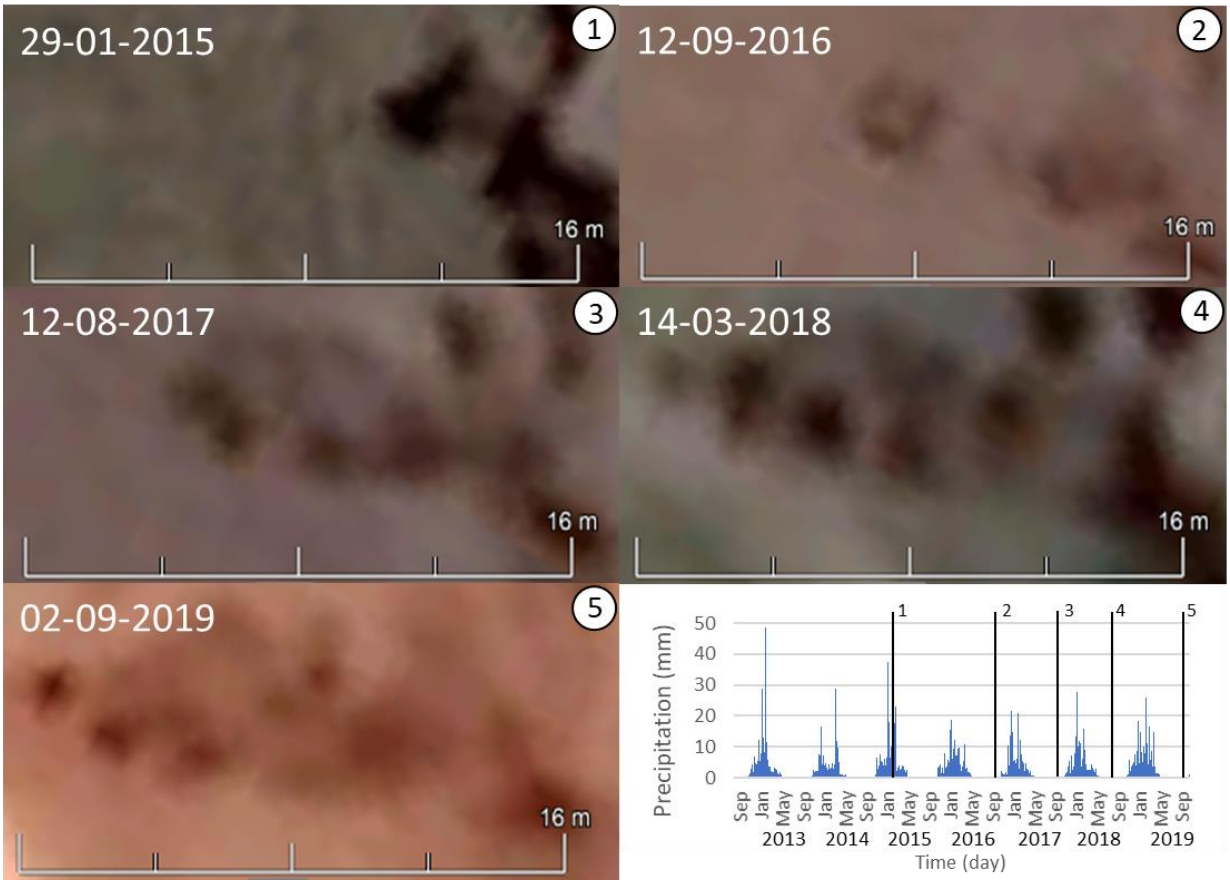


*Figure 17: The gully growth in the agricultural field from 2015 to 2019. The bottom right shows the precipitation per day for this area and the time of the imagery.*

### 4.1.2 Gully growth in the middle catchment

The gully density and growth rates in the middle catchment, which has a size of approximately 1050 km$^2$, are given in table 4. The gully density was observed to be on average 3.94 km/km$^2$ and the gully lengths increased by 4.1% during a time span of 15 years. Regions inside the middle catchment were slightly different, as the north had more agriculture than the south. A large flat area in the north consisted of slopes with less than 5°, while the south had slopes of 10-15°. The southern part of the middle catchment had a larger gully density and gully growth than the flat part.

Gullies were locally flattened for agriculture, which means that entire gullies were removed. At the same time, agricultural land use can initiate gullies as well. The initiation of new gullies was observed in lower areas next to newly constructed fields in higher areas (figure 18). While most gully growth was similar throughout the selected areas of the middle catchment, enhanced growth was found at the construction site.

*Table 4: Gully density and growth in the middle part of the Wadi al Wala catchment of Jordan, over the period 2004-2020.*

| Selected area (10 km$^2$) | nr of gullies | gully density (km/km$^2$) | growth (%) |
|---|---|---|---|
| South | 18 | 4.54 | 4.5 |
| Flat area | 10 | 3.35 | 3.6 |
| Average | 14 | 3.94 | 4.1 |

*Figure 18: Examples of removal (blue arrow) and initiation (red arrow) of gullies in combination with agricultural practices.*

Another example of the influence of construction was observed in a smaller area of 0.23 $km^2$, which had a tributary gully system connected to an ephemeral river (figure 19). This increased gully growth coincides with construction activities in the years 2017, 2018 and 2019. The fastest growth was detected between 2017 and 2018, which caused an increase of about 5 m headward erosion (figure 20). This was a remarkably fast growth considering that the growth in this area was less than 1 m/y under normal conditions.

Another 5 m growth was detected in 2019 after constructions and more frequent large rainfall events during the season 2018/2019 (figure 20).

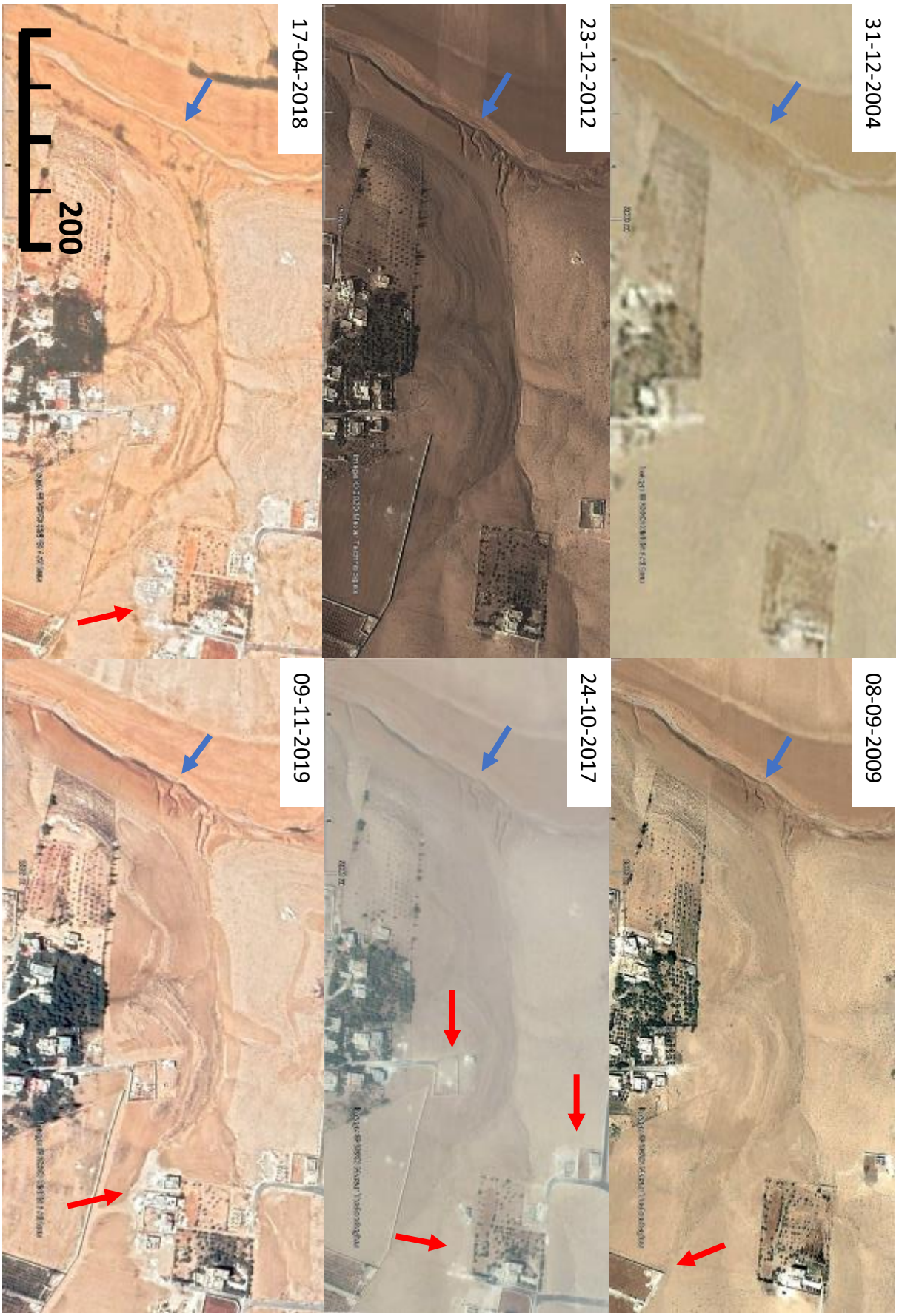


*Figure 19: Time lapse imagery of an area in the middle Wadi al Wala catchment in Jordan over the period 2004-2019. The tributary gully growth is indicated with a blue arrow and new construction with a red arrow.*

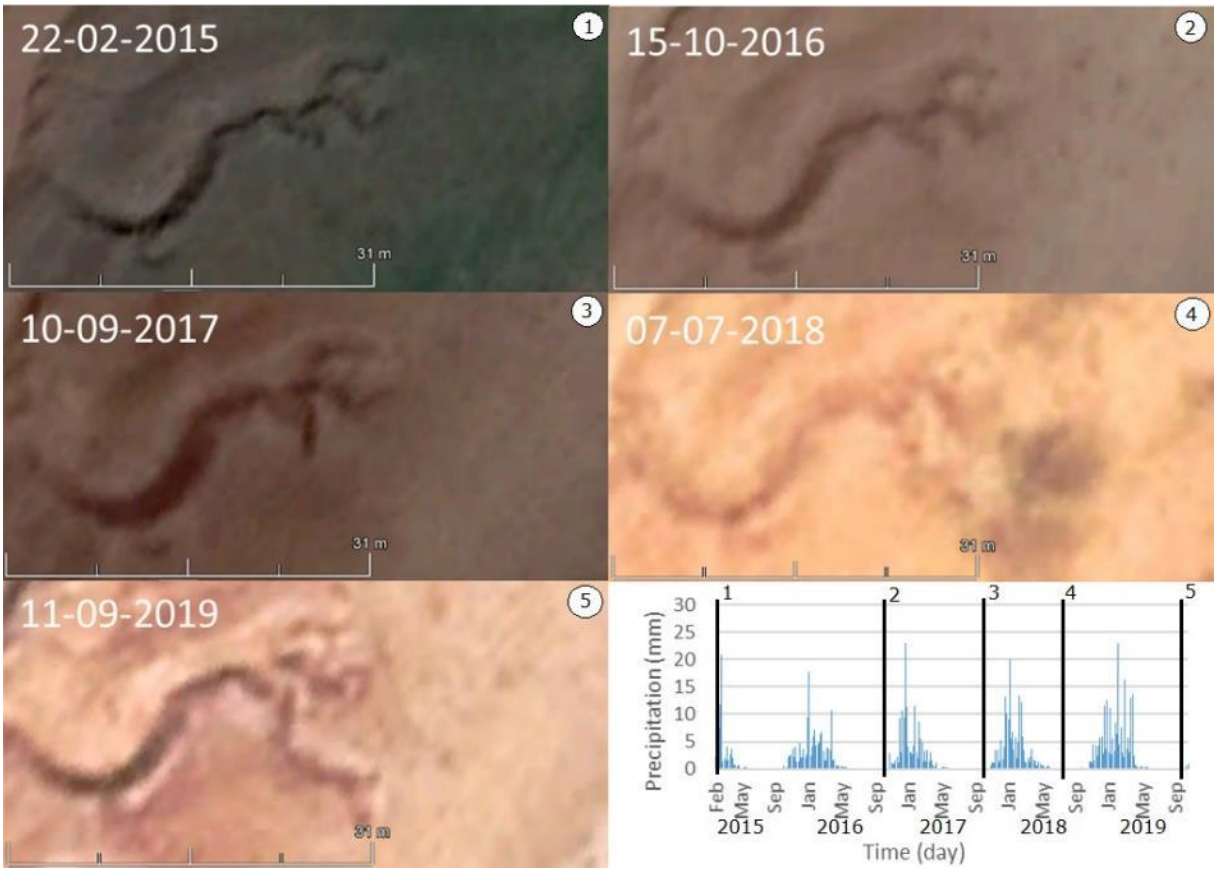


*Figure 20: Close up of the tributary gully growth in the middle Wadi al Wala catchment in Jordan over the period 2015 to 2019. The bottom right shows the precipitation per day for this area and the time of the imagery.*

### 4.1.3 Gully growth in the higher catchment

In the high catchment, which has a size of approximately 900 km$^2$, the gully density was on average 4.55 km/km$^2$, and the gullies grew 1.1% in length during a time span of 15 years (table 5).
The subareas within this catchment were similar, as the north and south had a gully density of respectively 4.90 and 4.19 km/km$^2$, and a gully growth of 1.0 and 1.2% between 2004 and 2019.

*Table 5: Gully density and growth in the high part of the Wadi al Wala catchment of Jordan, over the period 2004-2020.*

| Selected area (10 km$^2$) | nr of gullies | gully density (km/km$^2$) | growth (%) |
|---|---|---|---|
| North | 26 | 4.90 | 1.0 |
| South | 21 | 4.19 | 1.2 |
| Average | 23.5 | 4.55 | 1.1 |

A smaller area of 0.45 km$^2$ inside the high catchment was highlighted and consisted of a RWH treated and an untreated watershed (figure 21). The length of the gullies remained stable during the observation period, but the width and depth increased in both watersheds. Since the implementation of the RWH structures in 2017, the width and depth inside the treated site did not increase anymore.

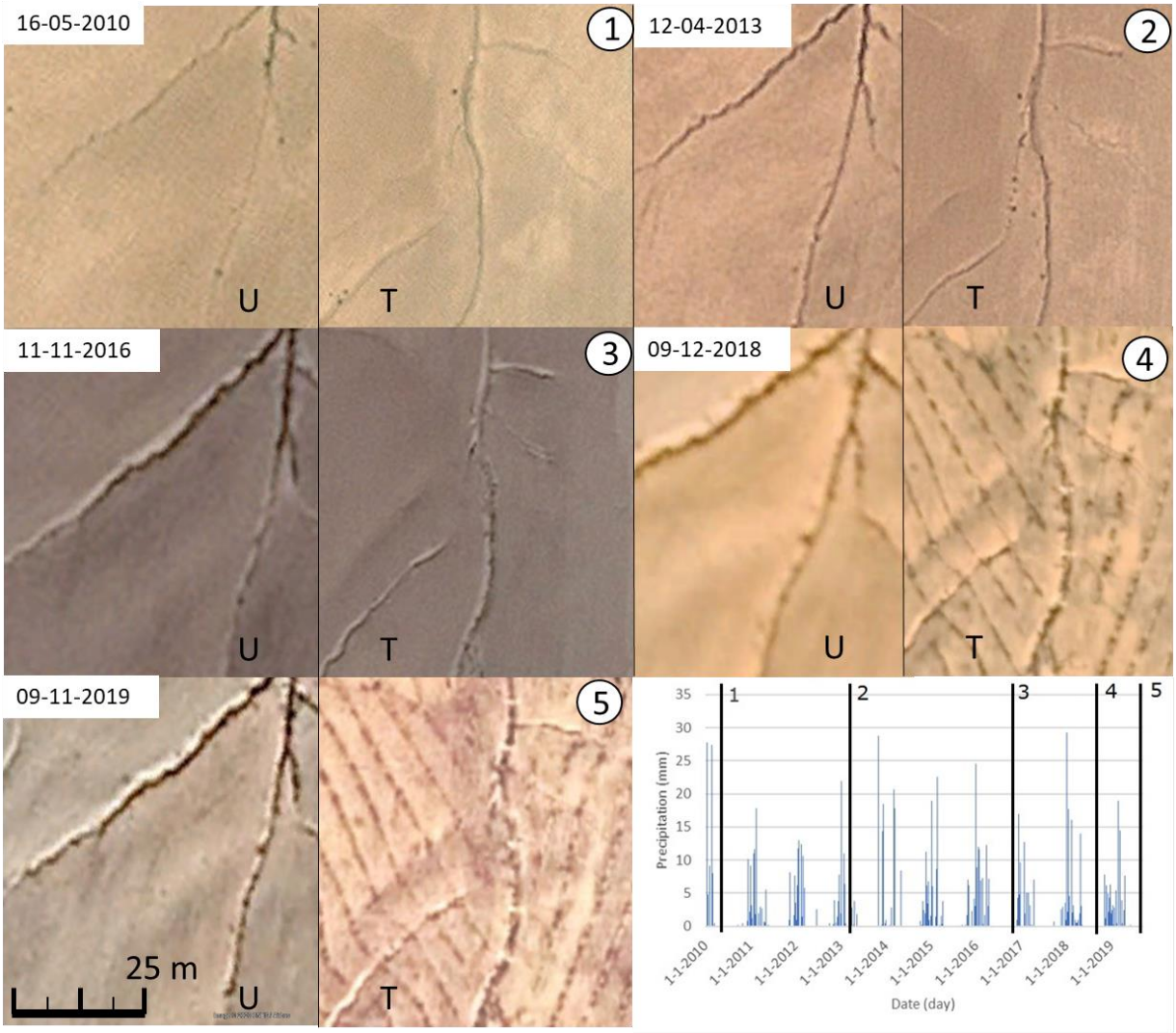


*Figure 21: Detailed timelapse of the untreated (**U**; left) and treated (**T**; right) watershed inside the higher Wadi al Wala catchment in Jordan, over the period 2010-2019. The bottom right shows the precipitation per day for this area and the time of the imagery.*

## 4.2 Intermediate scale: The Al-Majidiyya gully systems

### 4.2.1 Critical slope and drainage area correlation

The critical slope and drainage area (CSADA) correlation of the watersheds in Al-Majidiyya were determined for six different gully heads, which were measured in an RWH treated and an untreated watershed. The critical slope variated between 0.03 and 0.15 m/m inside these watersheds, and the area of the drainage catchments was in between 0.17 and 2.4 ha (figure 22). The CSADA threshold values were higher for the untreated than for the treated watershed. In addition, the critical slope in the treated watershed had a larger decrease per drainage area.

A power function was fitted between the determined CSADA measurement points in both RWH treated and untreated watersheds of Al-Majidiyya (figure 22). The two watersheds had an R-squared ($R^2$) value of respectively 0.86 and 0.72, the combined measurements points of both watersheds were determined at 0.80. The $R^2$ values indicate that all measurement points in the two watersheds are closely related.

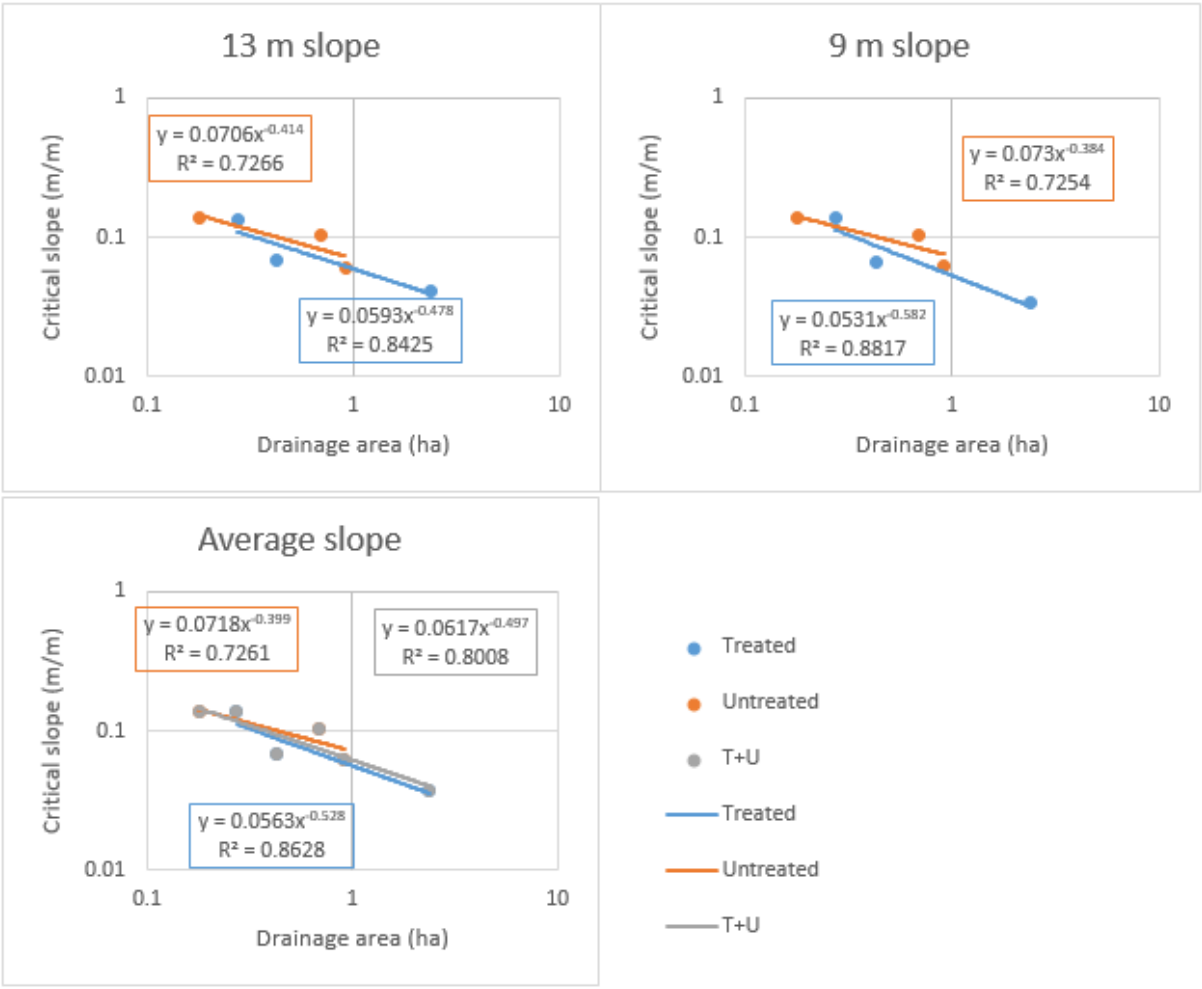


*Figure 22: Relation between the critical slope and drainage area for the 13-meter slope, the 9-meter slope and the average of these slopes on the Al-Majidyya watersheds. Blue colors represent the treated site, orange colors the untreated site and gray the average of all observation points.*

### 4.2.2 Surface runoff volume

The monitored gully heads received different amounts of surface runoff during the 2016/2017 and 2017/2018 rainy seasons (figure 23). Gully head 2 received the largest amount of water (>250 $m^3$), while gully heads 3 and 5 (<50 $m^3$) received the least amount of water. The total surface runoff at the gully heads was adjusted to the Vallerani capture for gully head 1, 2 and 3. However, the water volume increased mostly due to a larger drainage area (figure 8).

The total water volume towards the gully head depended more on individual large rainfall events than a distribution of several smaller events (figure 24). The total volume in the season of 2016/2017 consisted for 78% from the contribution of the largest rainfall event, while the other 17 events only contributed for 12%. The largest event within a number of 13 events in the season 2017/2018 contributed for 54% to the total water volume per season.

The surface runoff collected in the treated watershed was adjusted for Vallerani RWH structure capture inside the gully head drainage area (table 6). The amount of Vallerani was counted inside the drainage area (figure 8) and adjusted for a capture efficiency of 0.85%. Gully head 2 (GH2) observes a cut of almost half the total surface runoff it would normally receive, while GH1 did not change in the treated watershed as it did not have Vallerani RWH structures in its drainage area.

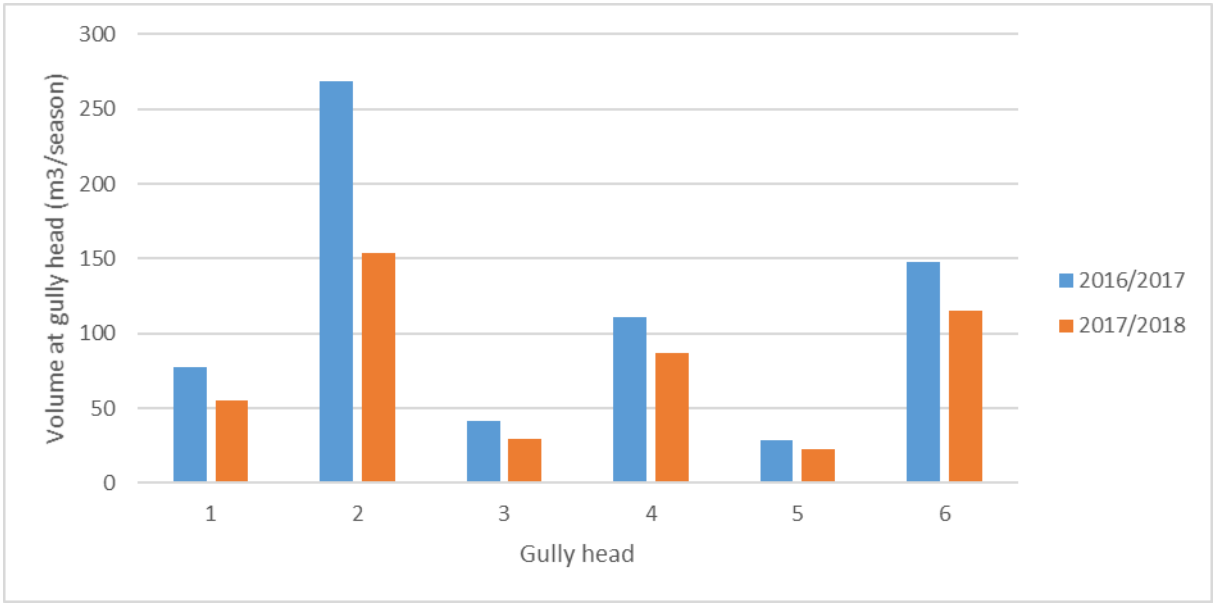


*Figure 23: Total runoff at gully heads in $m^3$/season. Gully head 1,2 and 3 are in the RWH treated watershed and 4, 5 and 6 are in the untreated watershed.*

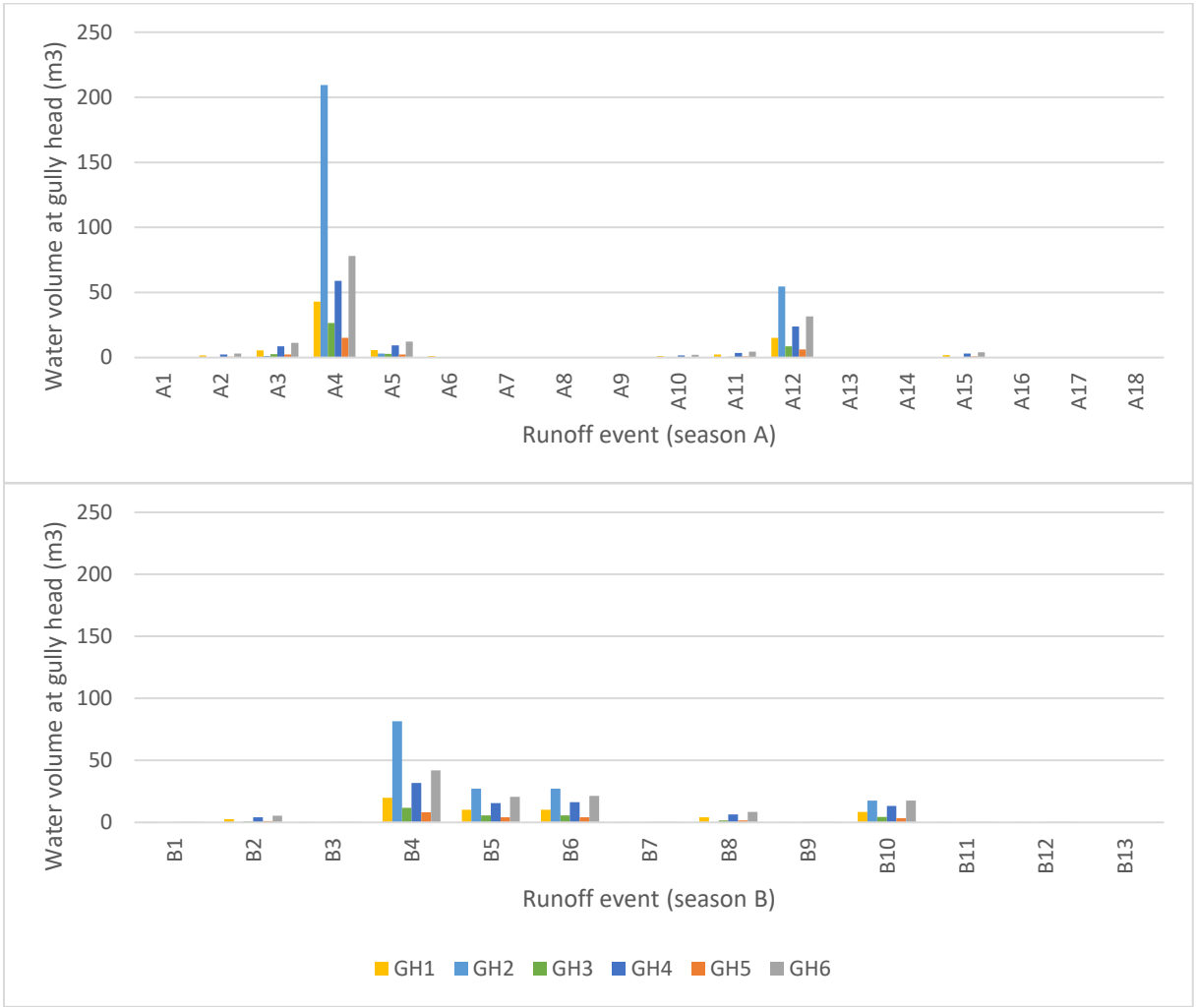


*Figure 24: Water volume at six gully heads in $m^3$ for every rainfall event in season 2016/2017 (A) and 2017/2018 (B). Gully heads 1, 2 and 3 are in the RWH treated watershed and gully heads 4, 5 and 6 are in the untreated watershed.*

*Table 6: Total surface runoff volume ($m^3$) collected per season inside the treated watershed with (V) and without (NV) Vallerani RWH structures inside the drainage area.*

| | GH1 | GH2 | GH3 |
|---|---|---|---|
| Amount Vallerani in gully head drainage area | 0 | 154 | 5 |
| V 16/17 | 77,8 | 268,3 | 41,4 |
| NV 16/17 | 77,8 | 431,4 | 49,7 |
| V 17/18 | 55,5 | 153,4 | 29,8 |
| NV 17/18 | 55,5 | 308,2 | 35,5 |

### 4.2.3 Reoccurrence time of rainfall and peak runoff events

Rainfall reoccurrence time is the average time a certain amount of rain reappears. This time was determined for the Al-Majidyya watersheds and shows the return period of all precipitation and runoff events (figure 25). The largest precipitation events in the last 10 years were recorded as 28.8 mm (20 November 2013), 29.2 mm (5 January 2018) and 35.7 mm (28 February 2019), and have a return period of 5 to 25 years. The return period runoff values were calculated on an average, 50 m slope without RWH structures in Al-Majidyya and peak discharge was estimated by the input of multiple similar precipitation events in the RHEM model. The peak runoffs of discharge events were estimated between extreme values of 6 and 47 mm/h (2013) and 6 and 46 mm/h (2018). These estimations were converted to the peak discharge for every gully head ($m^3$/h) by including drainage area (figure 26). The runoff return period (figure 25) is calculated as the average runoff during an event and must not be confused with the peak discharge (figure 26), which is much higher. The peak discharge of 2019 was measured by Cipoletti weirs and will be discussed in chapter 4.2.4.

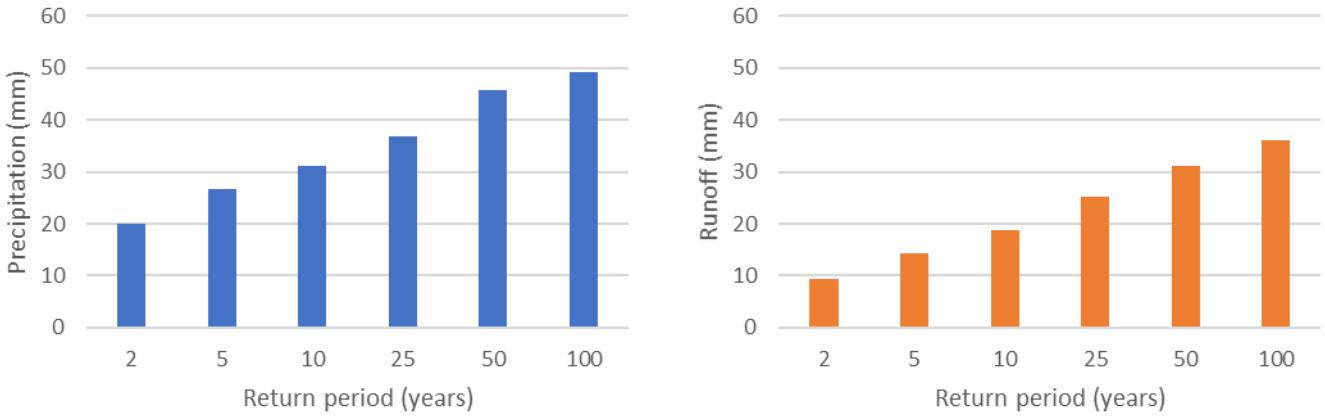


*Figure 25: Return period of precipitation and average runoff per event as calculated by RHEM for periods of 2, 5, 10, 25, 50 and 100 years for the combined Al-Majidiyya watersheds without RWH structures.*

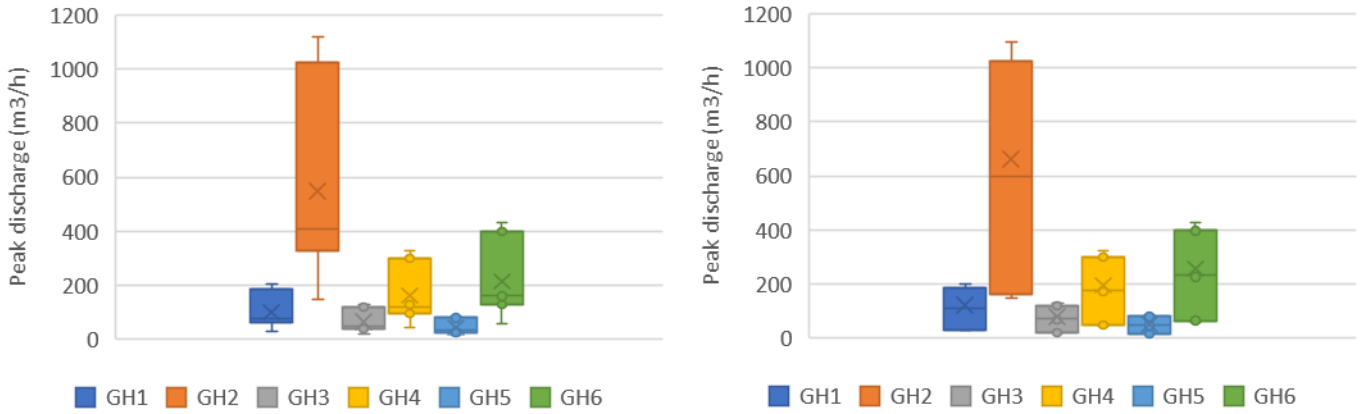


*Figure 26: Peak discharge at gully head on respectively 20-11-2013 and 05-01-2018 as estimated by RHEM for several generated precipitation events.*

### 4.2.4 Peak discharge measured by the Cipoletti weir

Four peak discharges of discharge events were determined using the Cipoletti weirs on 28-02-2019 (figure 27), 28-12-2019 (figure 28), 08-01-2020 (figure 29) and 24-01-2020 (figure 30). The event of 28-02-2019 was the largest rainfall event in 20 years and corresponds with a return period of approximately 25 years (figure 25). The other events were smaller and more common in a season.

The discharge in the treated watershed did not reach the outlet during smaller events, while outflow was occurring from the untreated watershed (figure 28, 29). However, the peak discharge was the same in both watersheds during larger events (figure 27, 30). Hence, the outflow from the untreated watershed was larger than from the treated watershed during small events, but similar during large events.

A large difference was observed between the peak discharges for each event inside the watersheds (table 7). They ranged from 26.6 to 352.4 ($m^3/h$) on the largest event (28-02-2019), while the other more common events ranged from 1.4 to 98.8 ($m^3/h$).


*Figure 27: Peak discharge event in the untreated (left) and treated (right) watersheds at 28-02-2019.*


*Figure 28: Peak discharge event in the untreated (left) and treated (right) watersheds at 28-12-2019.*


*Figure 29: Peak discharge event in the untreated (left) and treated (right) watersheds at 08-01-2020.*

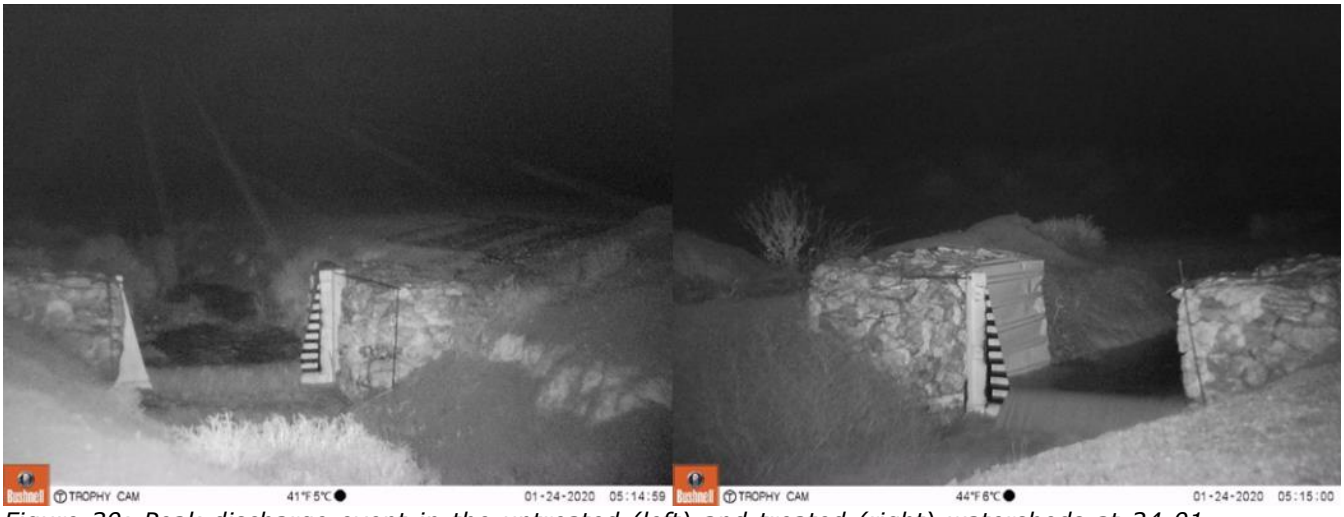


*Figure 30: Peak discharge event in the untreated (left) and treated (right) watersheds at 24-01-2020.*

*Table 7: Peak discharge per gully head for the monitored events of the season 2019/2020.*

| Date | G1 ($m^3/h$) | G2 ($m^3/h$) | G3 ($m^3/h$) | G4 ($m^3/h$) | G5 ($m^3/h$) | G6 ($m^3/h$) |
|---|---|---|---|---|---|---|
| 28-2-2019 | 63.5 | 352.3 | 40.6 | 102.9 | 26.6 | 136.3 |
| 28-12-2019 | n/a | n/a | n/a | 15.7 | 4.1 | 20.8 |
| 8-1-2020 | n/a | n/a | n/a | 5.6 | 1.4 | 7.4 |
| 24-1-2020 | 17.8 | 98.8 | 11.4 | 28.9 | 7.5 | 38.2 |

### 4.2.5 Soil moisture inside the gully side bank

The soil moisture patterns of gully cross sections were modeled with Hydrus 2D during three rainfall events for both watersheds of Al-Majidyya. The first rainfall event captures a smaller event inside the field and represents the more common rainfall throughout the year. The other two events capture more extreme events and their corresponding soil moisture patterns. The emphasize of this study was to see if the water infiltrates the channel, and if there are differences in infiltration due to rainfall intensity.

The first profile shows a common rainfall event of 15.8 mm in 2017 (figure 31), which wetted the inside of the gully and the soil directly in contact with the atmosphere. This was followed by an event the next day, which further increased the water content of the soil. The water content in the side bank of the gully decreased from 0.4 to 0.22 (-) during the following two days.

The water content patterns were similar in both watersheds. However, the water content volume in the side banks of the treated watershed was higher than in the untreated watershed. An increase of moisture content in the side bank was not observed after these rainfall events.

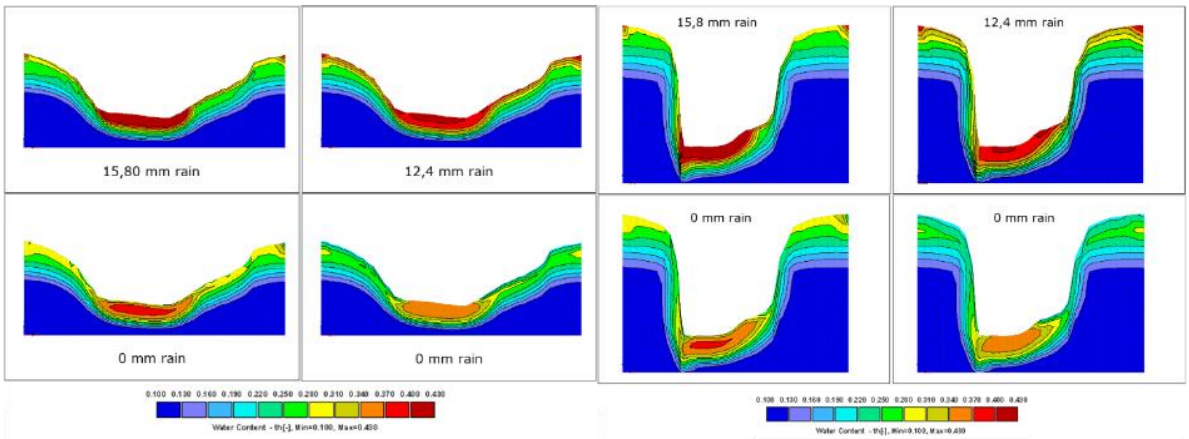


*Figure 31: The soil moisture content patterns along a gully cross section of the treated watershed (left) and the untreated watershed (right) during the period between 28-01-2017 and 31-01-2017. Modelling was done with the Hydrus 2D model. Rain fell on the first two days and was followed by two dry days (see appendix 1a).*

The moisture patterns were similar but had more soil moisture following a large rainstorm of 26.3 mm on 19-01-2018 (figure 32). A fast decrease in soil water content in the gully side bank was visible in the days after the rainfall event. A slower decrease of water content was observed on top and inside the gully.

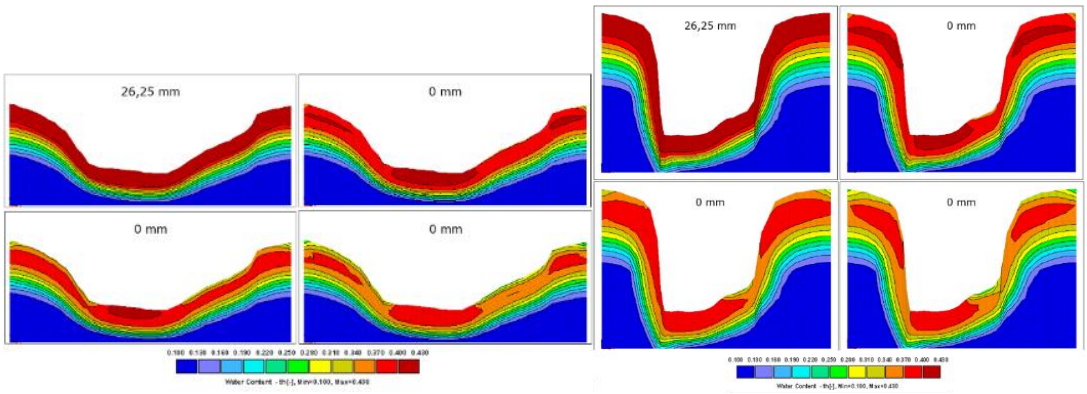


*Figure 32: The soil moisture content patterns along a gully cross section of the treated watershed (left) and the untreated watershed (right) during the period between 19-01-2018 until 22-01-2018. Modelling was done with the Hydrus 2D model. Rain fell on the first day and was followed by three dry days (see appendix 1b).*

The soil moisture content remained high (>0.4) in the days after the rainfall event of 28 February 2019 (35.75 mm), as the soil moisture decrease was minimal (figure 33). The untreated cross section observed a faster decrease in soil water content as the soil moisture in the treated cross section appeared constant days after the strong rainfall event. The water content in the right side of the untreated cross section appeared to evaporate faster than the left side.

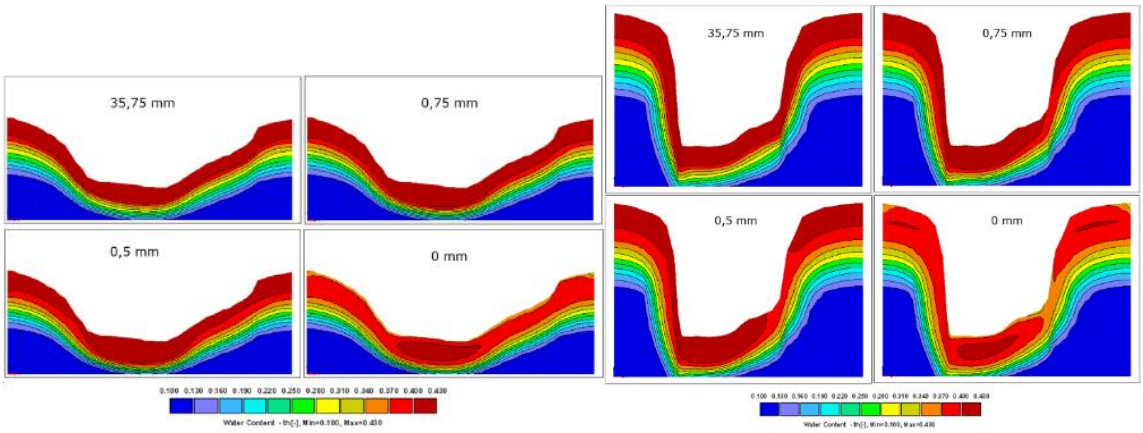


*Figure 33: The soil moisture content patterns along a gully cross section of the treated watershed (left) and the untreated watershed (right) during the period between 28-02-2019 until 03-03-2019. Modelling was done with the Hydrus 2D model. A large amount of rain fell on the first day and was followed by two days of a small rainfall amounts and one dry day (see appendix 1c).*

Soil moisture contents were measured directly after a rainfall event on 20 January 2020 (figure 34, 35), which provided information on flow paths and moisture content patterns inside the cross sections. The number of the moisture content measurements corresponds to the number of the cross sections (appendix 3, 4).

Soil moisture content patterns were variable within the cross sections of the watersheds (figure 34, 35). The soil moisture content was higher at the bottom as well as on top of the cross sections and the shadow part of the gully was wetter than the part that was heated by the sun. Another high moisture content pattern in either the left or right side at the bottom of the gully was measured, which corresponded to the location of the flow path.

The treated and untreated TDR measurements were not significantly different, as both watersheds observed similar water content patterns. However, the treated cross sections had higher moisture contents, and less steep side walls than the untreated cross sections. In addition, stony layers were more common in the untreated watershed.

| cross-section nr | water content (%) | | |
|---|---|---|---|
| 1 | 18.3 | | 19.3 |
| | 22.5 | | 24.0 |
| | 25.0 | 32.4 | 35.0 |
| 2 | 12.9 | | 15.7 |
| | 2.3 | | 8.7 |
| | 20.4 | 16.8 | 23.1 |
| 3 | 20.4 | | 11.7 |
| | 25.9 | | 3.9 |
| | 22.5 | 26.7 | 17.7 |
| 4 | 17.1 | | 6.7 |
| | 20.8 | | 8.4 |
| | 25.3 | 24.7 | 18.0 |
| 5 | 24.7 | | 15.3 |
| | 15.6 | | 1.2 |
| | 19.3 | 14.1 | 4.3 |
| 6 | 20.3 | | 16.6 |
| | 4.3 | | 20.0 |
| | 25.8 | 15.8 | 24.5 |

| cross-section nr | water content (%) | | |
|---|---|---|---|
| 7 | 29.8 | | 27.5 |
| | 4.3 | | 23.6 |
| | 21.0 | 23.5 | 4.9 |
| 8 | 24.6 | | 16.9 |
| | 18.8 | | 7.9 |
| | 30.5 | 12.2 | 34.3 |
| 9 | 26.8 | | 25.7 |
| | 26.4 | | 4.0 |
| | 28.3 | 29.2 | 14.5 |
| 10 | 25.2 | | 19.1 |
| | 28.7 | | 25.5 |
| | 28.2 | 32.4 | 20.8 |
| 11 | 31.8 | | 20.1 |
| | 24.3 | | 3.3 |
| | 24.0 | 28.7 | 3.4 |
| 12 | 27.0 | | 20.5 |
| | 16.8 | | (-) |
| | 33.1 | 31.0 | 23.7 |

*Figure 34: The soil moisture content in the cross sections of the gully in the treated watershed as measured by the TDR. The increase of water content is indicated by a darker green intensity. The brown color indicates either impermeable wall or bad measurement.*

| cross-section nr | water content (%) | | |
|---|---|---|---|
| 1 | 19.8 | | 18.8 |
| | 28.7 | | 4.4 |
| | 31.2 | (-) | 22.3 |
| 2 | 21.6 | | 17.2 |
| | 25.3 | | (-) |
| | 28.0 | 21.4 | 27.0 |
| 3 | 20.4 | | 20.3 |
| | 26.2 | | 6.9 |
| | 16.5 | 17.6 | 12.4 |

| cross-section nr | water content (%) | | |
|---|---|---|---|
| 4 | 17.2 | | 13.8 |
| | 16.2 | | (-) |
| | 27.3 | 32.2 | 8.2 |
| 5 | 23.0 | | 17.5 |
| | 20.5 | | 6.8 |
| | 24.7 | 24.4 | 16.0 |
| 6 | 19.5 | | 17.8 |
| | 7.6 | | 7.8 |
| | 25.6 | 28.0 | 21.6 |

*Figure 35: The soil moisture content in the cross sections of the gully in the untreated watershed as measured by the TDR. The increase of water content is indicated by a darker green intensity. The brown color indicates either impermeable wall or bad measurement.*

## 4.3 Observation and measurements of erosion at the small scale

### 4.3.1 Observations of the Al-Majidyya gully erosion

One of the erosion types in the Al-Majidyya gully is scouring, which was observed on average at 20 cm above the base of the gully (figure 36). Consequently, the elevation of the water level was at least below 20 cm. Variation of this scouring height was observed in locations where the gully was smaller or wider. Higher scouring heights were observed in smaller gully sections, while wider gully sections observed lower scouring heights.

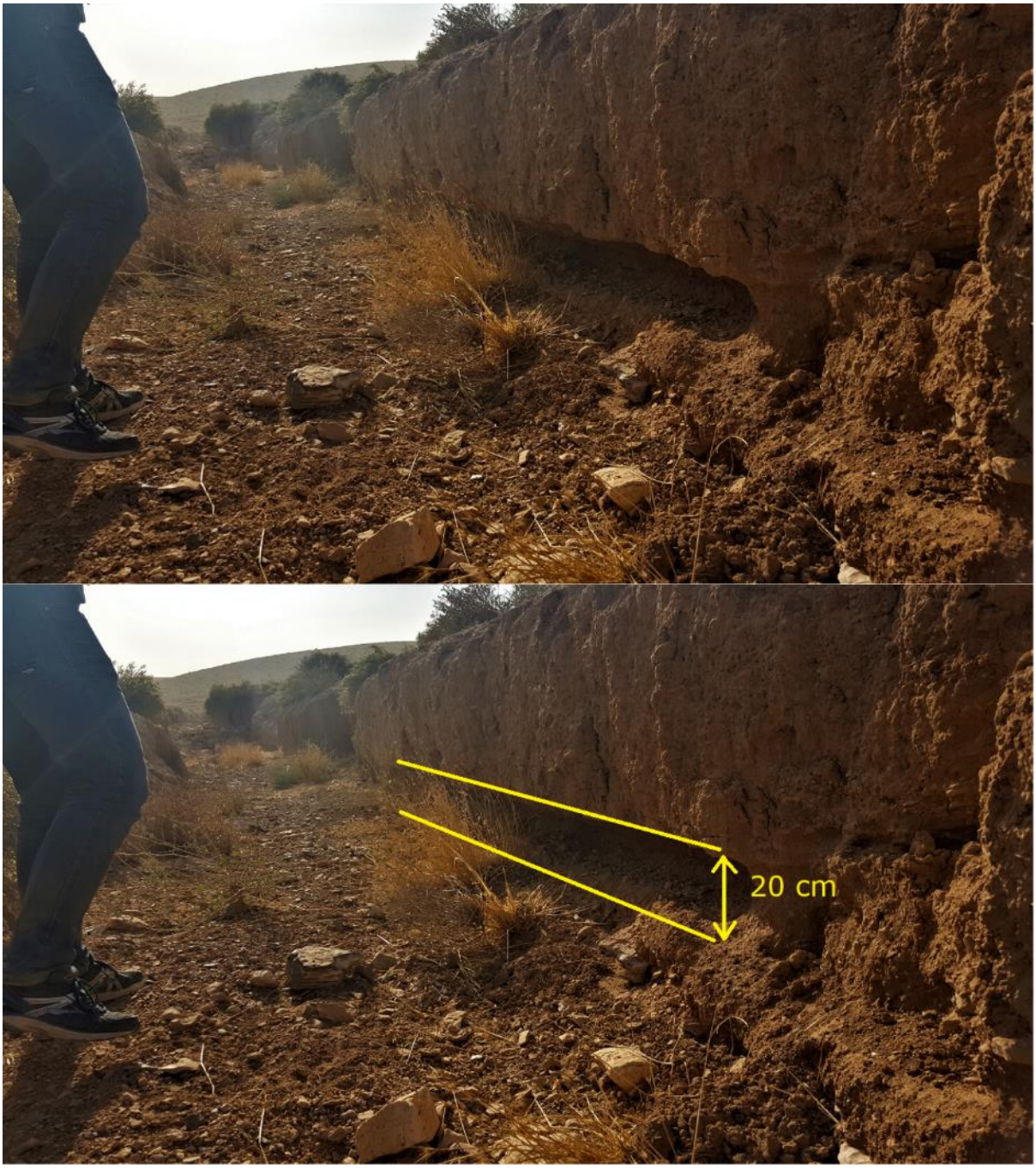


*Figure 36: Channel erosion scouring by water flow in the gully. Scouring in this gully system was on average up to 20 cm.*

The side bank can collapse under its own weight when scouring becomes more severe, which is first noticed by spliced earth (figure 37). The side wall cannot sustain the soil any longer and will eventually collapse. Severe scouring was more commonly observed at locations where tributaries merged, and in the bends of the gully where water is concentrated at the outside of the gully bend. This erosion process was widening the gully by channel erosion and did not influence the gully length.

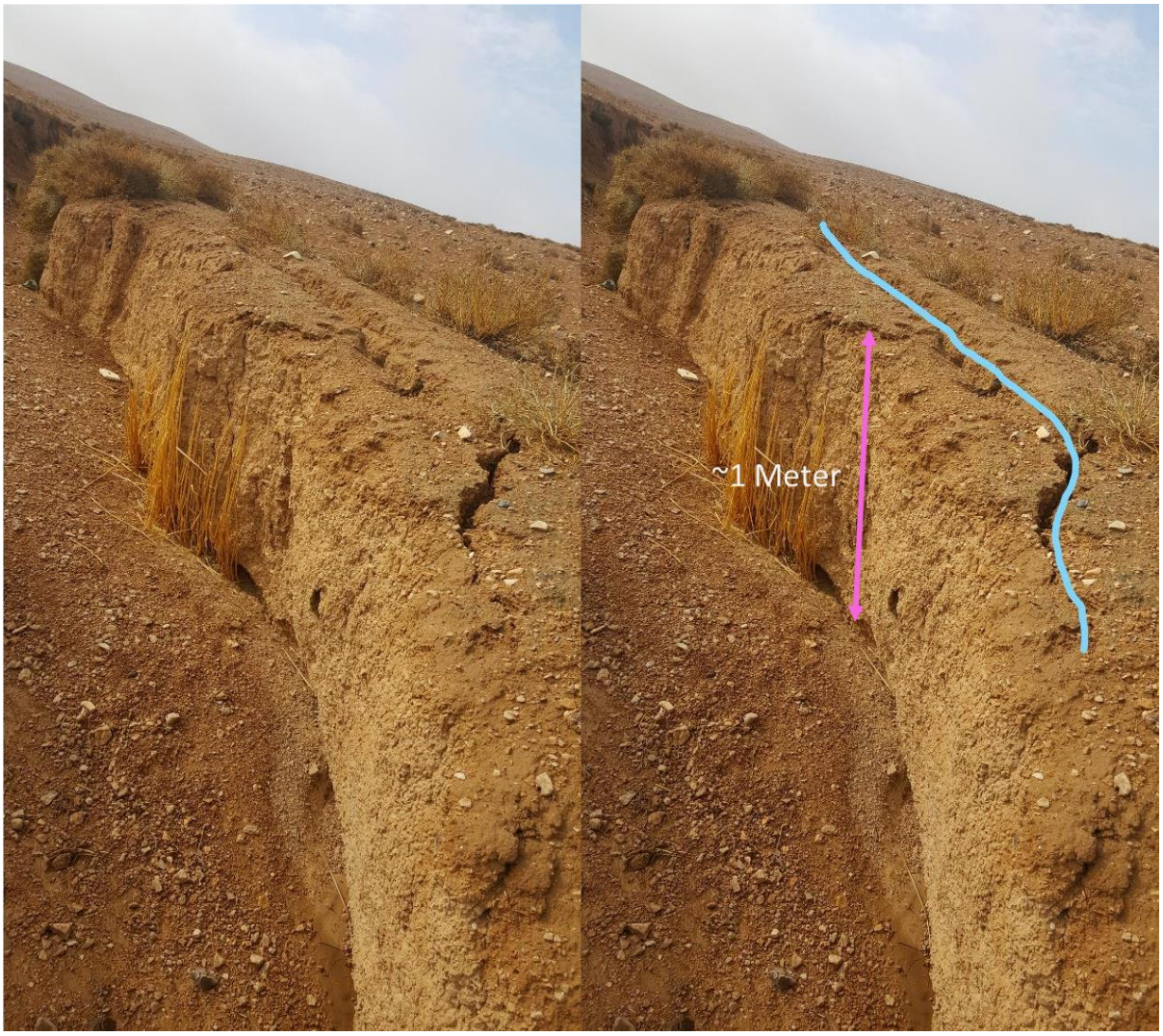


*Figure 37: Spliced earth as seen in the gully (blue line). The side bank can collapse after undermining by scouring.*

Funnel structures were observed in the gully's side bank, which were formed by small scale erosion processes (figure 38). The top of these structures had more erosion than the bottom, which resulted into plunge pools, as the falling water scours the basin deeper and wider. Plunge pools develop inside the channel side walls where water plunges into a small basin or pool (figure 38, 39).

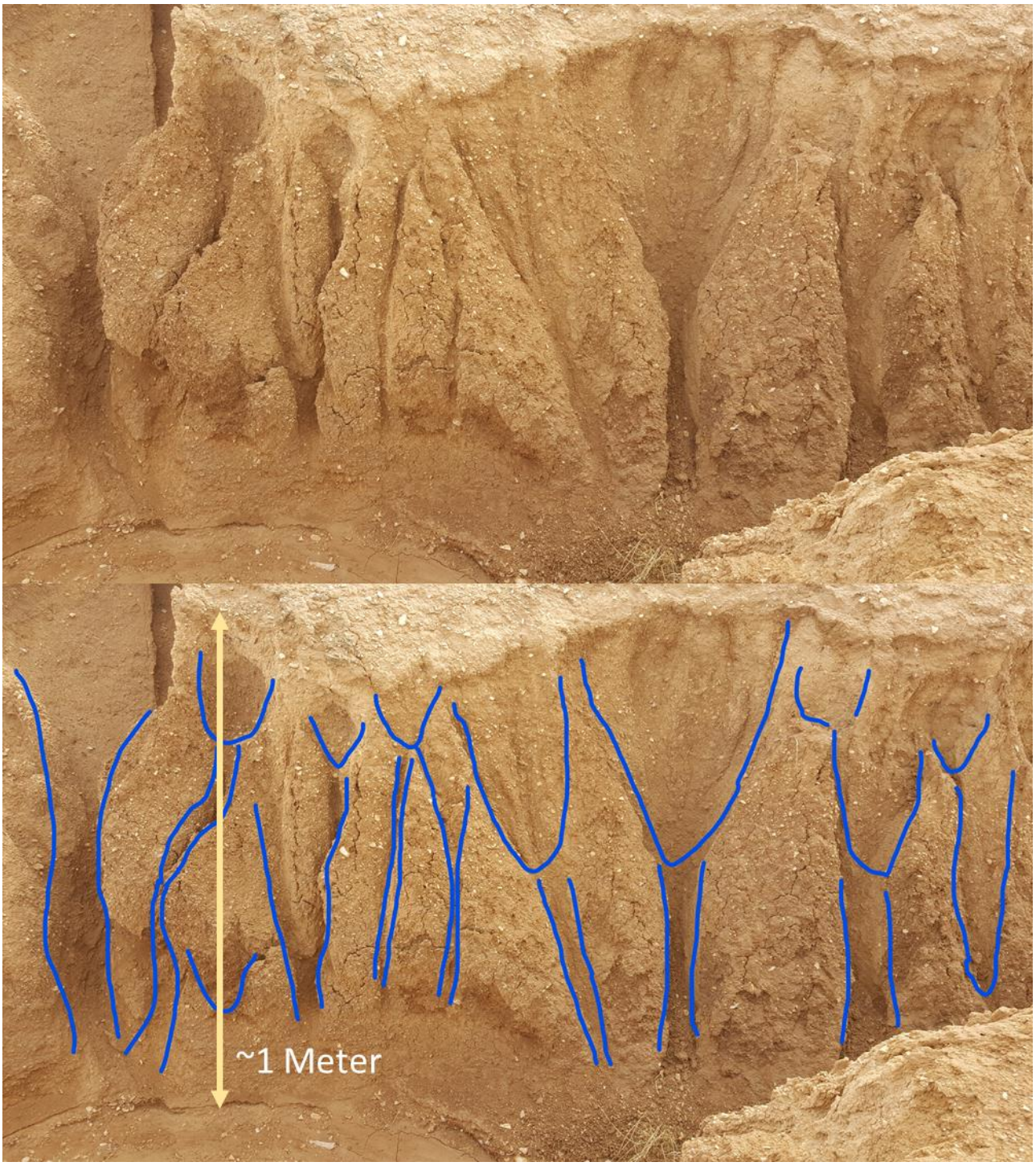


*Figure 38: Funnel structures and starting plunge pools at the side banks of the gully.*

Headward erosion was observed inside plunge pools, which were located at the end of rill erosion on the hillslope (figure 39). The direction of the headward erosion followed the path of the rill erosion. These headward erosion plunge pools have the potential to grow into tributaries, as formed tributaries have been observed following rills on the hillslopes draining into the gully.

*Figure 39: Headward erosion and undercutting in the side banks of the gully. Just right of the plunge pool an erosion rill is visible.*

The end of the rill and starting point of the gully or its tributaries is characterized by the combination of undercutting, headward erosion and spliced earth (figure 40). These are all formed by high energy water flow and high volumes, as all the surface runoff of the drainage catchments is collected here. Consequently, undercutting takes place at the boundary of the rill and gully. Concentrated water in the rill flows down into the gully and cuts below the head scarp, which collapses and progresses upslope. In addition, the runoff scours and led to gully's side banks collapse.

*Figure 40: The starting point of the gully and headward erosion as observed in the field. Undercutting takes place at the yellow line, the purple line depicts spliced earth.*

An incision inside a gully was observed at locations in the treated watershed (figure 41). These phenomena were observed inside the gully when water flow incises the old gully and creates a new smaller gully. The amount of vegetation growth is an indication of the time the incision started. In this case, the old gully has not been active for some time as vegetation grows directly on the sides of the new gully.

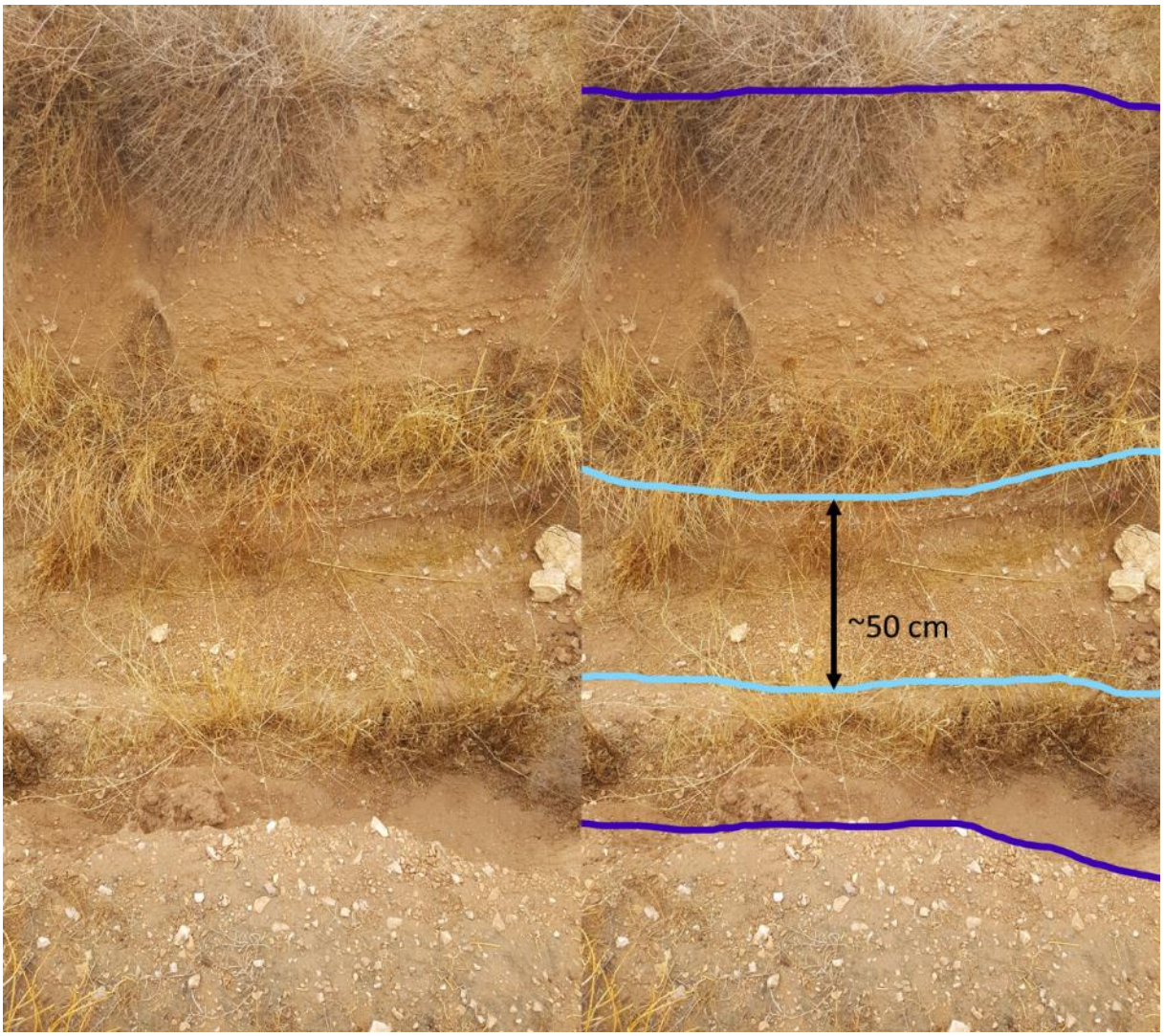


*Figure 41: Observation of a gully channel inside a gully channel in the treated watershed.*

The different types of gully erosion processes were indicated by color on the gully survey map before the rainfall events took place in the year 2019\2020 (figure 42). Several phenomena were recognized in this map: 1) plunging and scouring processes were often positioned opposite of each other, 2) pipe erosion was only seen in three places where animals dug tunnels, and 3) headward erosion was often seen at locations where erosion was more severe or at transitions between rill and gully erosion.

Parts of the gully in both catchments were missing at flat locations (figure 42). The water flow velocity and water volume at these locations were not sufficient to incise the soil. These phenomena were observed in areas where the slope was very gentle or flat.

The channel walls inside the untreated watershed were more severely eroded than the treated watershed (figure 42). More locations of headward erosion, spliced earth and wall breakage were observed in the untreated watershed, while the treated watershed observed more plunge pool and smaller scouring erosion. Various Vallerani RWH structures in the path of rill erosion were damaged as they could not withstand the surface runoff. These rills were already in the field when the Vallerani RWH structures were implemented.

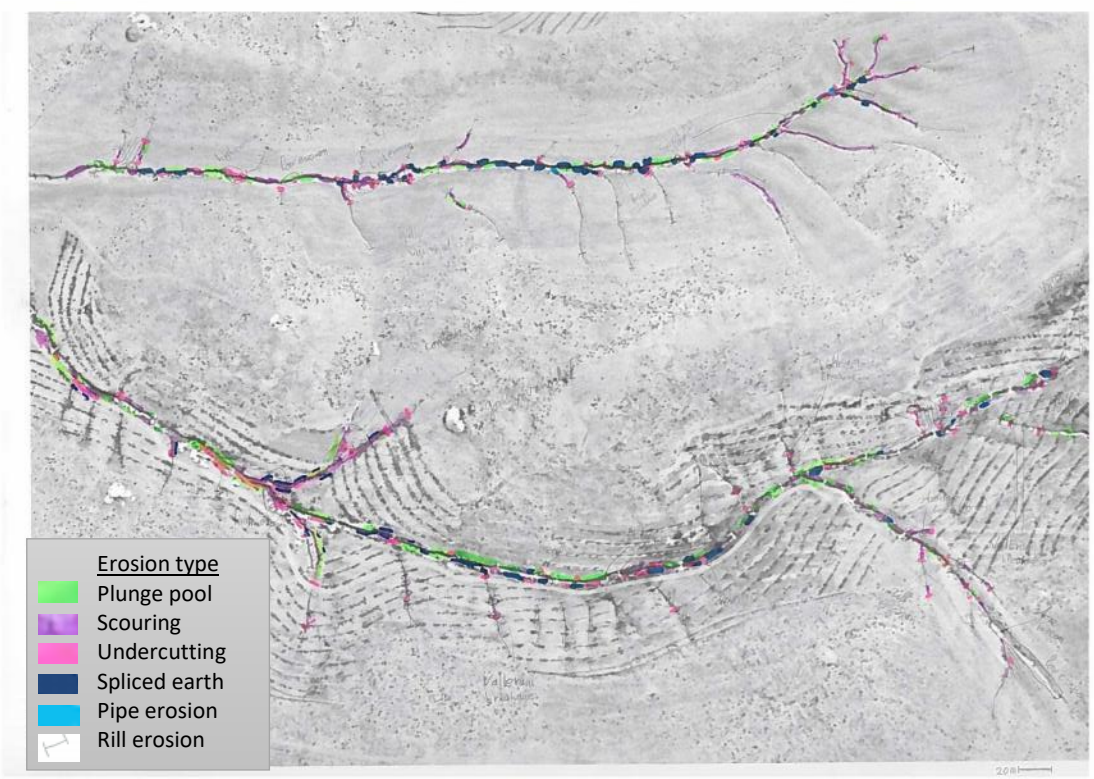


*Figure 42: Colored map of the treated and untreated watershed at the Al-Majidiyya fieldwork site. The colors indicate the erosional process observed in the field. Rill erosion and other observations were indicated by notation on the map (see appendix 2).*

### 4.3.2 Erosion phenomena by external influences

#### 4.3.2.1 Vegetation influences

Vegetation influenced the stability and erosion of the gully side banks (figure 43). The erosion observed around the vegetation was severe, but not strong enough to erode the vegetated soil as the side bank remained stable when the roots of the vegetation (Atriplex Halimus) increased the soil stability. In addition, the vegetation slowed down the flow of water with its stem and branches.

In contrast, the vegetation can converge water flow and increase the erosion towards the gully. The tributary curves around the vegetated soil while the upland of the tributary shows severe erosional processes of scouring, earth splicing and plunging (figure 43). Vegetation slows down the flow of water on the slope and concentrates the water in front of the vegetation. Normally, the flow would be equally distributed over the gully, but now the water concentrates around the vegetation. Erosional processes in the gully system are enhanced at these locations, as concentrated water flow increases plunging.

The formed tributary on the right of the vegetation captures most of the runoff in the area resulting in the stabilization of the left part (figure 43). The right tributary manages to capture more overland flow, because it has access to a wider area on the hillslope. Consequently, rapid growth can be observed. The plunging and undercutting processes show less activity on the left side as less of the overland flow reaches this side of the vegetation.

The amount of water for scour erosion increases downstream, as water captured by the tributary and water upstream merges inside the gully (figure 43). The gully side bank downstream of the tributary showed increased scouring. These effects last till the influence of the water from the tributary diminishes which varies for every tributary.

*Figure 43: Plunge pool and headward erosion next to vegetation. The vegetation stabilized the side wall, but enhanced erosion around the vegetation due to flow concentration on both sides.*

Roots of vegetation were observed to influence the stability of gully side walls. The root type of the vegetation did either stabilize or splice the channel walls. This depended on the root type of the vegetation. Fibrous roots will hold the soil in place, while a tap root (carrot formed) enhances splicing of the crust and soil, increasing the vulnerability of side banks to collapses.

A tap root has potential to bolster earth splicing by lowering the stability of the side bank as observed in the field (figure 44). The roots of vegetation can enhance earth splicing as tap roots of plants were often located at the crack inside the earth. When scouring takes place, the root spliced the soil fragmentarily in advance and the side bank is easily triggered to collapse.

Plant roots can increase the stability of the side wall during earth splicing as well, when soil was held by fibrous roots (figure 45). The side wall will not collapse even though the scouring at the bottom is more severe. The time of collapse is extended as the fibrous roots are strongly holding on to the soil.

*Figure 44: Earth splicing at the roots of vegetation.*

*Figure 45: Vegetation holding soil together while the side collapses.*

The stabilizing forces of the side bank vegetation are limited to the erosional forces of the water flow. Although vegetation stabilizes the soil, the side banks will collapse when this stabilizing threshold is exceeded. The side bank was less stable at the location of the flowpath inside the watershed (figure 46).

*Figure 46: Soil stability and vegetation. The side wall with vegetation has collapsed due to erosional forces exceeding the stability forces.*

#### *4.3.2.2 Land practice influence*

Contour plowing can evolve to rill erosion when plowed perpendicular to the main gully and parallel to the tributary (figure 47). The contour plowing inside the watershed was in down slope direction, which increased the scouring and concentrated the surface runoff. The rill can evolve into a tributary gully if left unattended. When the contour is located upslope from the tributary, it captures surface runoff that would normally flow into the tributary (figure 47). This results in an erosional shift, as the erosion inside the tributary decreases, while the erosion inside the plowed contour increases.

*Figure 47: Forming of rill erosion by contour plowing parallel to a gully tributary.*

New rills can evolve at the boundary of perpendicular contour plowing lines (figure 48). The surface runoff combines the water volume at this boundary and the additional water follows the contour line to the main gully. The contour line parallel to the tributary transports water downslopes and this accelerated the water velocity. In time, the erosional force and incision of the rill increases. Larger water volume and higher velocity enhanced the erosion at this location.

*Figure 48: Rill erosion at the boundary of perpendicular contour plowing lines. Blue lines represent contour plowing and the red line represents rill erosion.*

The gully plugs in the treated site collapse when the side bank fails by erosion (figure 49). Water flow is partly obstructed by the gully plugs and forms erosional eddies (small circular currents) in these locations, which scour the sides upstream of the gully plug and can result in extensive erosion. The water flow prefers a path around the plug as it requires less energy. The space of the preferential path is small and increases the velocity of the water flow and extensive erosion takes place.

*Figure 49: Failed gully plug located in the treated watershed. Increased erosion was seen on the right where the side bank collapsed.*

#### *4.3.2.3 Animal activity*

Animals were active in the side banks of the gully (figure 50). Small rodents dug tunnels that enhanced the susceptibility of the soil to erosion. The tunnels connected the gully with the surface in a distance of less than a meter. Surface runoff flows inside these tunnels and emerges in the gully. The slope inside these tunnels is steeper than the slope of the surface. Therefore, water flow became more energetic in these tunnels and erosion potential increased. The water erodes the tunnel which could collapse in time, which result in the initiation of a tributary gully. Such holes were observed at three locations in the site only (figure 42). Most tributaries were initiated by headward erosion and sufficient surface runoff.

*Figure 50: Animal perturbation as observed in the field.*

### 4.3.3 Cross-sections and headward erosion measurements

Small erosional growth was observed in cross sections of the gully in the treated watershed (figure 51). Measurements were taken before the rainfall events at the end of November 2019. Secondary measurements were taken after multiple rainfall events at the end of January 2020. Most erosion was observed in the lower part of the watershed, while the higher part observed less erosion. An exception was cross section 7, which was in a tributary with a steep slope in the high watershed. This cross section had increased erosion where the sidewall collapsed. This collapse took place before the measurements were taken, and the loose soil was partly eroded during the rainfall events. Most of the erosion inside the treated watershed took place at the channel walls, as the lowest point inside the gully remained similar (table 8).

The cross sections of the gully in the untreated watershed were observed to have less erosion than the treated watershed (figure 52). Sedimentation was observed in the lowest points of cross sections 1 and 4 while cross section 5 had erosion at the lowest point (table 8). Cross section 5 was located at the intersection of multiple gully tributaries which increased the runoff volume and erosion. The cross sections 5 and 6 observed deeper and smaller incisions compared to the upslope cross sections in the treated watershed.

*Table 8: Difference between the lowest point of the gully cross sections before and after rainfall events in the treated and untreated watersheds of Al-Majidyya. The difference indicates either erosion (negative) or deposition (positive) of sediment.*

| Cross section | 1 | 2 | 3 | 4 | 5 | 6 | 7 | 8 | 9 | 10 | 11 | 12 |
|---|---|---|---|---|---|---|---|---|---|---|---|---|
| Treated (cm) | 0 | 1 | -1 | 0 | 1 | 1 | 1 | 1 | 1 | -3 | 3 | -2 |
| Untreated (cm) | 8 | 1 | -1 | 11 | -7 | 2 | | | | | | |

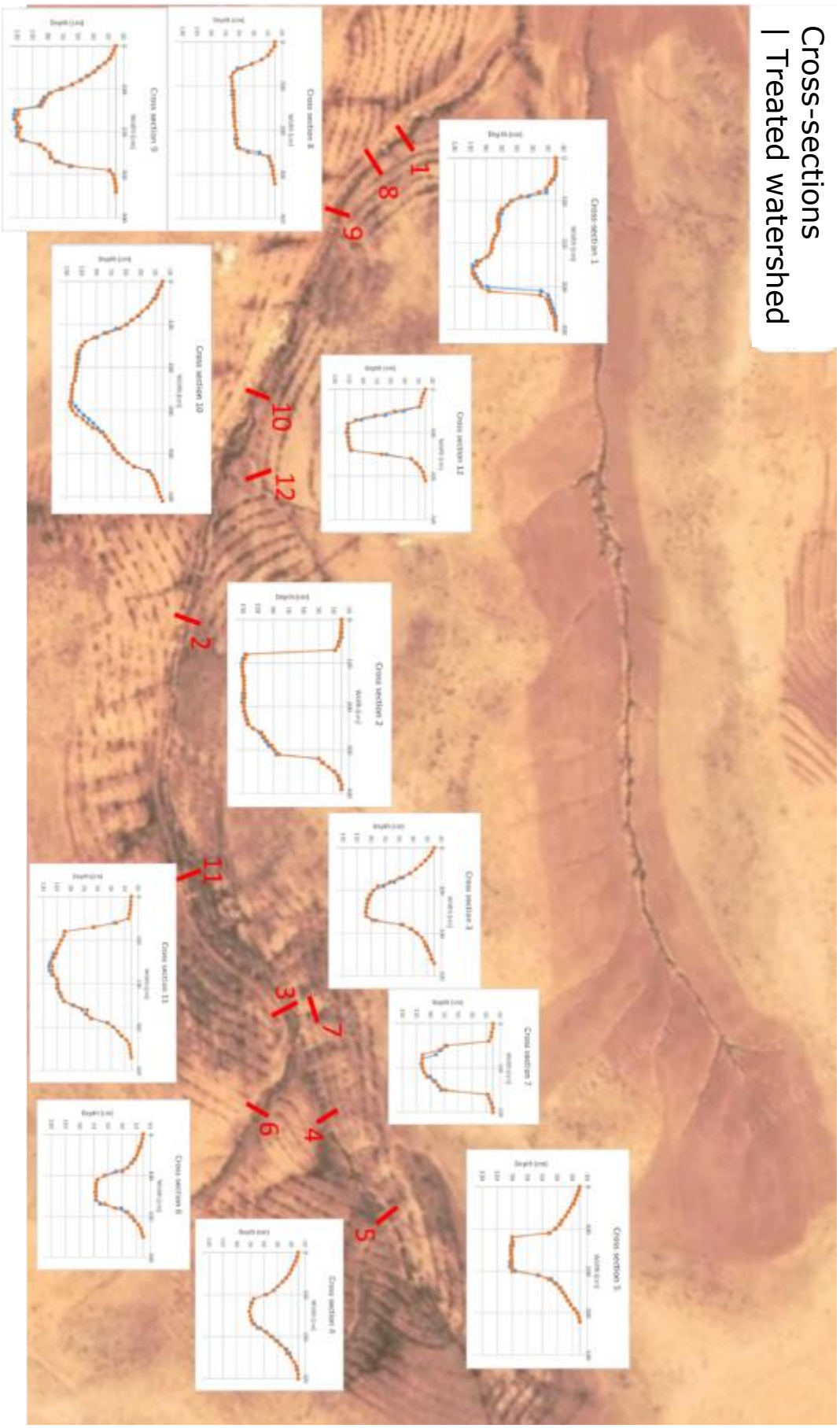


*Figure 51: Cross sections in the treated gully watershed (see appendix 3). Blue lines represent measurements before rainfall events, orange lines represent measurements after rainfall events.*

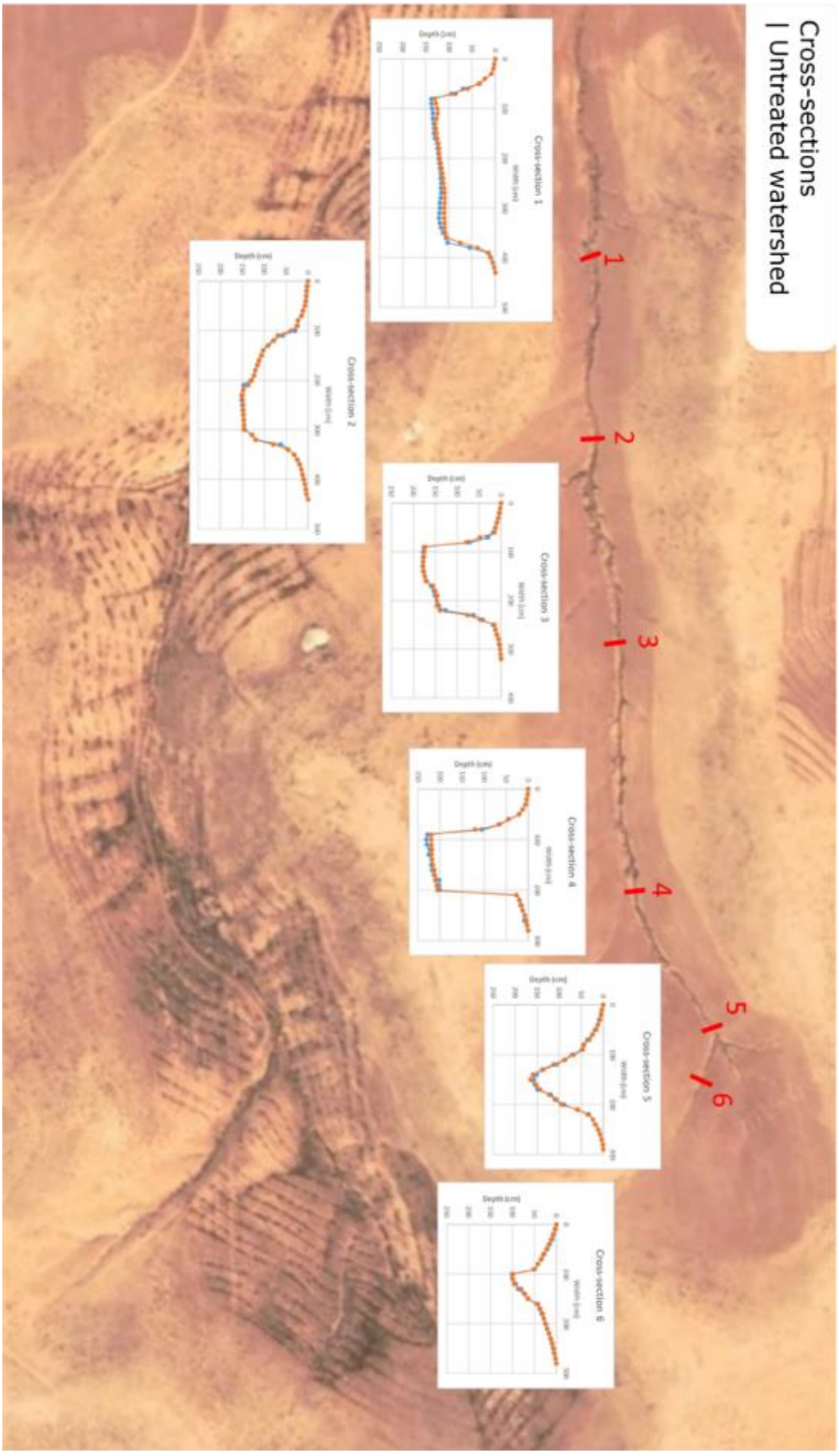


*Figure 52: Cross sections in the untreated watershed (see appendix 4). Blue lines represent measurements before rainfall events, orange lines represent measurements after rainfall events.*

The growth of headward erosion was measured in the treated site at three different locations before and after rainfall events (figure 53). Growth was observed at the sides in every gully head, while growth in headward direction was mostly detected in the profile of headward erosion 1 (~17 cm) (table 9). Large growth was measured in the left side of headward erosion 3 as well (~15 cm), which had a larger drainage area, the slope is steeper and Vallerani RWH structures were not implemented. In addition, Vallerani RWH structures at the right of the gully head hindered runoff flowing into the gully and showed no erosion. Almost no growth was observed in the measurement of headward erosion 2 (~3 cm).

The three headward erosion measurements in the untreated watershed had different growth directions (table 9, figure 54). Headward erosion 1 expands to the front left of the gully head (~20 cm). Part of the left side collapsed, as the surface runoff was collected from upslope. At the right of this measurement, another gully is located. Most of the surface runoff on the right was captured by this gully. Headward erosion 2 expanded in upslope direction (~12 cm). The gully head is located almost parallel to the major gully and is upslope connected to the end of a separate gully. Hence, headward erosion 2 is connected to a "missing" gully as water from this upslope gully flows directly into the gully head and receives water at the front, increasing headward erosion. The right side of the profile in headward erosion 3 experienced more erosion (~20 cm). Collected water from the hillslope flowed directly into the contour lining towards the gully head. This contour line follows a gentle slope and leads water towards the left of the gully head. Hence, the right of the gully head received more runoff than the left of the gully head similarly as in headward erosion 1.

The untreated watershed experienced more growth at the gully heads than the treated watershed (table 9, figure 53, 54). Areas with converged water flow, due to rills and vegetation, were observed to have more erosion than other areas. In addition, the profiles of the treated watershed show smaller growth than the profiles of the untreated watershed. The cross-sectional profiles of the untreated watershed (figure 52) had more sedimentation, while the treated watershed (figure 51) had more erosion during the 2019/2020 rainy season. Overall, growth changes inside the profiles were more visible in the untreated watershed than in the treated.

*Table 9: Headward growth in both watersheds of Al-Majidyya in three different directions.*

| | Treated | | | Untreated | | |
|---|---|---|---|---|---|---|
| Direction | HE1 | HE2 | HE3 | HE1 | HE2 | HE3 |
| Left | ~5 cm | ~3 cm | ~15 cm | ~20 cm | 0 cm | 0 cm |
| Upslope | ~17 cm | ~3 cm | ~3 cm | ~13 cm | ~12 cm | ~5 cm |
| Right | 0 cm | 0 cm | ~3 cm | 0 cm | ~4 cm | ~20 cm |

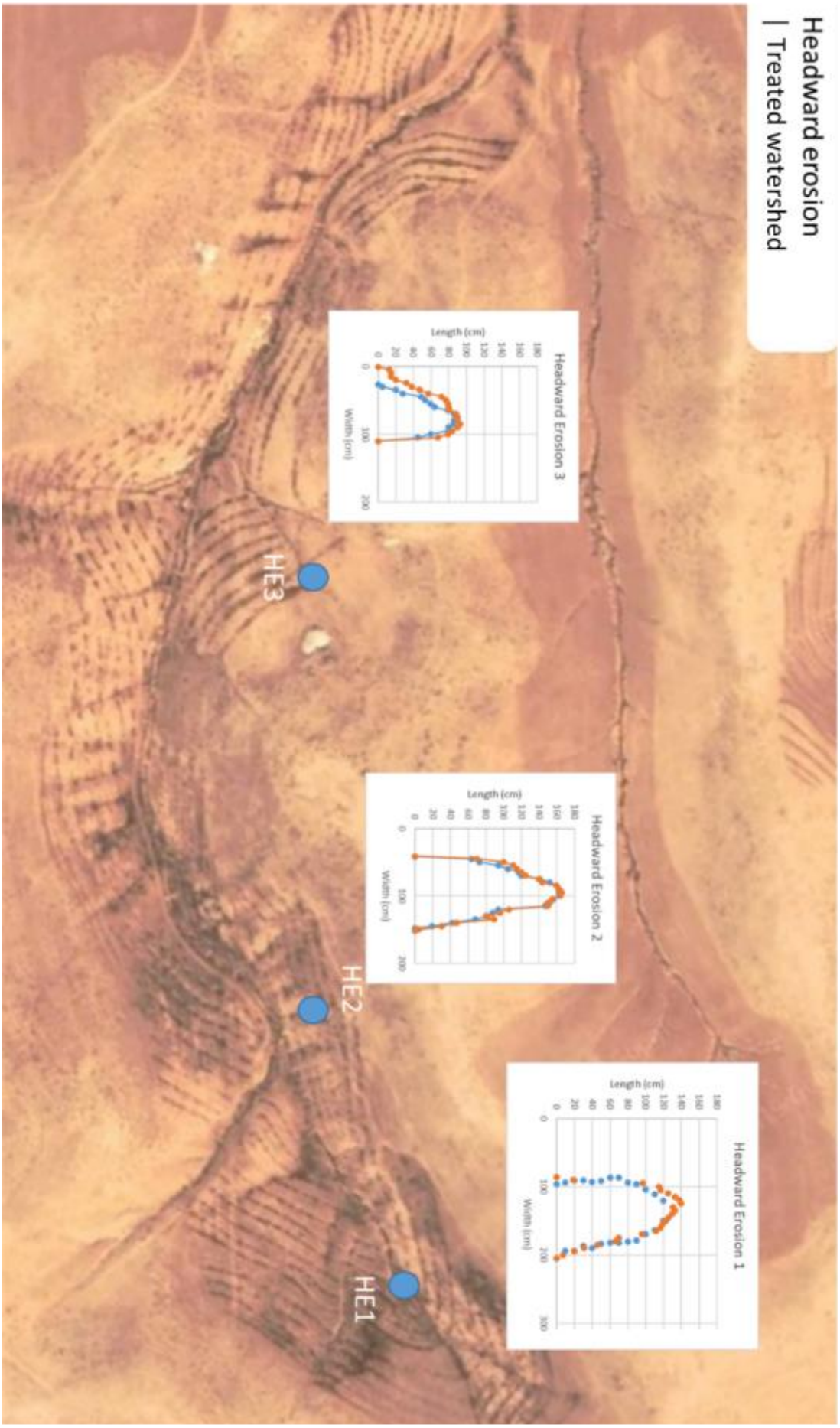


*Figure 53: Headward erosion in the treated watershed (see appendix 5). Blue lines represent measurements before rainfall events, orange lines represent measurements after rainfall events.*

*Figure 54: Headward erosion in the untreated watershed (see appendix 6). Blue lines represent measurements before rainfall events, orange lines represent measurements after rainfall events.*

# 5 Discussion

## 5.1 Activity of identified gullies inside the Wadi al Wala in the Jordan Badia

Google Earth Engine and Google Earth Pro provided much information on the gully activity in the Wadi al Wala catchment. However, the landscape variable maps, and time lapse imagery provided only coarse observations of the watersheds and lack visibility for small scale changes. The resolution was acceptable for the extensive growth of the gullies (larger than a meter) but was insufficient for the small scale observations. The best available resolution was used in this large scale study and resolution will improve over time as imagery becomes less coarse. The gully growth determination will improve in future studies, as it will become easier to study small scale growth with higher resolution.

The landscape variables inside the subdivisions of the Wadi al Wala catchment had influence on the density and growth of the gullies. The studies of Zhao et al. (2016) and Guyassa et al. (2018) found that gully density was dominated by topographic factors and vegetation cover and not by human actions. This study was not able to test the influence of vegetation cover in the Wadi al Wala since the area has very little vegetation cover. Topographic and human factors could be correlated to gully density changes, as these were different between regions. The gully density was less in the high plateau compared to the hills inside the lower catchment. The high plateau is mostly flat, which decreased water velocity, and could not easily erode compared to the area of the hills (Moore et al., 1988; Morgan, 2005). The gully density was in addition low in the flat area of the middle catchment, which had $<10^{\circ}$ slopes. This area had more constructions (e.g. agriculture, towns) which need gully removing or instead initiated gullies. Likewise, the high catchment had a large gully density, the least constructions and consisted mostly of 10-15$^{\circ}$ slopes. The construction density in the area relates more to the gully density than vice-versa, as constructions are easier to build in areas with less gully density. Space was created for constructions by removing gullies, when the flat area became too full to fit new constructions.

The low and middle catchment have the most gully growth compared to the higher catchment. This agrees with the study of Shahrivar and Christopher (2012) who determined that silty clay soils in Iran resulted in more gully growth than other soil textures. In addition, the areas inside the lower and middle catchment have more precipitation, which result in larger soil detachment and transport, due to higher runoff volumes and faster discharge (Moore et al., 1988; Morgan, 2005; Poesen et al., 2003).

The large scale study determined that gully growth rates largely depend on individual rainfall events, as gully growth does not increase in a constant rate per year. This observation was made in several other studies as well (Capra et al., 2009; Morgan, 2005; Poesen et al., 2003; Valentin et al., 2005). The length of the gully increased abrupt by several meters between consecutive time lapse imagery, while in other imagery over longer time periods no change was detected. This increase was observed when rainfall events appeared more often, and the magnitude of rainfall events were larger throughout the season. The results of the water volume in every gully head of Al-Majidyya determined that most of the surface runoff in the year is only generated in one or two rainfall events. The erosion inside the gully became stronger, when larger events were seen more often in a season. This was observed in both the lower and middle catchment of the Wadi al Wala.

The gullies inside the middle catchment show only small growth rates (<1 m), except for the sudden increase of 5 meter between 2017 and 2019. The landscape variables in this area are similar to the other regions except for the slopes (0-15$^{\circ}$), which are less steep than in the other regions. This difference alone would not explain the increase of the identified gully, as the growth rate is not constant over years and the slopes remained the same. The large increase in gully growth coincides with construction in the area and an increase of rainfall events. This combination could have resulted in increased erosion as this observation was done in the study of Nyssen (2001) as well. This study took place in the Ethiopian Highlands, where a gully grew after construction activities in the study area.

The magnitude of human actions is difficult to measure, as constructions have varying influence and can either increase or decrease the erosion inside the area.

No sudden increase of gully length was identified in the imagery of the gullies inside the high catchment. The differences of this region compared to others, is that this region has gentle slopes (<10°), less yearly precipitation (<200 mm/y) and the land use is dessert/barren. The Al-Majidyya watersheds inside the high catchment appeared to be inactive, as no severe erosion took place in either RWH treated or untreated site. Several large events were found over eleven years, which did not lead to severe erosion inside the watersheds. The largest event of 28 February 2019 has a reoccurrence period of 25 years. Even this rainfall event was not enough to lead to severe erosion as seen in the GEP imagery. Monitoring this catchment on a smaller scale determined that gully growth took place, but compared to the rest of the Wadi al Wala, only in small amounts (< 1m).

The importance of the five landscape variables on gully growth in the Wadi al Wala can be graded by most to least influence in this study. The most influence is amount of rainfall, as generated surface runoff is needed to detach and transport soil (Moore et al, 1988; Morgan, 2005). Second is the slope inside the watersheds, as this influences water velocity the most. The water flow becomes more energetic on a steep slope, which leads to larger transport and detachment (Morgan, 2005). Third is the soil texture, which influences the soil stability directly as textures have varying susceptibility to erosion (Shahrivvar and Christopher, 2012). Fourth and fifth are the land use and vegetation, which influence both soil stability and water velocity, by changing the infiltration, obstructing the flow path and influence soil detachment (Morgan, 2005; Nyssen, 2001; Shahrivvar and Christopher, 2012). However, these landscape variables were less common in the desert of the Jordan Badia and are therefore less influential than the other variables.

## 5.2 Gully and hillslope hydrology in the Al-Majidyya watersheds

The critical slope and drainage area (CSADA) correlation helped to understand the processes of growth, as it determines the slope threshold value for the initiation and growth of gullies (Begin and Schumm, 1979; Moore et al., 1988). The CSADA results determined the variable b to be larger than 0.2, which is associated as surface flow dependent by several studies (Begin and Schumm, 1979; Moore et al., 1988; Poesen et al., 2003). However, the amount of measurement points was limited for these watersheds, and the CSADA correlation for Al-Majidyya could be reflected better with more input. In addition, the treated and untreated watershed were not different before 2017, as the Vallerani RWH structures were not yet implemented. Hence, all measurements together have a good fit for one relationship in the area. A longer time period is needed to determine changes in CSADA between the watersheds.

Measurements below the threshold line of the CSADA correlation do not grow as either the slope is not steep enough for erosion by water flow, or the drainage area is not large enough to generate enough surface runoff for water erosion (Begin and Schumm, 1979; Poesen et al., 2003). However, it is possible for gullies to grow and exceed beyond the CSADA correlation due to rill erosion, which gathers surface runoff and concentrates the discharge. This increases the flow forces for detachment and transportation of the soil particles on the hillslope (Morgan, 2005).

The width and depth of the gully channel cross section can be linked to the drainage area and slope of the gully channel. The width of the gully channel is determined by the volume of surface runoff generated on the drainage area (Di Stefano et al., 2013). The cross-section becomes wider when larger volumes of discharge flow through the channel. Hence, the widest gully channel was found at the end of the watershed. Tributaries connected to a larger drainage area had a wider channel. Cross section depth can be linked to slope and water velocity but likewise by water volume (Di Stefano et al., 2013). The depth of the cross sections was the deepest in the middle of the watershed, where the slope is still steep enough to incise the bottom and volume is large enough for transport. The slope was less steep at the end of the watershed and the gully became wide but shallow. In contrast, the slope was steepest in the higher watershed, but the water volume could not incise to the depth of the middle watershed.

The three largest rainfall events of the last 10 year did not result in severe erosion, and the gully remained mostly inactive after these large rainfall events. The largest rainfall event took place on the 28th of February 2019 and consisted of 35.75 mm of rainfall, which corresponds to a return period of 25 years. The generated peak discharges of this event were determined 26.6 and 352.3 $m^3/h$ between the gully heads, which correspond to a reoccurrence time of 5 years. The other two rainfall events on 20th of November 2013 (28.8 mm) and 5th of January 2018 (29.2 mm) have a reoccurrence time of 5-10 years and a discharge approximated by boxplots in between 10 and 1000 $m^3/h$, which correspond to a reoccurrence time of 5-25 years. This difference in reoccurrence time is possible, as the time of rainfall can variate for each event. The generated surface runoff is larger when the rainfall amount falls in less time (Morgan, 2005). Hence, rainfall with short reoccurrence time can have runoff with long reoccurrence time when the rain falls in a short period.

Common rainfall events that occur in the Al-Majidyya watersheds, result in discharge events that are only energetic enough for small scale erosion (1-2 cm). The peak discharge in the gully heads of the more common rainfall events ranged from 1.4 to 98.8 ($m^3/h$), which was at times lacking to flow out of the RWH treated watershed. However, erosion took place as changes were observed in the cross-section measurements. Peak discharge was not determined as the Cipoletti weirs couldn't measure this discharge.

The water content patterns determined by Hydrus2D did not show an increase in soil moisture towards the channel walls after rainfall events. Hence, the channel walls are not susceptible to collapse by oversaturation. The first evaporation took place inside the channel walls, as the water content showed a rapid decrease in consecutive days. This observation was made by the TDR as well, as most of the water content was hold at the bottom or at the shadow side of the gully's cross section, where sun heating had less influence on evaporation.

## 5.3 Observations of erosion inside the watersheds of Al-Majidyya

The erosion inside the Al-Majidyya gullies either originated from water flow inside the gully channel or surface runoff on the hillslope. Subsurface flow was not observed inside the field except for water flow through tunnels dug by rodents at three locations. The water flow inside the channel led to channel erosion by scouring, which will eventually result in channel wall collapse and widening of the gully (Kirkby and Bracken, 2009; Mishra, 2013). The surface runoff on the hillslope flowing into the gully led to funnels, plunge pool erosion and eventually headward erosion. Funnels and plunge pools were processes widening the gully, while headward erosion resulted in an increase of length.

The incised gully phenomena originated from smaller water volume inside the channel, which could be caused by two factors. The first factor is a decrease in generated surface runoff. When rainfall events generate less runoff, the smaller discharge can result in a new incision inside the old gully. The water flow was not able to erode the whole gully channel, but only a small lower part. The second factor is the implementation of the Vallerani RWH structures in the treated site since 2017. These RWH structures captured surface runoff and decreased the discharge inside the gully. Consequently, less water was available to erode the whole gully, and the smaller amount of discharge resulted in the creation of a secondary gully inside the old gully.

The survey of the Al-Majidyya watersheds led to recurring patterns of erosion types. Plunge pools and scouring were often found opposite of each other. When water flows down the hillslope into the gully and creates plunge pools, it will flow towards the other side of the gully channel and merges with the channel flow. The turbulent water flow increases local instability, resulting in increased detachment and transport capacity of the water (Kirkby and Bracken, 2009; Morgan, 2005). Another observation was that most locations of headward erosion are connected to rill erosion on the hillslope. The surface runoff on the hillslope is first collected by the rill erosion before reaching the tributary head scarp. The larger volume of water undercuts the head scarp and advances upwards to the hillslope (Kirkby and Bracken, 2009; Morgan, 2005). Consequently, other plunge pools do not advance as surface runoff was not concentrated by the rill, and the force of water was not

enough for erosion. The gully remained stable as the soil stability threshold was not reached.

Although the vegetation was scarce inside the watersheds, it had a lot of influence on erosion. Vegetation increased the soil stability at the location of the plant, while at the same time, vegetation increased the erosion around the plant. Stability was expected, as vegetation acts as an obstacle to the water flow and decreases its velocity (Morgan, 2005). In addition, roots stabilize the soil, which decreases the potential for erosion (Karrou et al., 2011; Valentin et al, 2005). However, the increased erosion was not expected, but can be explained by redirection and converging of the water flow around the plant. As water flows down the slope, it is distributed over the whole hillslope. When vegetation redirects the water flow, this water volume is added to the volume flowing down next to the plant. This increased water volume is capable of incising and forming rill erosion, as detachment and transport of soil increase linearly with discharge (Kirkby and Bracken, 2009).

The erosion by land practice influence was seen in multiple locations. Contour plowing parallel to tributaries resulted often in further incision and rill erosion. The larger concentrated discharge increased detachment and transportation of soil on the hillslope (Kirkby and Bracken, 2009; Morgan, 2005). On the large scale, human actions created and removed gully tributaries after agricultural practice (e.g. tillage), as seen in this study and others (Nyssen, 2001; Valentin et al., 2005). Practices inside the gully, such as gully plugs, acted as an obstacle to the normal flow of water, which lead to strong erosion of the channel walls and gully bottom.

The cross sections of the gully in the treated watershed were observed to have more erosion in the channel walls than the cross sections of the gully in the untreated watershed, while the untreated watershed had more sedimentation. This can be explained by the RWH structures in the field. The Vallerani RWH structures slowed down the water flow and decreased the detachment and transport capacity of the surface runoff on the hillslope in the treated watershed (Vallerani, 2013). In addition, large volumes of water and detached soil were captured by the Vallerani RWH structures and did not reach the gully channel. Consequently, the surface runoff that reached the channel was less and had low soil content. Surface runoff with low soil content is more capable to transport, and erode the gully of the lower catchment when discharge is large enough (Kirkby and Bracken, 2009; Morgan, 2005). The surface runoff in the untreated watershed detached soil on the hillslope and transported it to the gully channel. This soil settled inside the channel and resulted in sedimentation on the gully bottom.

Headward erosional growth was larger in the untreated watershed than in the treated watershed. The Vallerani RWH structures caused a large decrease in surface runoff on the slopes of the treated watershed as the monitored gully heads received less of the total surface runoff. The headward erosion profiles and measurements showed that erosion was stronger at a side without obstacles and the direction in which most surface runoff entered the gully head. Diversion by obstructions on the hillslope (e.g. vegetation, Vallerani, stones) or other tributaries influenced the speed and direction of headward erosional growth. In addition, the erosional growth speed depended on the steepness of the slope, and the size of the drainage area in which surface runoff entered the gully head. These factors influenced the water velocity and water volume of the surface runoff (Moore et al., 1988; Morgan, 2005; Poesen et al., 2003). The erosional growth is stronger on the side of the gully head with higher velocity and larger water volume.

The climate in the Jordan Badia is becoming drier and rainfall events become more extreme (Dregne, 2002; Karou et al., 2011). This will have effect on the gully erosion as most surface runoff was generated in individual strong rainfall events. Hence, the maximum capture capacity by Vallerani RWH and the maximum infiltration rate of the soil are reached earlier when extreme rainfall events become more common. An increase of these events would result in an increase of runoff volumes per event, which can exceed the runoff threshold value and initiate gullying.

# Conclusion

The different gully densities inside the three regions of the Wadi al Wala showed that topographic factors had the most influence on gully density. Areas with gentle slopes were less dense than areas with steep slopes. Lower gully density was not a result of construction but a cause, as high gully density challenges the building of constructions. Hence, flat areas were preferred for constructions and space limitation led to removal of gullies. Human action initiated gullies when constructions changes the hillslope hydrology, increasing discharge at water concentrated locations. However, this was at a small scale and did not made a huge impact on density. Other studies connect vegetation cover to gully density. This could not be tested in the Wadi al Wala, as Enhanced Vegetation Index (EVI) values were similar and the area was barren.

Gully growth depended on individual rainfall events, as the gullies did not grow in a constant rate each year. The water volume measurements by RHEM showed that most of the surface runoff volume was generated in only one or two rainfall events. The time lapse imagery showed that severe gully growth took place when precipitation was larger in magnitude and occurred more often in a season.

The five landscape variables were graded in this study by influence on gully growth inside the Wadi al Wala catchment. First is precipitation amount, as it determines surface runoff volume. Second is the slope, as it determines the flow velocity. Third is the soil texture, as this determines soil stability and infiltration. Fourth and fifth are land use and vegetation as both influence soil stability, water velocity and infiltration. The influence of the last two were small as they were less common inside the Jordan Badia.

The speed of growth was different inside the Wadi al Wala catchment. The lower catchment had an average growth of 6.1%, the middle catchment 4.1% and the high catchment 1.1% in 15 years. The growth did not have a constant rate over the years as observed by the time lapse imagery. An increase of 10 meter was observed in one of the gullies inside an agricultural field of the high catchment between 2015 and 2019. The middle catchment observed a 5 meter increase between 2017 and 2019. More common growth rates detected were below a meter during this time. This enhanced increase was observed during constructions and an increase of rainfall events. The high catchment had no severe erosion in a time lapse of eleven years. The headward erosion measurements of the small scale in Al-Majidyya showed that growth took place at small rates during the 2019-2020 season (<15 cm).

The Vallerani RWH technique influenced water flow inside the watersheds after implementation, while the technique did not influence other factors yet. At the large scale, the two watersheds had similar growth rates during the time lapse of 15 years. Changes were not observed yet as the Vallerani RWH structures were implemented since 2017, which seemed not long enough for affecting gully growth. The critical slope and drainage (CSADA) correlation has not changed and a longer time period is needed before possible changes can be determined. However, changes in discharge and erosion have been observed from 2017 onwards. Peak discharges inside the gullies were at times not large enough to flow out of the treated watershed, while peak discharges were observed in the untreated watershed. Vallerani RWH structures captured the runoff and decreased the outflow in the treated watershed. The gully heads observed centimeters less erosion in the treated watershed compared to the untreated watershed. The smaller discharges have resulted in the observed incision inside the gully, as less discharge was available for erosion of the whole gully. In addition, the Vallerani RWH structures influenced the side of which headward erosion took place, as the structures captured and diverted water flow towards the head scarp. The gully channel wall without the structures was stronger eroded than the side with the structures.

The cross sections of the gully in the treated watershed were observed to have more erosion in the channel walls than the cross sections of the gully in the untreated watershed, while the untreated watershed had more sedimentation. The Vallerani RWH structures slowed down water flow and decreased the detachment and transportation capacity of surface runoff. Detached soil was captured, which led to smaller sedimentation inside the

gully of the treated watershed. The low content of soil inside the discharge resulted in less sedimentation and more channel wall erosion of the gully. The surface runoff of the untreated watershed is not captured by Vallerani RWH structures and transports soil from the hillslope to the gully. This resulted in the sedimentation of the untreated gully.

Initiation and growth of gullies was largely influenced by the hillslope hydrology in Al-Majidyya. The survey and the CSADA correlation determined that the watersheds were surface flow related, as subsurface flow was not observed inside the field. Gully initiation depended mostly on the CSADA correlation. Conditions below this threshold did not result in gullies as either the slope was not steep enough for erosion, or the drainage area did not generate enough surface runoff. Rill erosion could result in erosion above the CSADA threshold, as the converged surface runoff increases the discharge of the flow. Therefore, headward erosion was often preceded by rill erosion. The width and depth of the gully channel could in addition be linked to drainage area and slope. Channels were wider when larger volumes of surface runoff were discharged, and channels were deeper when slopes were steeper. The depth was also connected to runoff volume, as channels in the higher catchment were less deep than channels in the middle catchment.

The surface runoff on the hillslope was often diverted by obstacles, which changed the direction and degree of growth in gully heads. An example of an obstacle is vegetation, as plants decreases water velocity directly and decreases erosion. Simultaneously, plants divert water flow, which increases erosion around the plant. In addition, plant roots can either delay or speed up erosion, as tap roots increase splicing, while fibrous roots stabilize the soil. Parallel tributaries or contour plowing can in addition influence growth, as surface runoff is divided over several gully and rill branches and redirect them on the hillslope. The headward erosion measurements show that the side without obstacles on the hillslope was more eroded than the side with obstacles.

Erosion inside the gullies either originated from water flow inside the channel or surface runoff on the hillslope. Water flow inside the channel resulted in scouring of the channel walls, which will eventually break, as the weight exceeds the soil stability in time. Surface runoff flowing into the gully resulted in funnels, plunge pools and headward erosion. The water flows down towards the opposite side of the channel, merges with the channel flow, and creates turbulent flow, which enhances scouring. Consequently, plunge pools and scouring are often observed on the opposite side of the channel. Scouring, funnels and plunge pool erosion widens the gully channel, while headward erosion increases length.

The gullies inside the Al-Majidyya watershed only had small scale erosion and the gully remained mostly inactive. The three largest rainfall events of the last 10 years did not result in severe erosion. Even the largest event, with a rainfall reoccurrence time of 25 years and a peak discharge reoccurrence time of 5 years, did not result in severe erosion, as observed in the middle and lower Wadi al Wala. Most of the rainfall in a year falls in one or two events, while the common events increase the gully 1-2 cm. In addition, the channel walls were not susceptible to collapse by oversaturation after the rainfall events. Hydrus 2D and the handheld TDR measurements found that soil moisture evaporated in the channel walls and did not increase by standing water.

Concluding, gullies were initiated and growing when the discharge forces exceeded the soil stability threshold. This was observed with the CSADA correlation and the changing water velocity by obstacles on the hillslope (Vallerani RWH structures, vegetation, rocks, etc.). Human landscape changes have potential to initiate gullies by increasing the water shear force due to discharge increasing practices (i.e. contour plowing). The growth speed is mostly influenced by precipitation amount, slopes and soil texture type.

Erosion is likely to become more severe in the future, as rainfall events become more extreme due to climate change. The maximum capture capacity by Vallerani RWH and the maximum infiltration rate of the soil are reached earlier when extreme rainfall events become more common. An increase of these events would result in an increase of runoff volume per event, which can exceed the runoff threshold value and initiate gullying.

# References


Begin, Z.B. and Schumm, S.A. (1979). Instability of alluvial valley floors: a method for its assessment. Transactions of the American Society of Agricultural Engineers 22: pp 347–354.

Capra, A., Porto, P., and Scicolone, B. (2009). Relationships between rainfall characteristics and ephemeral gully erosion in a cultivated catchment in Sicily (Italy). Soil and Tillage Research, 105(1), pp 77-87.

Castillo, C. and Gómez, J. A. (2016). A century of gully erosion research: Urgency, complexity and study approaches. Earth-Science Reviews, 160, pp 300-319.

Conacher, A. J., and Sala, M. (1998). Land degradation in Mediterranean environments of the world: nature and extent, causes and solutions. John Wiley and Sons Ltd.

Dis4Me. (2004). Desertification indicator system for Mediterranean Europe. (accessed 26 October 2019). https://esdac.jrc.ec.europa.eu/public_path/shared_folder/projects/DIS4ME/issues/issue_degradation.htm

Di Stefano, C., Ferro, V., Pampalone, V., and Sanzone, F. (2013). Field investigation of rill and ephemeral gully erosion in the Sparacia experimental area, South Italy. Catena, 101, pp 226-234.

Dodge, R. (2001). Water measurement manual: A guide to effective water measurement practices for better water management. Government Printing Office.

Dregne, H. E. (2002). Land degradation in the drylands. Arid land research and management, 16(2), pp. 99-132.

Dunne, T. (1990). Hydrology, mechanics, and geomorphic implications of erosion by subsurface flow. In Groundwater Geomorphology: The Role of Subsurface Water in Earth-Surface Processes and Landforms (Vol. 252, pp. 1-28).

Gui, M. W., and Wu, Y. M. (2014). Failure of soil under water infiltration condition. Engineering geology, 181, pp 124-141.

Guyassa, E., Frankl, A., Zenebe, A., Poesen, J., and Nyssen, J. (2018). Gully and soil and water conservation structure densities in semi-arid northern Ethiopia over the last 80 years. Earth Surface Processes and Landforms, 43(9), pp 1848-1859.

Haddad, M. (2019). Exploring Jordan's rangeland transition: merging restoration experiment with modeling – a case study from Al Majidiyya village. Thesis, university of Jordan. Amman. Pp. 134

Hashemite fund. (2019). Jordan Badia. The Hashemite fund for development of Jordan Badia, http://www.badiafund.gov.jo/en/node/310 (accessed 9 September 2019).

Hernandez, M., Nearing, M. A., Al-Hamdan, O. Z., Pierson, F. B., Armendariz, G., Weltz, M. A., and Holifield Collins, C. D. (2017). The rangeland hydrology and erosion model: A dynamic approach for predicting soil loss on rangelands. *Water Resources Research*, 53, pp 9368– 9391. https://doi.org/10.1002/2017WR020651

Janeau, J.L., Bricquet, J.P., Planchon, O., and Valentin, C. (2003). Soil crusting and infiltration on steep slopes in northern Thailand. European Journal of Soil Science, 54 (3), pp. 543-554

Karrou, M., Oweis, T., Ziadat, F., and Awawdeh, F. (2011). Rehabilitation and integrated management of dry rangelands environments with water harvesting. Community-based optimization of the management of scarce water resources in agriculture in Central and West Asia and North Africa. Aleppo, Syria: ICARDA.

Kirkby, M. J., and Bracken, L. J. (2009). Gully processes and gully dynamics. Earth Surface Processes and Landforms: The Journal of the British Geomorphological Research Group, 34(14), pp 1841-1851.

Moore, I.D., Burch, G.J. and Mackenzie, D.H. (1988). Topographic effects on the distribution of surface soil water and the location of ephemeral gullies. Transactions of the American Society of Agricultural Engineers 34: 1098–107.

Morgan R. P. C. (2005) Soil erosion and conservation. National Soil Resources Institute. Cranfield University. Blackwell publishing, third edition. ISBN 1-4051-1781-8

Middleton, N., Stringer, L., Goudie, A., and Thomas, D. (2011). The forgotten billion: MDG achievement in the drylands. In United Nations Convention to Combat Desertification, Bonn.

Mishra, A. (2013). Soil and water conservation. (Accessed on 18-09-2019). http://ecoursesonline.iasri.res.in/mod/page/view.php?id=2103

Nyssen, J., (2001). Erosion processes and soil conservation in a tropical mountain catchment under threat of anthropogenic desertification—a case study from Northern Ethiopia. PhD thesis, Dept. Geography–Geology, K.U. Leuven, Belgium.

Pitt.edu. (2019). Running water: The geology of streams and floods. Geology 800. (Accessed on 18-09-2019). http://www.pitt.edu/~mabbott1/climate/mark/Teaching/GEOL_800_Geology/14GeoLec9.pdf

Poesen, J., (1986) Surface sealing as influenced by slope angle and position of simulated stones in the top layer of loose sediments. Earth Surface Processes and Landforms, 11, pp. 1-10

Poesen, J., Nachtergaele J., Verstraeten G., and Valentin C., (2003). Gully erosion and environmental change: importance and research needs. Catena 50: pp 91–133.

Prasad, S., and Romkens, M. (2004). Mechanical energy and subsurface hydrologic effects in head-cut processes. In International Symposium on Gully Erosion Under Global Change Proceedings pp 109-120.

Rawls, W. J., Brakensiek, D. L., and Saxtonn, K. E. (1982). Estimation of soil water properties. Transactions of the ASAE, 25(5), pp. 1316-1320.

Rawls, W. J., Gimenez, D., and Grossman, R. (1998). Use of soil texture, bulk density, and slope of the water retention curve to predict saturated hydraulic conductivity. Transactions of the ASAE, 41(4), 983.

Reed, M. S., Stringer, L. C., Dougill, A. J., Perkins, J. S., Atlhopheng, J. R., Mulale, K., and Favretto, N. (2015). Reorienting land degradation towards sustainable land management: Linking sustainable livelihoods with ecosystem services in rangeland systems. Journal of Environmental Management, 151, pp 472-485.

Saba, M., Mudabber, M., Kaabneh, A., Obeidat, E., Muhaisen, R., and Khriesat, M., (2017). Marab water harvesting techniques. Jordan. DOI: 10.13140/RG.2.2.19088.3584

Shahrivar, A., and Christopher, T.B.S. (2012). The effects of soil physical characteristics on gully erosion development in Kohgiloyeh and Boyer Ahmad Province, Iran. Advances in environmental biology. pp 367-405.

Šimůnek, J., M. Th. van Genuchten, and M. Šejna (2018). The HYDRUS software package for simulating two- and three-dimensional movement of water, heat, and multiple solutes in variably-saturated media, PC progress technical manual, Version 3.0, Prague, Czech Republic, pp 274.

Strohmeier, S. (2018, April). Restoring Degraded Rangelands in Jordan: Optimizing Mechanized Micro Water Harvesting using Rangeland Hydrology and Erosion Model (RHEM). 1st World Conference on Soil and Water Conservation under Global Change-CONSOWAAt: Lleida, Spain.

USBR, (1997) United States. Bureau of Reclamation, & United States. Natural Resources Conservation Service. (1997). Water measurement manual. The Bureau.

USDA, (2016). General Description of the CLIGEN Model and its History. (Accessed on 10-03-2020). https://www.ars.usda.gov/midwest-area/west-lafayette-in/national-soil-erosion-research/docs/wepp/cligen/

Valentin, C., Poesen, J., and Li, Y. (2005). Gully erosion: impacts, factors and control. Catena, 63(2-3), pp 132-153.

Vallerani. (2013). How it works. Vallerani system, http://www.vallerani.com/wp/?post_causes=how-it-works (accessed 22 Oct 2019).

WRMD. (2010) Water Resource Management Division, Water resources in Jordan: a primer. Department of Environment and Conservation, Government of Newfoundland and Labrador. (Accessed on 26-11-2019). http://esystem.mutah.edu.jo/main/pubs/SfP984072_Primer.pdf

Zhao, J., Vanmaercke, M., Chen, L., and Govers, G. (2016). Vegetation cover and topography rather than human disturbance control gully density and sediment production on the Chinese Loess Plateau. Geomorphology, 274, pp 92-105.

# Appendix

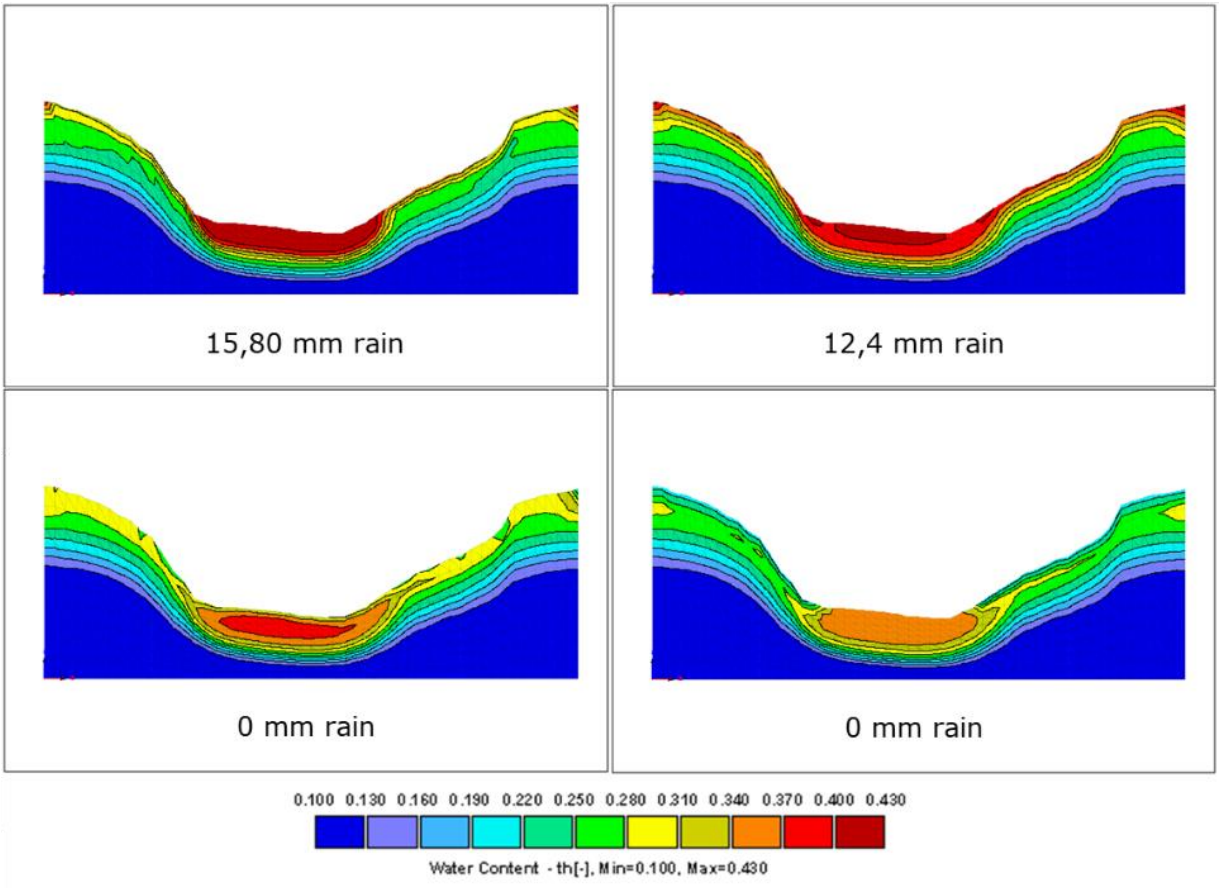


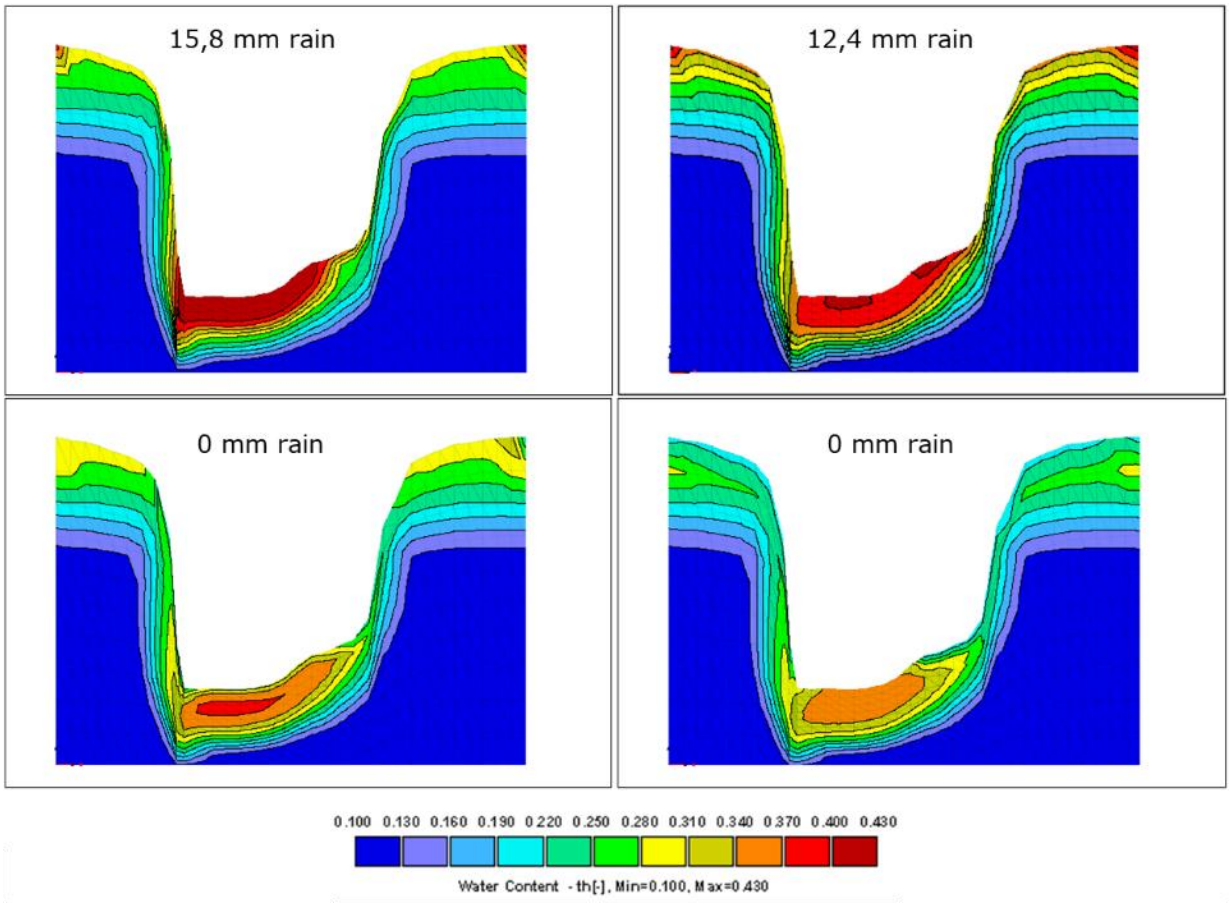


Appendix 1a

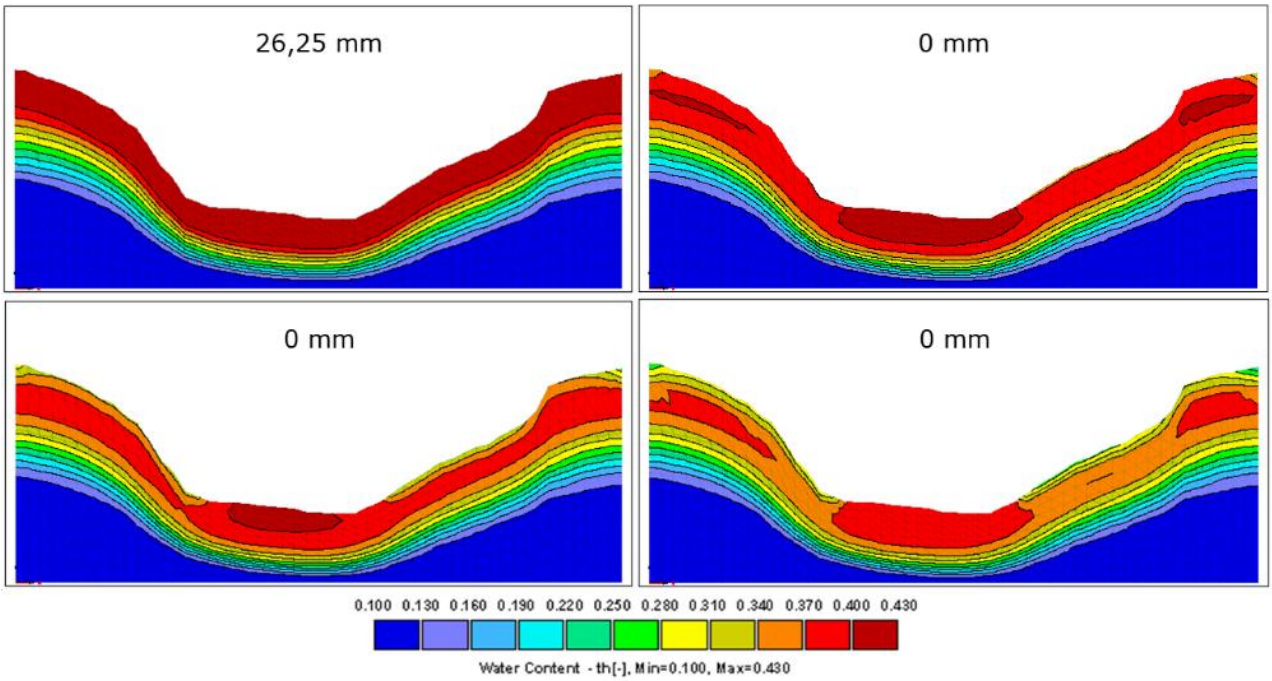
26,25 mm
0 mm
0 mm
0 mm
0.100 0.130 0.160 0.190 0.220 0.250 0.280 0.310 0.340 0.370 0.400 0.430
Water Content - th[-], Min=0.100, Max=0.430

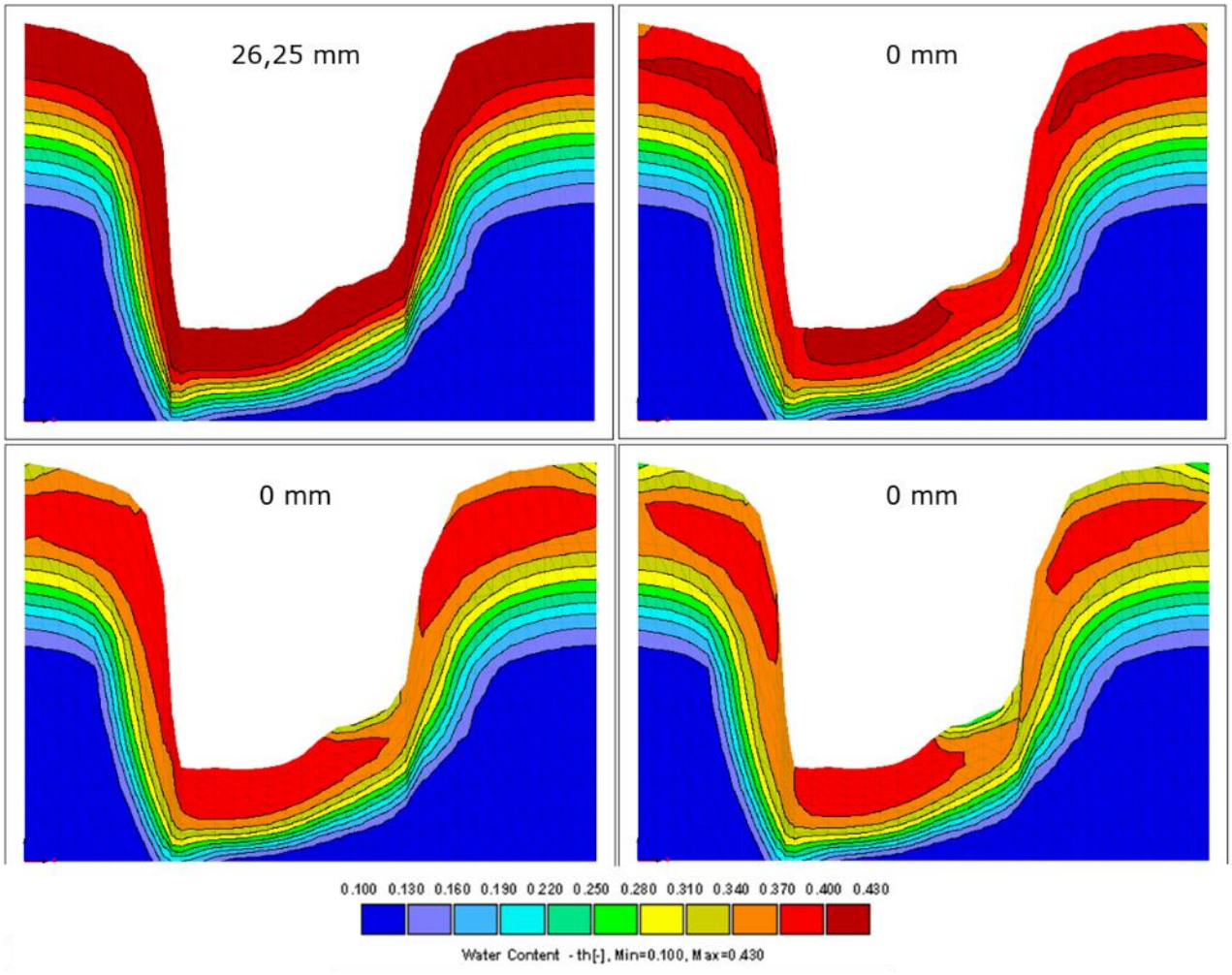
26,25 mm
0 mm
0 mm
0 mm
0.100 0.130 0.160 0.190 0.220 0.250 0.280 0.310 0.340 0.370 0.400 0.430
Water Content - th[-], Min=0.100, Max=0.430

Appendix 1b

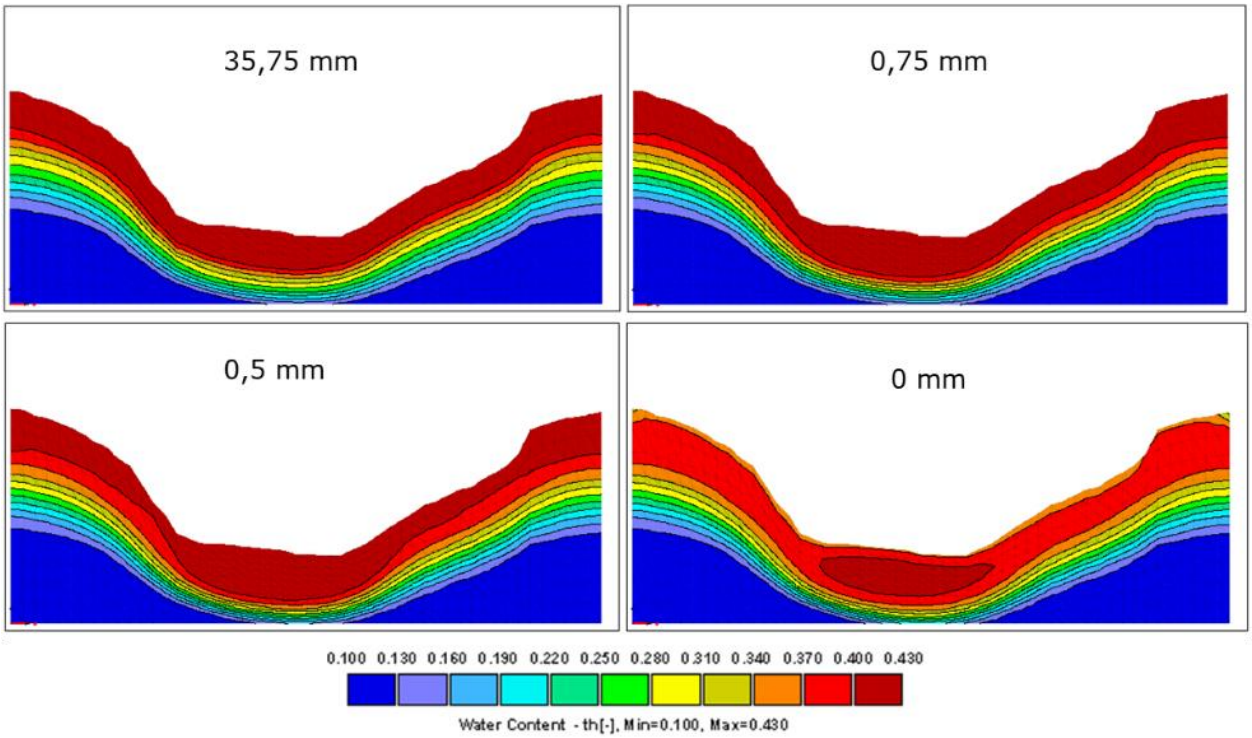
35,75 mm
0,75 mm
0,5 mm
0 mm
0.100 0.130 0.160 0.190 0.220 0.250 0.280 0.310 0.340 0.370 0.400 0.430
Water Content - th[-], Min=0.100, Max=0.430

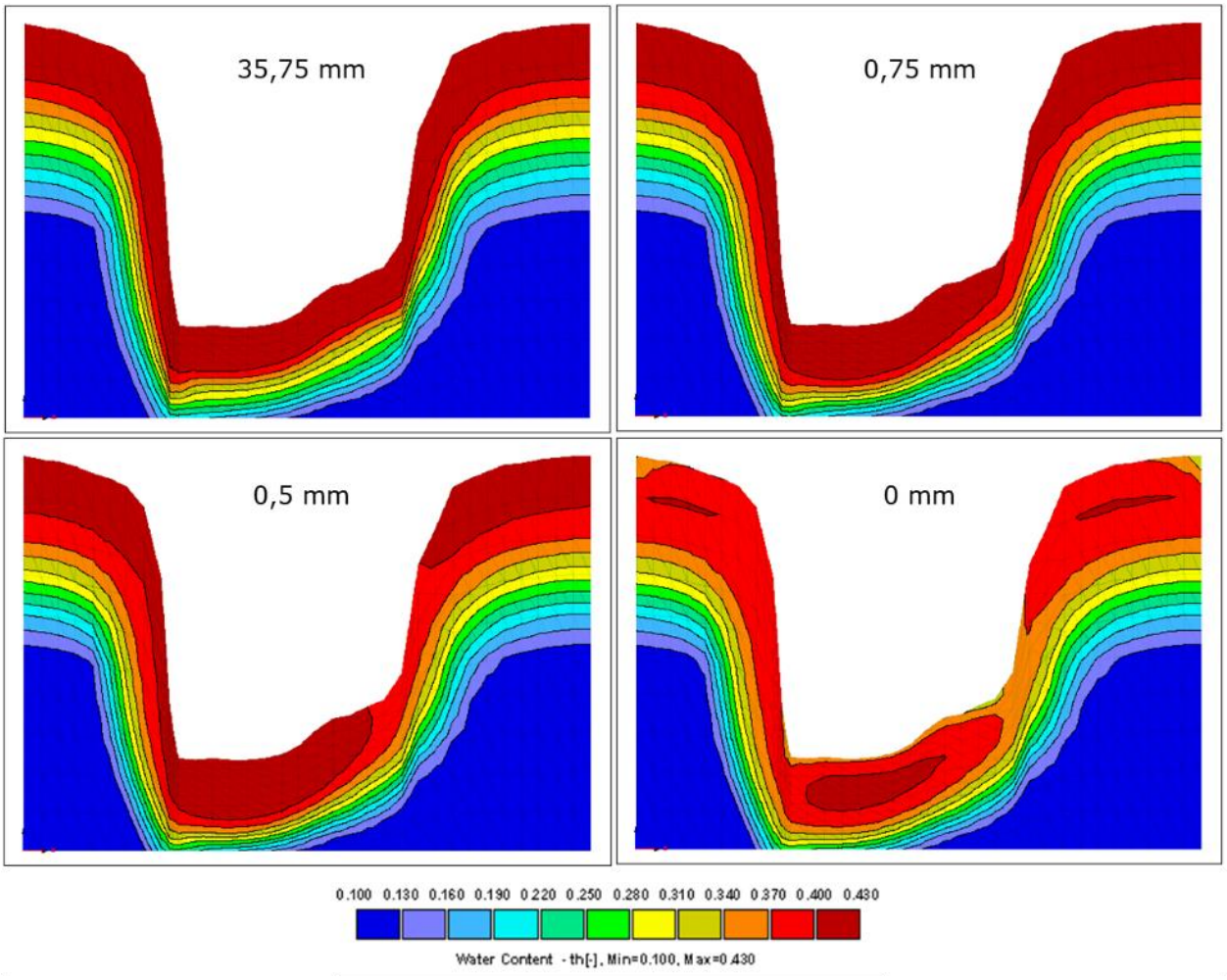
35,75 mm
0,75 mm
0,5 mm
0 mm
0.100 0.130 0.160 0.190 0.220 0.250 0.280 0.310 0.340 0.370 0.400 0.430
Water Content - th[-], Min=0.100, Max=0.430

Appendix 1c

Appendix 2

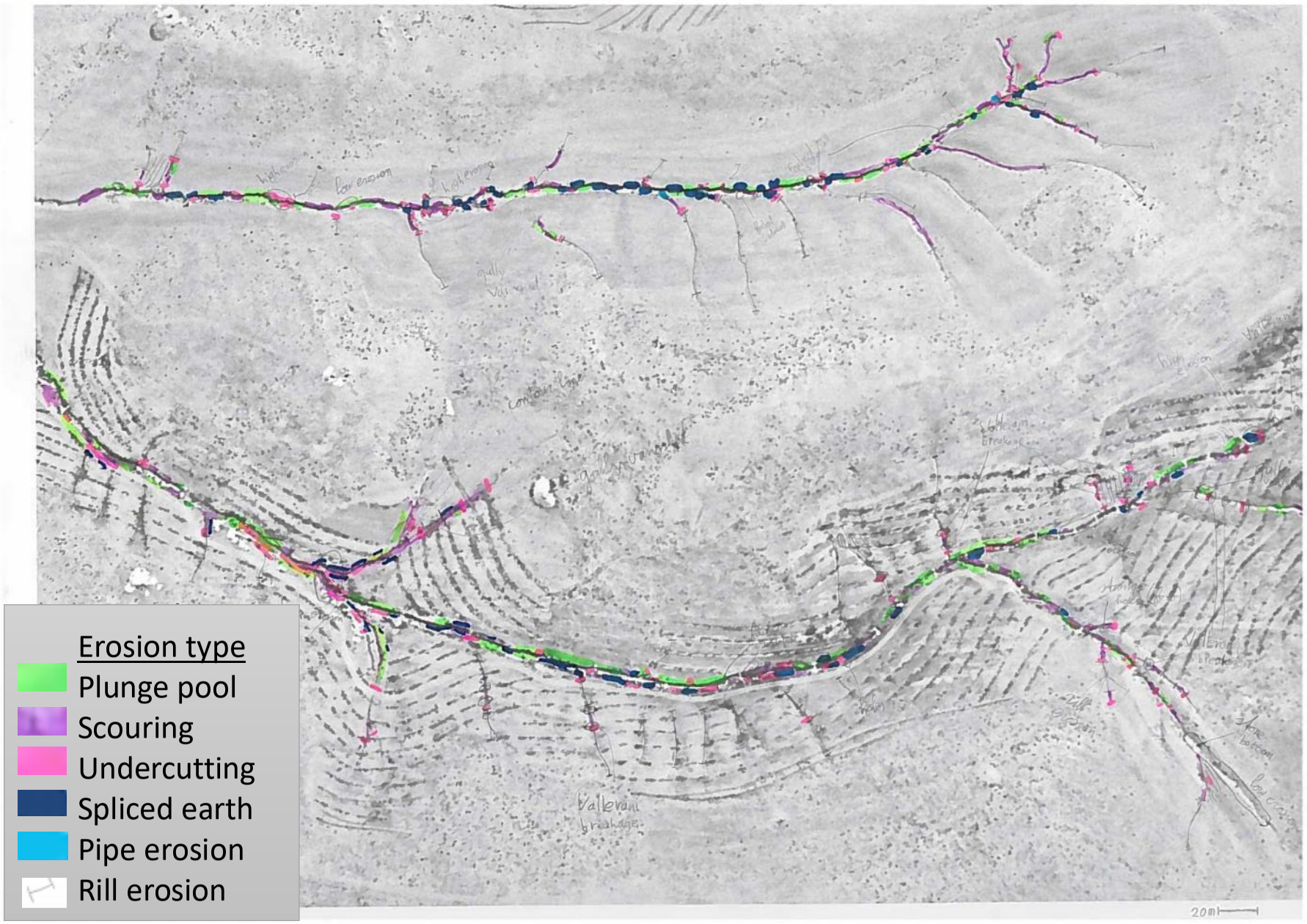
Erosion type
Plunge pool
Scouring
Undercutting
Spliced earth
Pipe erosion
Rill erosion
20m

Appendix 3

Treated watershed

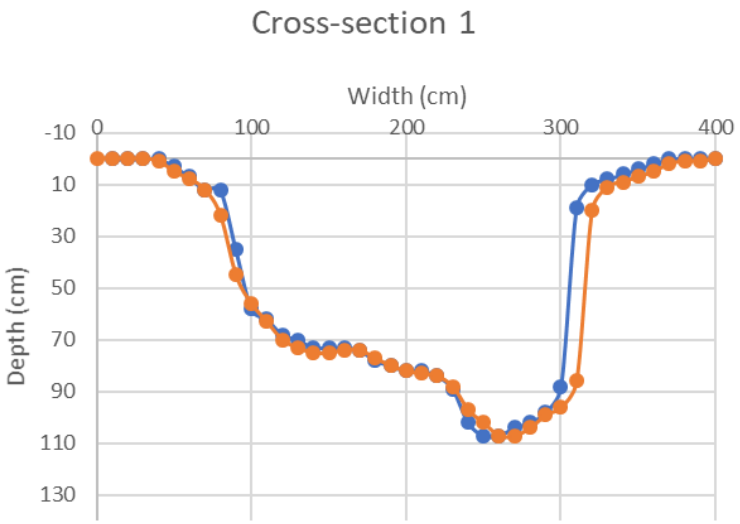


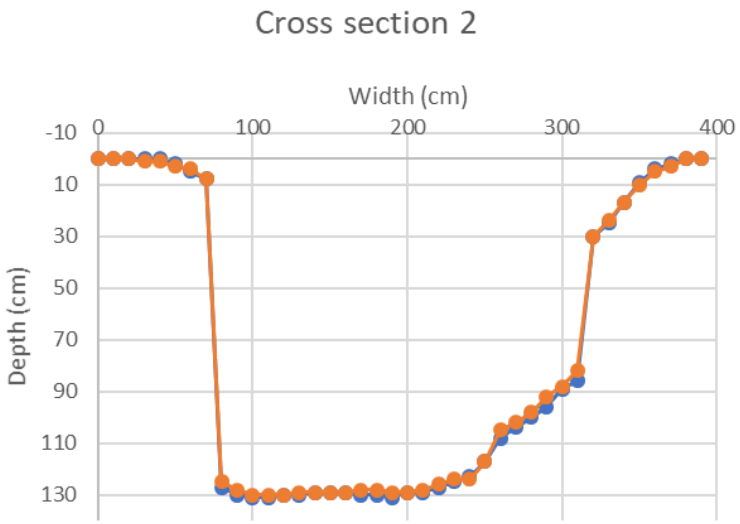


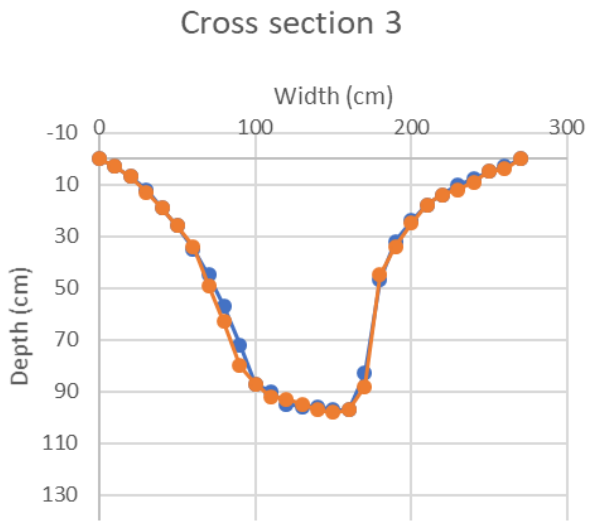


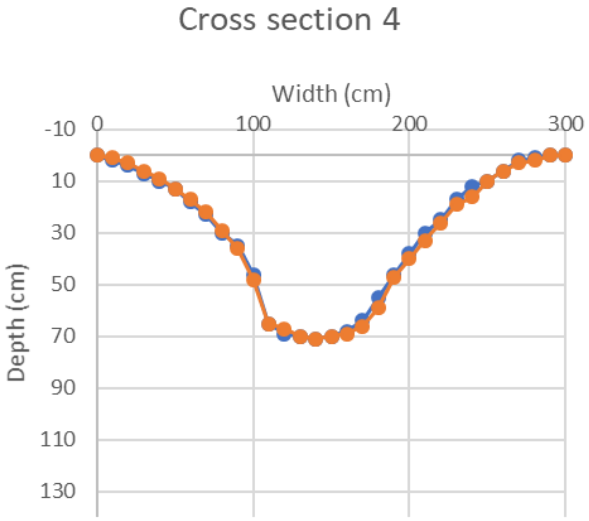


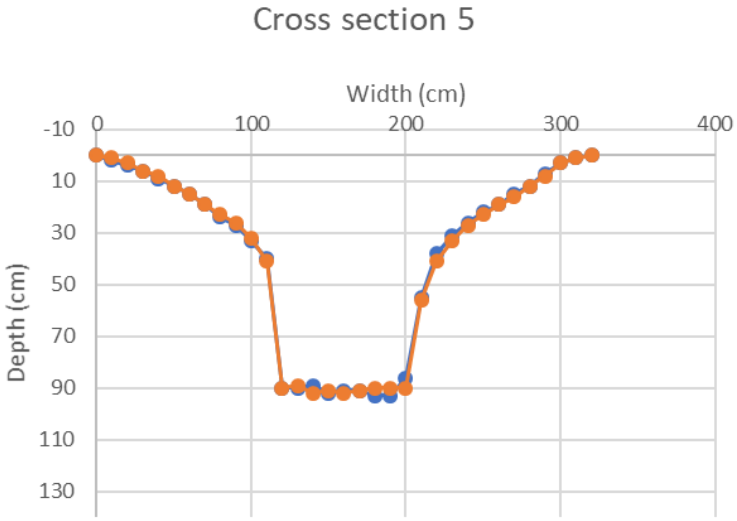


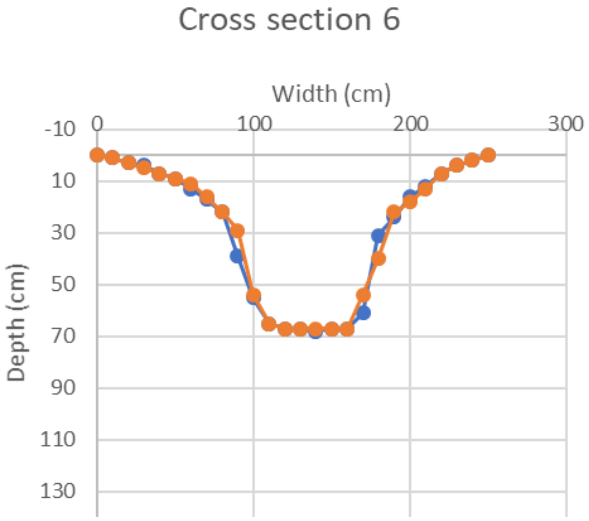

# Treated watershed

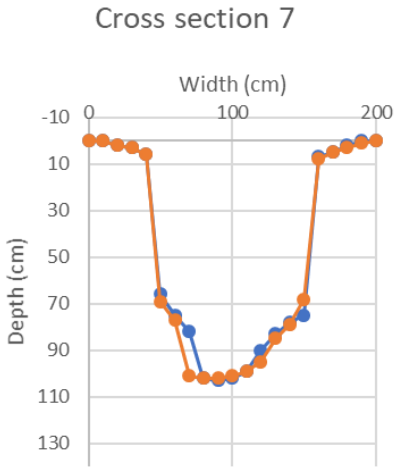


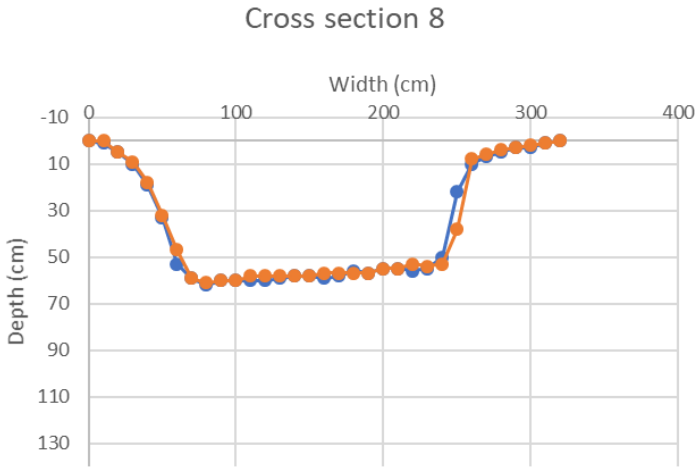


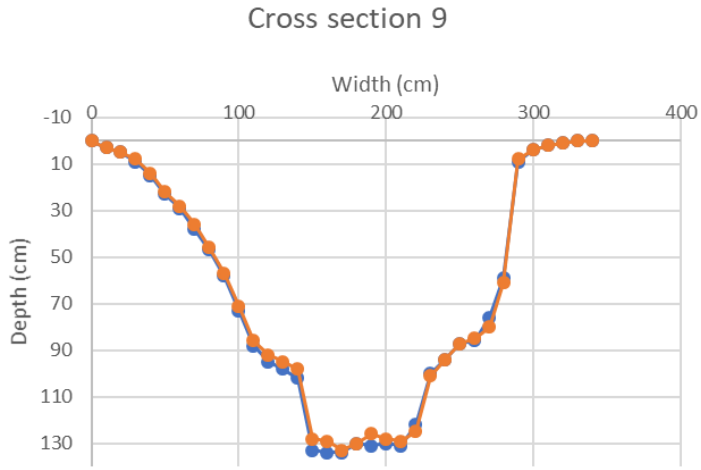


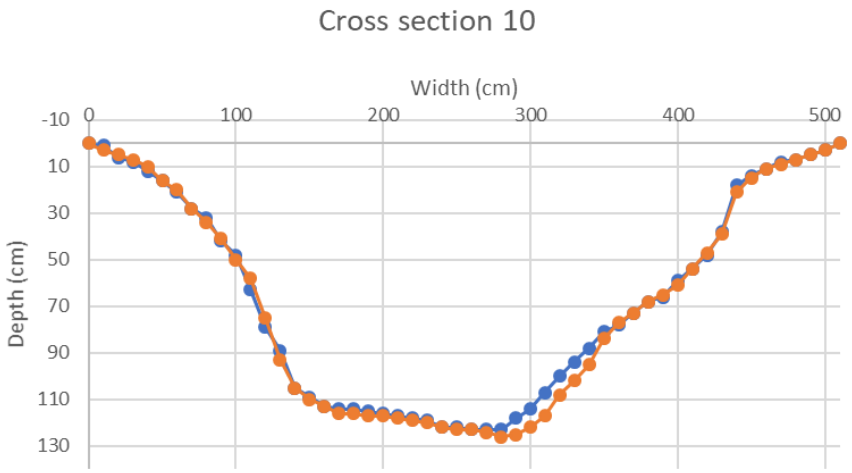


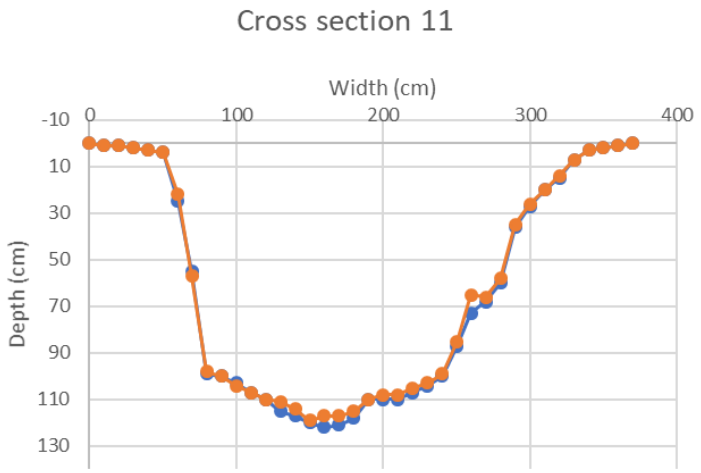


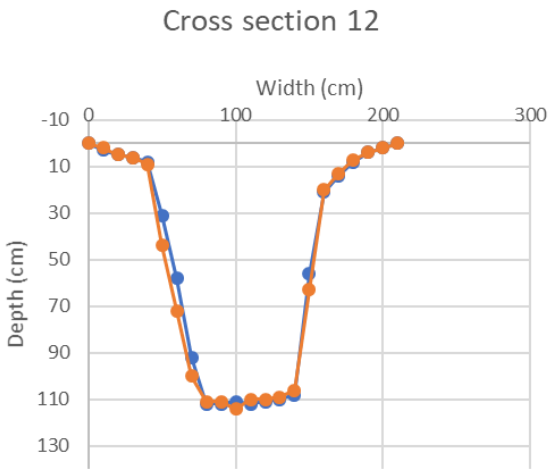

# Appendix 4

## Untreated watershed

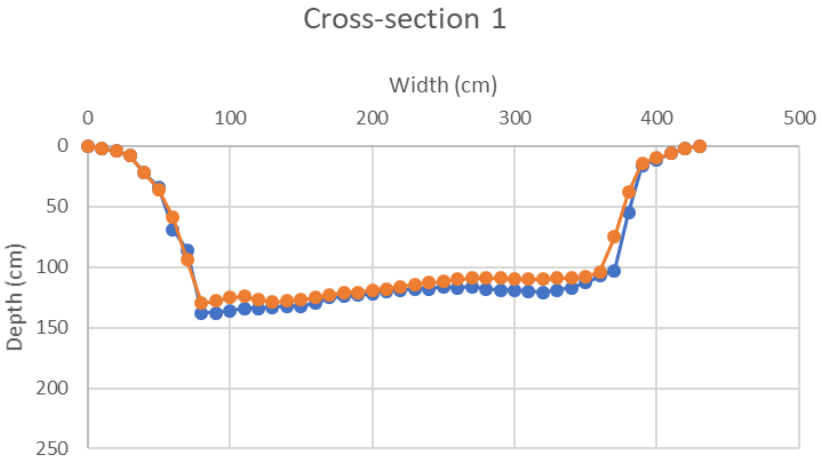


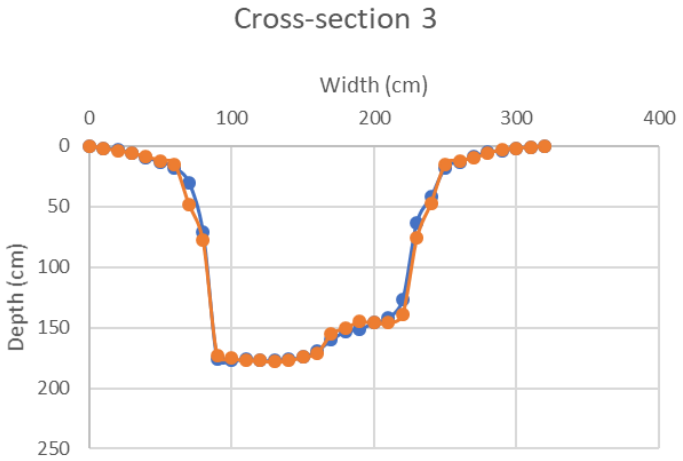


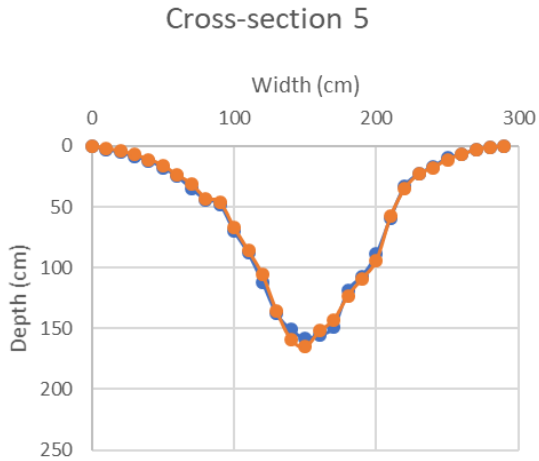


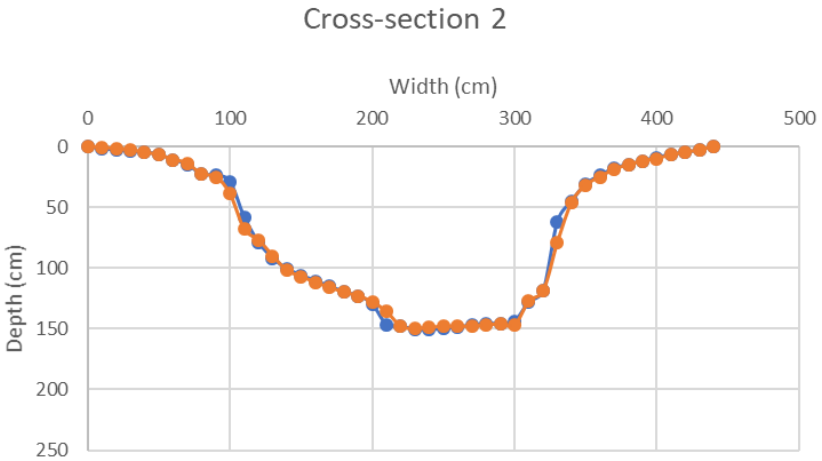


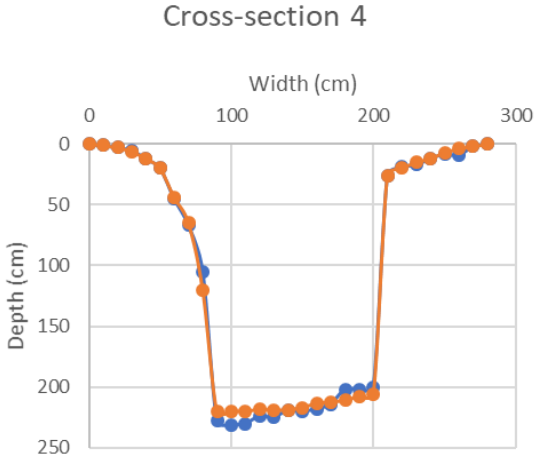


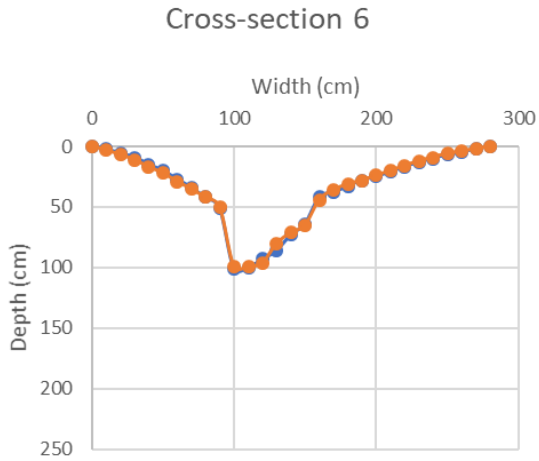

Appendix 5

Treated watershed

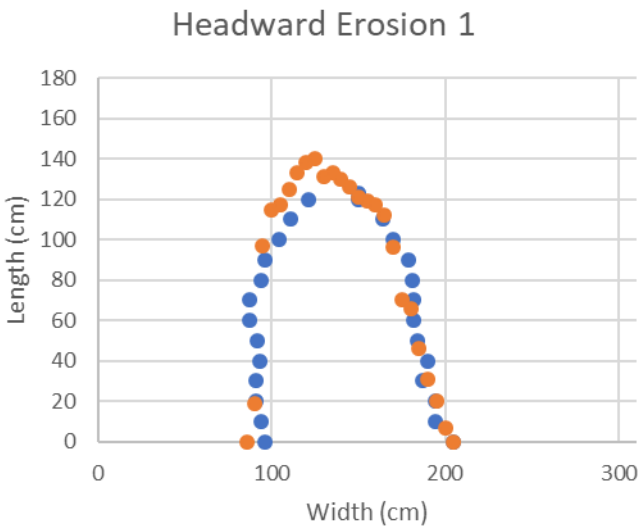


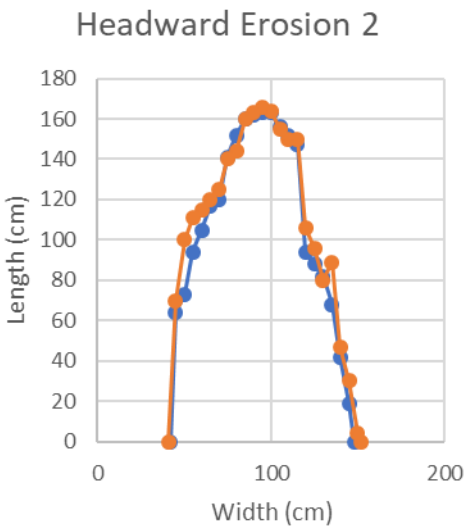


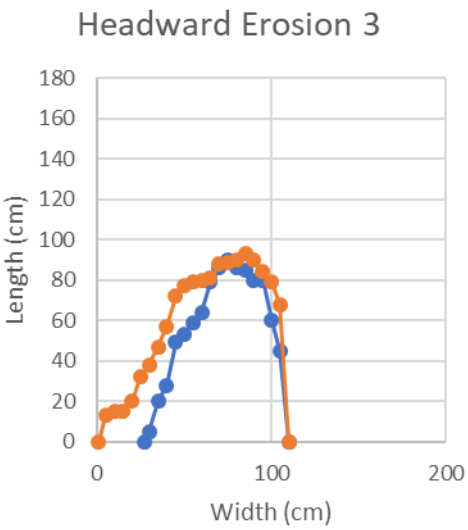

Appendix 6

Untreated watershed